Order Number 1346715

Fatigue damage due to vibration testing

Topham, Keith Craig, M.S.

The University of Arizona, 1991

U·M·I
300 N. Zeeb Rd.
Ann Arbor, MI 48106

FATIGUE DAMAGE DUE TO VIBRATION TESTING

by

Keith Craig Topham

A Thesis Submitted to the Faculty of the

DEPARTMENT OF NUCLEAR ENGINEERING

In Partial Fulfillment of the Requirements
For the Degree of

MASTER OF SCIENCE

In the Graduate College

THE UNIVERSITY OF ARIZONA

1 9 9 1

STATEMENT BY AUTHOR

This thesis has been submitted in partial fulfillment of requirements for an advanced degree at The University of Arizona, and is deposited in the University Library to be made available to borrowers under the rules of the library.

Brief quotations from this thesis are allowable without special permission, provided that accurate acknowledgment of source is made. Requests for permission for extended quotation from or reproduction of this manuscript in whole or in part may be granted by the head of the major department or the Dean of the Graduate College when in his or her judgment the proposed use of the material is in the interests of scholarship. In all other instances, however, permission must be obtained from the author.

SIGNED: Keith C. Tyldam

APPROVAL BY THESIS DIRECTOR

This thesis has been approved on the date shown below:

L. B. Scott

L. B. SCOTT Jr.
Professor of Aerospace and Mechanical Engineering

Nov. 20, 1991
Date

ACKNOWLEDGEMENTS

I would like to thank all the people who have helped me in my endeavor to complete this thesis. They are: my thesis advisors, Dr. George Nelson, Dr. Larry Scott Jr., and Dr. Robert Seale; my mentor, Mr. Richard Oedy; my supervisor, Mr. Tom Johnson; and my colleagues, Mr. Bob Stuart, Mr. Dave Brown, Mr. Jim Rollins, Mr. Mark Ewing, and Mr. Dave Stroup. Without their help, I would not have obtained the results that I did, let alone completed this thesis.

I want to thank Ms. Dorothy Graves, who helped me with all the technical details required to complete this thesis and to comply with the University's regulations. I would also like to express my appreciation to Ms. Sue Tippet, who helped me prepare this thesis for publication. Finally, I would like to thank my wife, Donna, who married me without knowing that I would spend the first 2 years of our marriage working on and writing this thesis. My wife's support and patience at home was crucial to my struggle to complete this thesis.

TABLE OF CONTENTS

TABLE OF CONTENTS -- Continued

LIST OF ILLUSTRATIONS

LIST OF ILLUSTRATIONS -- Continued

LIST OF ILLUSTRATIONS -- Continued

LIST OF TABLES

LIST OF SYMBOLS

ACM	Air Combat Maneuver
b	Spacing between holes (in)
c	Distance from neutral axis to cross section surface (in)
d	Diameter (in); subscript denotes inside (in) or outside (out)
D	Damage
f	Frequency (Hz); subscript denotes 1^{st}, 2^{nd}, 3^{rd} modes
f_n	Natural frequency; fundamental frequency (Hz)
G_{RMS}	Root mean square acceleration in gravity units (G)
h	Height (in)
I	Moment of inertia (in^4)
k_t	Stress concentration factor
M	Bending moment ($in\text{-}lb_f$)
n_i	Actual number of fatigue cycles
N_i	Number of cycles to failure
PSD	Power spectral density (G^2/Hz); subscript denotes input (in)/output (out)
Q	Transmissibility
R	Stress ratio, maximum stress divided by minimum stress
RMS	Root mean square
S_b	Stress (psi); subscript denotes bending
t	Time (Hr, Min, or Sec)
WUT	Windup-turn
σ	Standard deviation

ABSTRACT

The first objective of this study was to determine and compare the fatigue damage from two different vibration events versus the fatigue damage from an envelope of both events. The second objective was to determine and compare the fatigue damage from the equipment test versus the fatigue damage from a section test while using the same vibration envelope. Both objectives were accomplished using NASTRAN models to calculate internal loads for use in the fatigue analysis.

This study proved that the vibration envelope produced three times more fatigue damage than the worst vibration event, and two times more fatigue damage than both events applied sequentially. When the same vibration envelope was used in an equipment test and a section test, the analytical results showed the internal loads were quite different. Furthermore, this study demonstrated the need to validate and update analytical models with actual test data to derive accurate equipment loads.

CHAPTER 1

INTRODUCTION

Most types of equipment will experience a wide range of dynamic environments over their lifetimes. Of these, vibration is perhaps the least predictable environment and has the most severe damage potential. It is often cited as the major cause in structural failures that are due to fatigue.

Manufacturers often design their products to have lifetimes of ten years or more. Obviously, it is impractical to conduct any vibration test for a period of 10 years. Therefore, the equipment's field vibration data is overlaid on one graph and straight line segments are drawn above the acceleration peaks to completely "envelope" all the data. Next, the level of the envelope is then raised to account for not measuring every vibration event or every vibration level. Finally, the level of the envelope is usually raised even higher to accelerate the laboratory test in order to facilitate accumulating years of usage in a matter of days.

These envelopes are used in accelerated vibration tests to demonstrate the equipment's design adequacy. Sometimes the same envelope is used to control the responses of the test item in both the equipment and the section tests. An equipment test is one where all the sections are assembled together to form the "equipment". The equipment is simulated as mounted to its platform, and then vibrated with a shaker. A section test is where one or more assemblies are joined together to form one of the equipment's sections. Each section is in turn attached to a shaker table and then vibrated by the shaker table. The envelopes used in these vibration tests have the potential to significantly change the equipment's structural response to vibration. However, these changes may be more dramatic for laboratory tests that support the equipment differently than were used in actual usage from which the vibration data was originally measured.

Purpose

This study will (a) determine and compare the fatigue damage from two different vibration events versus the fatigue damage from an envelope of these events; and (b) determine and compare the fatigue damage resulting from use of the same vibration envelope for both the equipment test and for the section test. The study's purpose is to show that the fatigue damage from each of the vibration events when applied sequentially is not as high as that from the envelope of all the events. Its other purpose is to show that the fatigue damage that results from using the same vibration envelope for two different support conditions is not the same.

Scope

This study will attempt to validate the estimated mission profile with an actual mission profile. It will discuss the results and assumptions used in deriving the estimated profile. Then, it will derive the vibration envelopes and test times used to control laboratory vibration tests. Next, it uses the equipment's finite element models to calculate the structural loads. Finally, it uses the fatigue analysis to tie together the results from the structural analysis with the effects that frequency and test duration have on cumulative fatigue damage.

This study will evaluate whether different vibration events should be enveloped, or if they should be treated as unique events. This study also will evaluate whether the same vibration envelope should be used to control a vibration test with different support conditions than the data was originally measured, or if the envelope should be modified to account for these support conditions. This evaluation investigates the differences in fatigue life from using vibration envelopes versus using individual vibration events to control the laboratory vibration tests. This study also investigates the effects of using the same vibration envelope in laboratory tests with different support conditions.

Assumptions

Enveloping vibration data is a common practice among many different manufacturers and test organizations. The procedures used in this study apply to other engineering disciplines as well. Essentially, this process starts when

the equipment's user defines the equipment's anticipated usage. This guides the equipment's manufacturer in measuring the equipment's vibration environments, and aids him in developing vibration test levels and test times. Finally, this process usually concludes with the equipment's laboratory vibration tests. All the above steps are generic in nature, consequently, any type of equipment may be used to determine the cumulative fatigue damage due to vibration.

Approach

This study will evaluate the effects that vibration envelopes and different support conditions have on fatigue damage. As such, it is irrelevant what type of equipment or platform is used to meet these objectives. The equipment used in this study is the Advanced Medium Range Air-to-Air Missile (AMRAAM), and its platform is the McDonnell Douglas F-15 Eagle. This platform produces and generates some very intense vibration levels while carrying the equipment during its mission phase. Low frequency vibration is transmitted directly from the platform to the equipment, while high frequency vibration of the equipment results from the aerodynamic flow surrounding both the platform and its equipment.

This study evaluates and compares two different mission profiles. The estimated mission profile describes the different segments in terms of two parameters (time and altitude). Unfortunately, this format does not provide enough information regarding the events that occur in one particularly critical mission segment. The actual mission profile is built entirely from test data. It will be used to validate the estimated mission profile, and to define the events within the critical mission segment. This study will compare the two mission profiles in order to evaluate how well the estimated mission profile mirrors reality.

Either the estimated or the actual mission profile will be used to guide the vibration analysis. Vibration envelopes are usually made by overlaying numerous power spectral density (PSD) plots from different events. A curve is drawn around the peaks to form a vibration envelope. The laboratory test

durations are derived from an analysis of the G_{RMS} vibration levels of the various categories of events when grouped by environmental conditions.

The equipment's computerized vibration data base provides the means to define the PSD envelopes for the two vibration events. This study will sort all the vibration data by: event, location on the equipment, axis, environmental condition, and the equipment's location on its platform. This effort should produce a couple of events with distinct vibration spectra that defines the vibration envelope used in the equipment's laboratory tests.

The equipment's manufacturer built the NASTRAN model used in this study. This model contains the equipment's masses, material properties, stiffnesses, and damping characteristics. It does not include the equipment's attachments or the structural characteristics of its platform. However, the present study will model the equipment as mounted to its platform or to a shaker table for the structural analysis.

The platform's structural characteristics are unknown, and are not available for use in this study. The properties of the platform are simulated with rigid masses and springs. This permits the same degrees-of-freedom to exist between the equipment and its platform that exist in the field. The resulting model simulates those support conditions that exist during equipment's mission phase and during the laboratory tests (Fig. 1-1).

The equipment's finite element model is then cut in half to simulate a section test. Two large yokes attach the forward section at the cut and at its center directly to a shaker table. Rigid masses and springs are used to simulate the properties of the section's support structure. This model simulates only those conditions that exist during the laboratory section tests (Fig. 1-2).

Vibration envelopes are used in laboratory tests to control the equipment's dynamic responses. The same procedure is used by the present study to control both finite element model's responses during these simulated laboratory tests. First, this study conducted a modal analysis on each model and the compared the results to modal test data. Second, the support structure's stiffnesses are iteratively adjusted unit the analytical models predicted the first

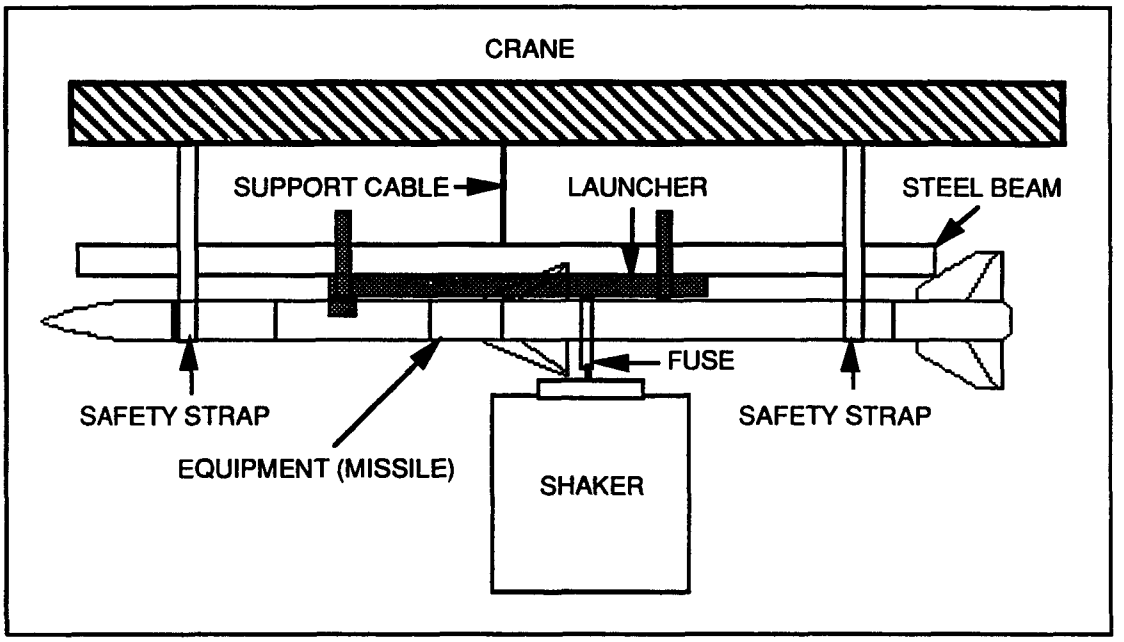

Figure 1-1 Equipment Laboratory Test Setup

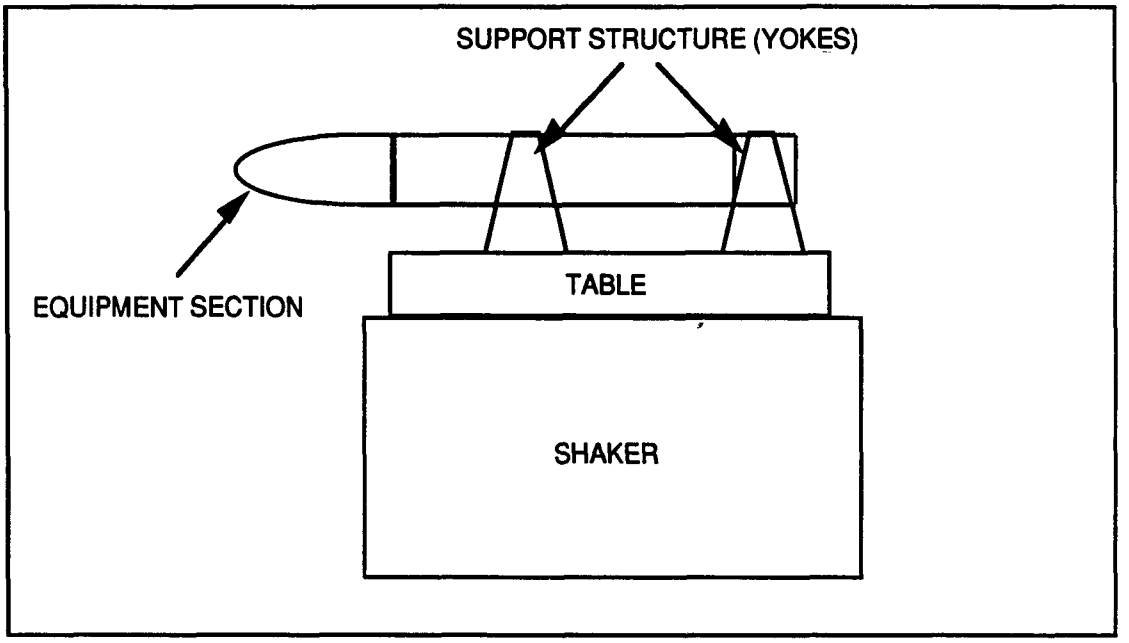

Figure 1-2 Equipment Section Laboratory Test Setup

two frequencies and mode shapes contained in the modal test data. Finally, a 1 G^2/Hz base excitation was applied to both models to produce their respective transmissibilities.

The present study uses these transmissibilities to derive the appropriate vibration inputs for each of the desired vibration responses. These derived inputs are used to excite the finite element models to obtain the desired responses at a particular control station on the equipment. The NASTRAN models are used to calculate internal bending moments, shear forces, bending stresses, and accelerations due to each of the different vibration response envelopes.

The present study applies Miner's rule to sum the fatigue damage due to different vibration envelopes for each different vibration event. Miner's rule uses the material's S/N curve to calculate the number of cycles to failure at each of the different stress levels. The number of cycles consumed at a particular stress level is a function of the equipment's resonant frequency and time spent at that stress level. Miner's rule sums the ratios of the number of cycles consumed to the number of cycles to failure for each of the different stress levels to arrive at the cumulative fatigue damage.

This study uses the fatigue analysis to assess the effects of enveloping vibration data versus using the PSDs for each of the different unique vibration events to control the response of the vibration tests. It also uses the fatigue analysis to assess the effects of using the same vibration envelope for tests with different support conditions without compensating for the changes in the equipment's dynamic characteristics. This study intends to show that analytical tools must be used in conjunction with laboratory tests in order to correctly interpret the results from the laboratory tests, and to derive accurate equipment loads.

The following sections will: introduce vibration; define the mission profiles; derive the vibration envelopes and test times; model the equipment as attached to its platform or a shaker table; model the equipment section attached to a shaker table; discuss the results of the structural analysis; and discuss the results of the fatigue analysis. Finally, this study concludes with its conclusions, and recommendations.

CHAPTER 2

VIBRATION

For nearly every part, sub-system, and assembly in an equipment, vibration is potentially one of the most damaging of all the natural and induced environments. Consequently, military specifications require the equipment's manufacturer to account for all the potential vibration environments that his equipment will be exposed during its lifetime. However, the magnitude, the length, and even the vibration environments themselves are in most cases unknown until the equipment is designed, constructed, and finally produced. The present study demonstrates a methodology that was used to deal with this lack of information about a particular vibration environment during the early stages of the equipment's design.

Figure 2-1 shows that the equipment's vibration environment is not measured until late in its development program. The equipment's dynamic response is a function of its configuration, interaction with its platform, and interaction with its environment. Therefore, the equipment manufacturer must use field data to upgrade the equipment's test levels and to evaluate its design.

Vibration Sources

It is extremely difficult to identify all the potential vibration environments the equipment will see in its lifetime. Although Fig. 2-2 applies specifically to military equipment, it does show the immense size of this task. Figure 2-2 also shows that there are three distinct phases in the equipment's life cycle. These are the transportation phase, the storage phase, and the mission phase. The equipment's manufacturer usually has the responsibility for determining those phases and events that have the greatest damage potential.

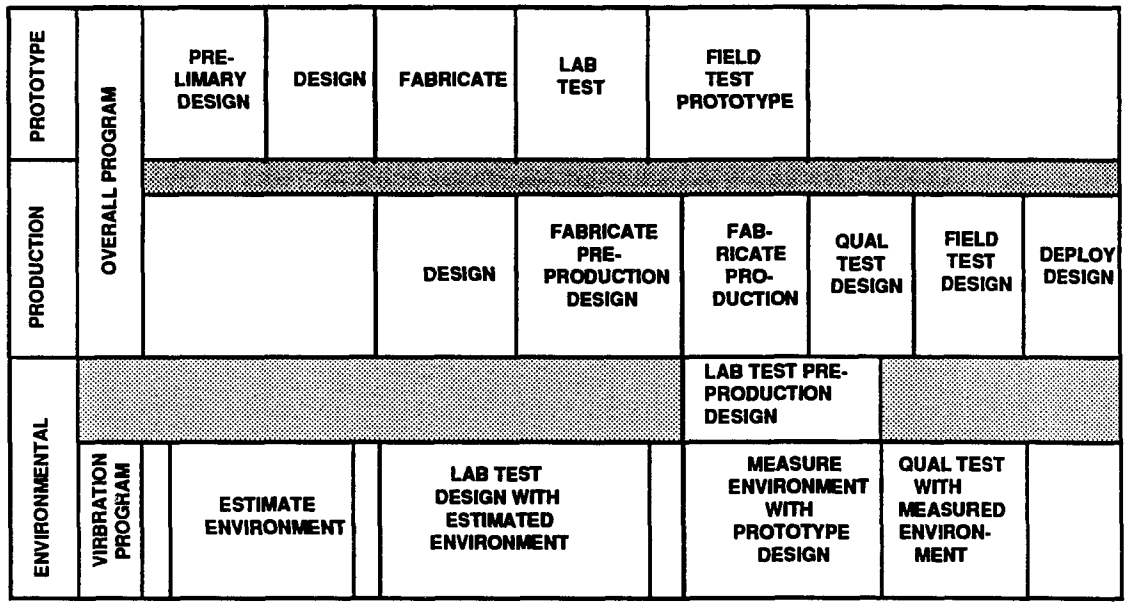

Figure 2-1 Comparison Between the Equipment's Development Program and its Vibration Program (Curtis 1962, p. 112)

Vehicles that travel through a medium such as air or water all experience some type of vibration. For instance, aircraft vibration is usually caused by the interaction between the aircraft's surfaces and the air. This interaction is most often induced by the aircraft's maneuvers and also by atmospheric turbulence. Similarly, ship vibration is usually caused by the interaction between the ship's hull and the water. This interaction is caused by the ship's maneuvers and also by the various sea conditions (DOD 1976, p. 43). Aircraft in particular and to a lesser degree ships, are sources of intense vibration during all three phases of the equipment's life cycle.

Transportation vibration is one source of vibration that all equipment will experience during their lifetimes. Usually, the equipment is first transported by either truck or by train, and will experience vibration due to its carrier traveling over a combination of rough surfaces or rough terrains (DOD 1976, p. 43). When the equipment is transported by either ship or aircraft to overseas locations, it experiences vibration environments that have similar levels and spectral shapes as those for the permanently installed equipment.

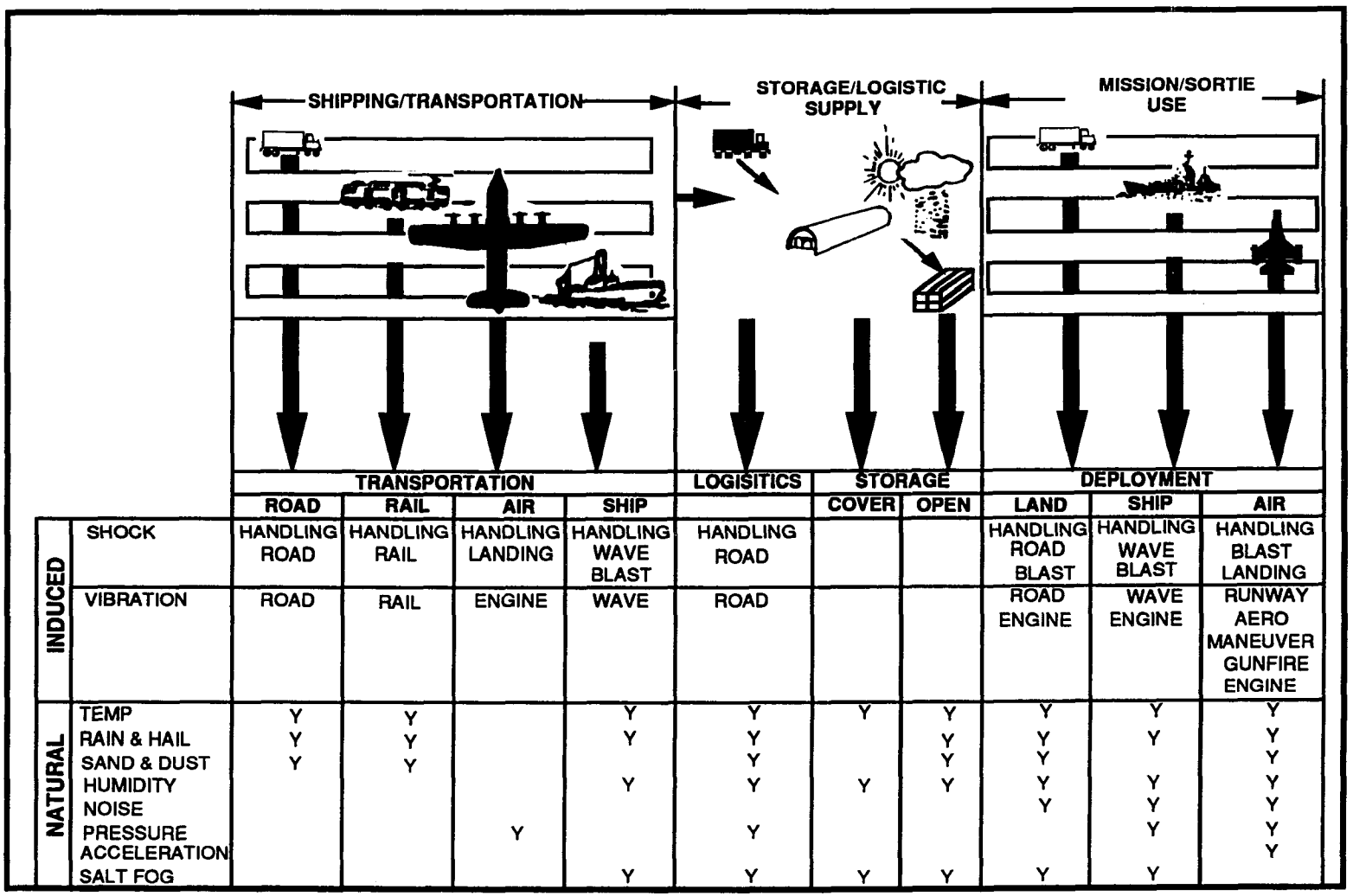

		TRANSPORTATION				LOGISITICS	STORAGE		DEPLOYMENT		
		ROAD	RAIL	AIR	SHIP		COVER	OPEN	LAND	SHIP	AIR
INDUCED	SHOCK	HANDLING ROAD	HANDLING RAIL	HANDLING LANDING	HANDLING WAVE BLAST	HANDLING ROAD			HANDLING ROAD BLAST	HANDLING WAVE BLAST	HANDLING BLAST LANDING
	VIBRATION	ROAD	RAIL	ENGINE	WAVE	ROAD			ROAD ENGINE	WAVE ENGINE	RUNWAY AERO MANEUVER GUNFIRE ENGINE
NATURAL	TEMP	Y	Y		Y	Y	Y	Y	Y	Y	Y
	RAIN & HAIL	Y	Y		Y	Y		Y	Y	Y	Y
	SAND & DUST	Y	Y			Y		Y	Y		Y
	HUMIDITY				Y	Y	Y	Y	Y	Y	Y
	NOISE								Y	Y	Y
	PRESSURE			Y		Y				Y	Y
	ACCELERATION										Y
	SALT FOG				Y	Y	Y	Y	Y	Y	

Figure 2-2 Life Cycle Histories for Military Equipment (DOD 1989, pp. 6-7)

Structural Effects

The ultimate structural effect of excessive exposure to vibration is usually a permanent failure of some kind or the other. Repeated exposure to severe vibration levels causes fatigue, which accumulates until the structure can no longer absorb any more damage. At this point cracks will eventually develop and then propagate within the equipment's structural members and within the mounting brackets of various electronic components.

Structural fatigue is caused by external forces that are repeatedly applied to the equipment's surfaces. If the equipment's resonant frequencies are low, its structure will usually see large displacements and consequently high internal stresses (Fisher and Forkois 1988, p. 43-2). An increase in the equipment's resonant frequencies can significantly reduce its displacements, which in turn reduces its internal stress levels (Fisher and Forkois 1988, p. 43-2). However, random vibration contains and excites all frequencies within its bandwidth, and it is often the most damaging type of vibration. There is nothing the equipment's manufacturer can do to avoid random vibration other than design for it.

Vibration Theory

An equipment's response to external excitation is primarily a function of its dynamic characteristics, material characteristics, mass distributions, and its degrees-of-freedom. The equipment's vibration response is influenced by its number of degrees-of-freedom. At each equipment resonant frequency there is a set of motions associated with that frequency called the "mode shape". Each mode shape or deformation involves periodic motion of the equipment at various locations involving one or more degrees-of-freedom. This is clearly shown in Fig. 2-8 for the equipment used in this study. The first mode (38.9 Hz) is the equipment's fundamental mode or resonant frequency. This mode, when excited, usually produces the largest displacements and the highest stresses within the equipment's structure (Steinberg 1988, p. 6).

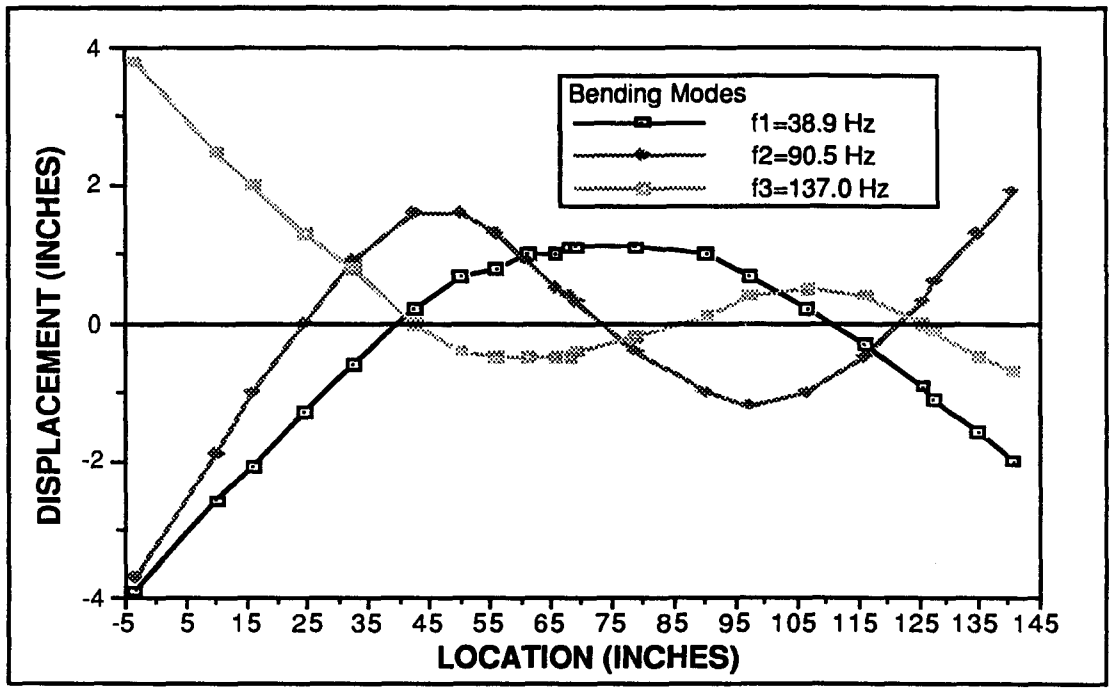

Figure 2-3 A Multiple Degree-of-Freedom System

Random Vibration

A random vibration is one whose instantaneous value is unpredictable. It consists of a continuous distribution of sine waves at all frequencies, the amplitudes and the phase angles of which vary in an unpredictable manner as a function of time. Random vibration cannot be described by an explicit mathematical relationship because each observation of the phenomenon is unique.

Random vibration can be categorized as being either stationary or non-stationary. Stationary vibration is that special case of vibration in which all ensemble averages and all possible moments and joint moments are time invariant i.e., any translation of the time origin in the calculations leaves the statistical properties unaffected. Stationary random vibration can be further categorized as being ergodic or nonergodic. Stationary vibration is ergodic when time averages of moments and joint moments computed for a specific sample function yields the same results as the ensemble averages of those same moments and joint moments. (Bendat and Piersol 1986, pp. 9 -14)

The type of random vibration associated with equipment carried on aircraft has, for the vibration events considered herein, been show by flight measurements and statistical analysis to be strongly stationary and ergodic (Bendat and Piersol 1986, p. 61). Thus, for the present study the random vibration was considered to be stationary and ergodic in the strict sense. Numerous studies have show that the type of random vibration associated with equipment carry on aircraft is fairly well described by a Gaussian "normal" distribution of its instantaneous acceleration peaks. The Gaussian probability density function is graphically illustrated in Fig. 2-4.

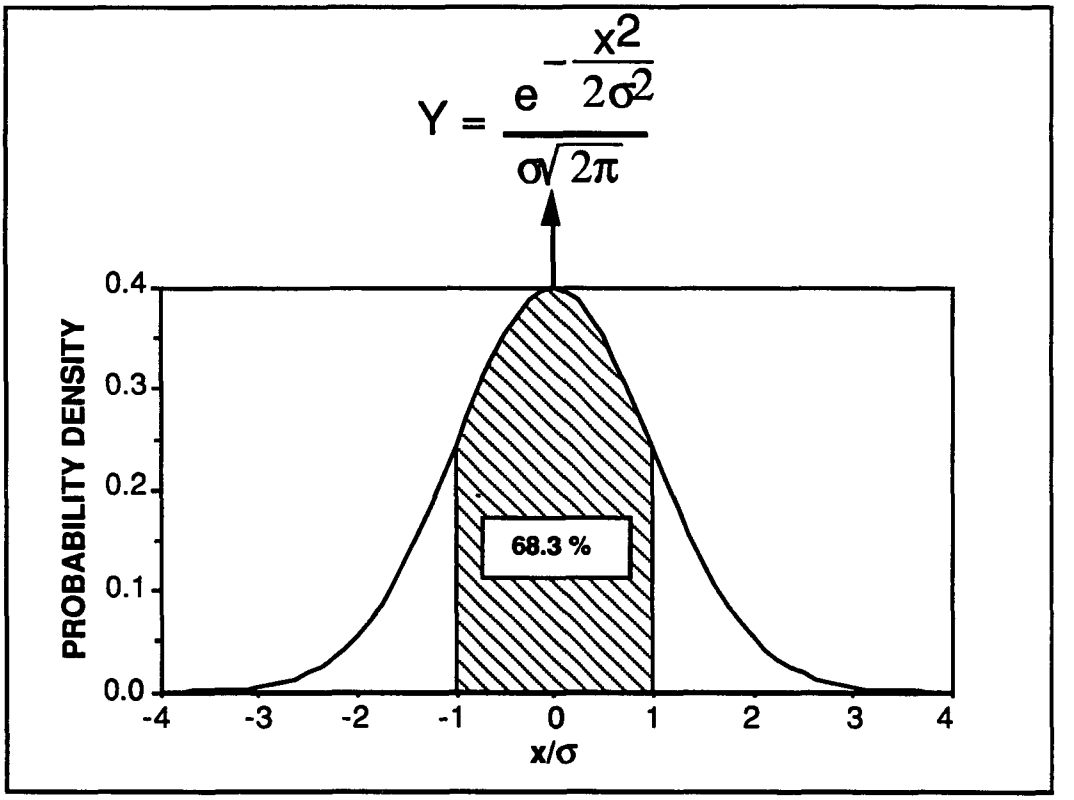

Figure 2-4 Gaussian Distribution Curve (Steinberg 1988, p. 221)

The above equation assumes that the mean acceleration, x_m, is zero. If this is true, the instantaneous acceleration is equal to, x, and the standard deviation, σ, is now equal to the G_{RMS} acceleration. The Gaussian distribution

curve describes the probability, Y, of occurrence of a particular instantaneous acceleration peak when plotted as a function of the ratio of the instantaneous acceleration peak, x, divided by the G_{RMS} acceleration, σ, of the vibration spectrum. If the random vibration is "normally" distributed (according to the Gaussian distribution) then the instantaneous acceleration peaks will lie between $\pm 1\sigma$ G_{RMS}, $\pm 2\sigma$ G_{RMS}, and $\pm 3\sigma$ G_{RMS} levels 68.30%, 95.40%, and 99.73% of the time, respectively. In addition, if one looked at a random vibration event's peak acceleration time history, one finds acceleration peak levels greater than 1σ G_{RMS}, 2σ G_{RMS}, and 3σ G_{RMS} occurring 31.7%, 4.60%, and 0.27% of time, respectively. Although, there are acceleration peaks that exceed 4σ G_{RMS} and 5σ G_{RMS}, the probability is almost 100% that all will lie within $\pm 3\sigma$ G_{RMS}. For laboratory simulations of the random vibration environment, machines called "shaker tables" or "shakers" employ controllers which apply the Gaussian distribution principle to control the vibration spectrum. The controllers simply clip any peak acceleration level exceeding $\pm 3\sigma$ G_{RMS}, thereby preventing an accidental equipment overtest.

Spectral Analysis

The fundamentals of vibration spectral analysis are covered by Bendat and Piersol 1986, pp. 1-25; and by Curtis 1986, pp. 22-1 to 22-28. The reader is referred to these two works for additional details concerning spectral analysis. In this section we will only briefly introduce the terminology, units, and properties that are important in the spectral analysis of random vibration as it relates to the present study. The power spectral density function for random vibration describes the general frequency composition of the vibration in terms of the spectral density of its mean square value. The amplitude of the acceleration spectral density has the units of gravity squared per unit cycle of bandwidth (G^2/Hz).

Power spectral density (PSD) plots show the mean squared power spectra rate of change versus frequency (Miles and Thomson 1988, p. 11-5). Engineers usually use the log-log format to show the spectral density of a vibration event over a wide frequency range. The abscissa on the PSD plot denotes the logarithm of frequency (Hz), while the ordinate denotes the logarithm of acceleration power spectra density (G^2/Hz). The area under the curve is integrated over the desired frequency range and the mean square root taken to obtain the RMS acceleration level (G_{RMS}) for the PSD plot.

Figure 2-5 shows three different types of vibration spectra. The left figure (Fig. 2-5a) illustrates the characteristics of a sine wave, which has only one fundamental frequency, and appears as a straight line on the PSD shown in Fig. 2-6a. The center figure (Fig. 2-5c) shows the characteristics of narrow-band random vibration. Narrow-band vibration may contain a number peaks at different frequencies. Each peak is concentrated within a narrow frequency bandwidth as illustrated in the PSD shown in Fig. 2-6c. Finally, the right figure (Fig. 2-5b) shows the characteristics of broad-band random vibration. Broad-band vibration contains an infinite number of frequencies, and usually covers a broad frequency band as illustrated in the PSD plot shown in Fig. 2-6b. Broad-band vibration has the most damage potential of the three types of vibration just discussed, since it simultaneously excites all frequencies in multiple degrees-of-freedom systems such as the equipment used in this study.

Test Envelopes

Test specifications describe the processes used to control and run the various equipment laboratory vibration tests. These specifications are written before the equipment is built, consequently, the vibration test envelopes are general in nature and are often devoid of spectral detail. The envelopes are produced by overlaying numerous PSD plots on the same graph. Next, a series of straight line segments are draw above the acceleration peaks to "envelope" all the data. Finally, to ensure the equipment does not fail its intended vibration tests, the envelopes are raised in magnitude to cover, as yet, unmeasured vibration events or unanticipated extremes (Morrow 1988, p. 20-14).

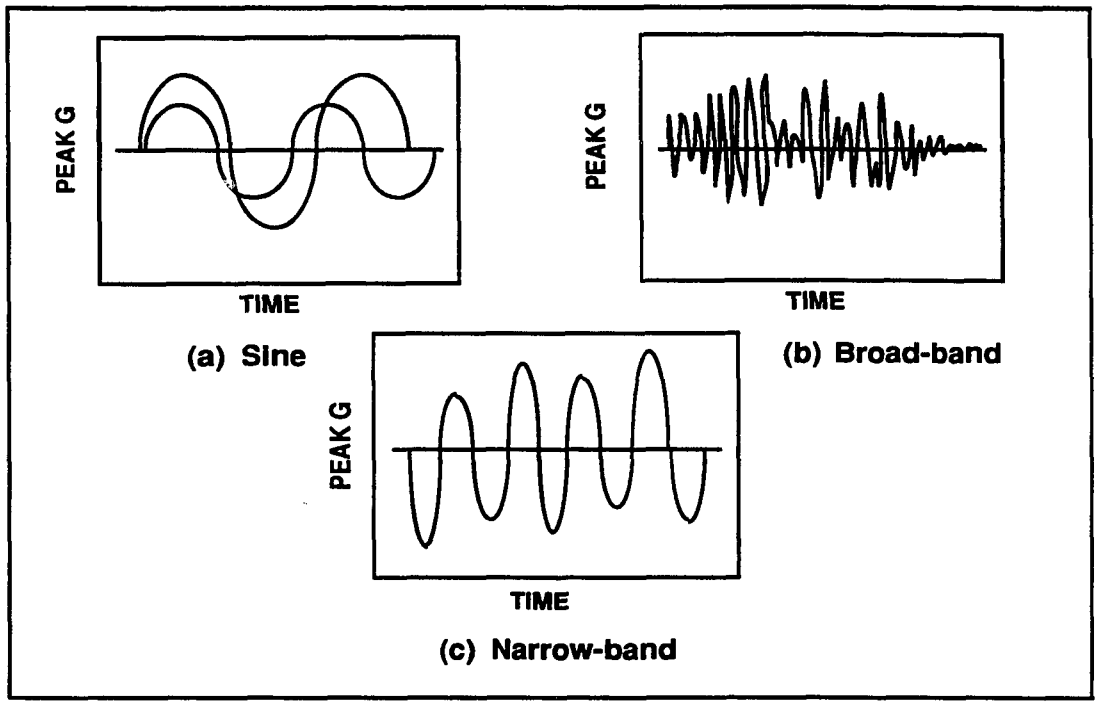

Figure 2-5 Comparison Between Different Acceleration Time Histories (Curtis 1988, p. 22-2)

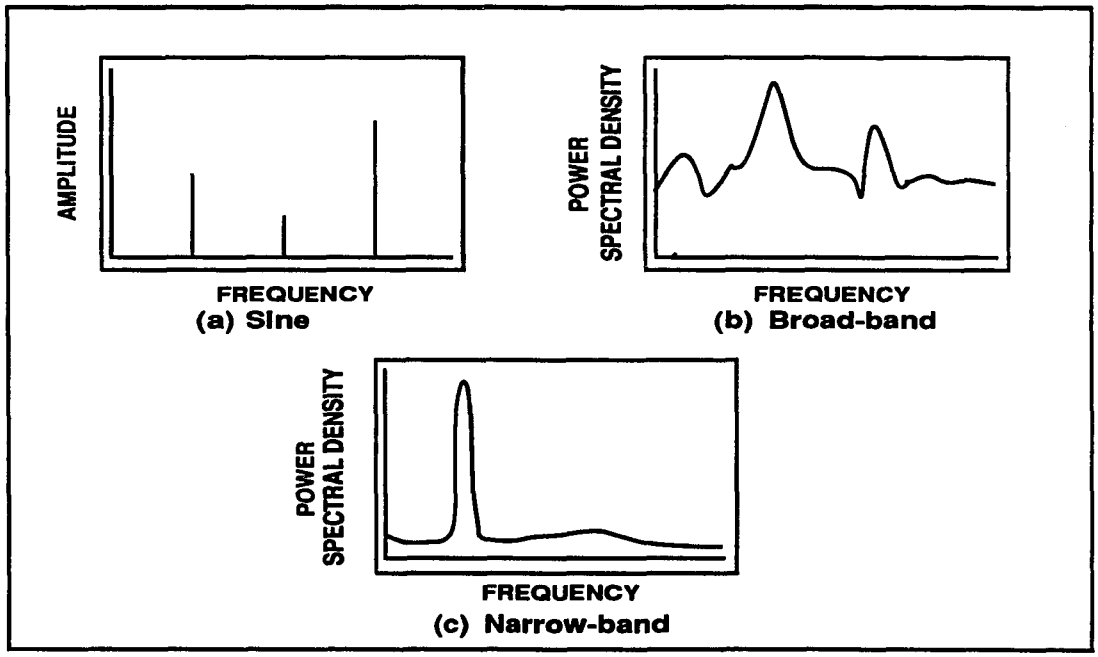

Figure 2-6 Comparison Between Different Power Spectral Densities (Curtis 1988, p. 22-2)

Design and development engineers overlay the acceleration peaks from numerous PSD plots derived from field measurements to develop a vibration envelope, like the one shown in Fig. 2-7. The problem with this process in a laboratory vibration test, is that the envelope omits the equipment's interactions with its platform, and any structural limitations that the platform might have had if it were to sustain that vibration level by the equipment. (Fackler 1972, p. 113).

In the next chapter, we describe the methodology used to correct this omission, through the use of "equipment mission profiles". A mission profile describes the different vibration events the equipment is expected to encounter in its field environment, and paves the way to derive more realistic vibration envelopes and test times for the laboratory tests. The next chapter defines two equipment mission profiles. The first is an estimate of the types of maneuvers and the environmental conditions that might occur in a training mission, and it is referred to as an estimated mission profile. The second is derived from an actual training mission, and it is referred to as an actual mission profile.

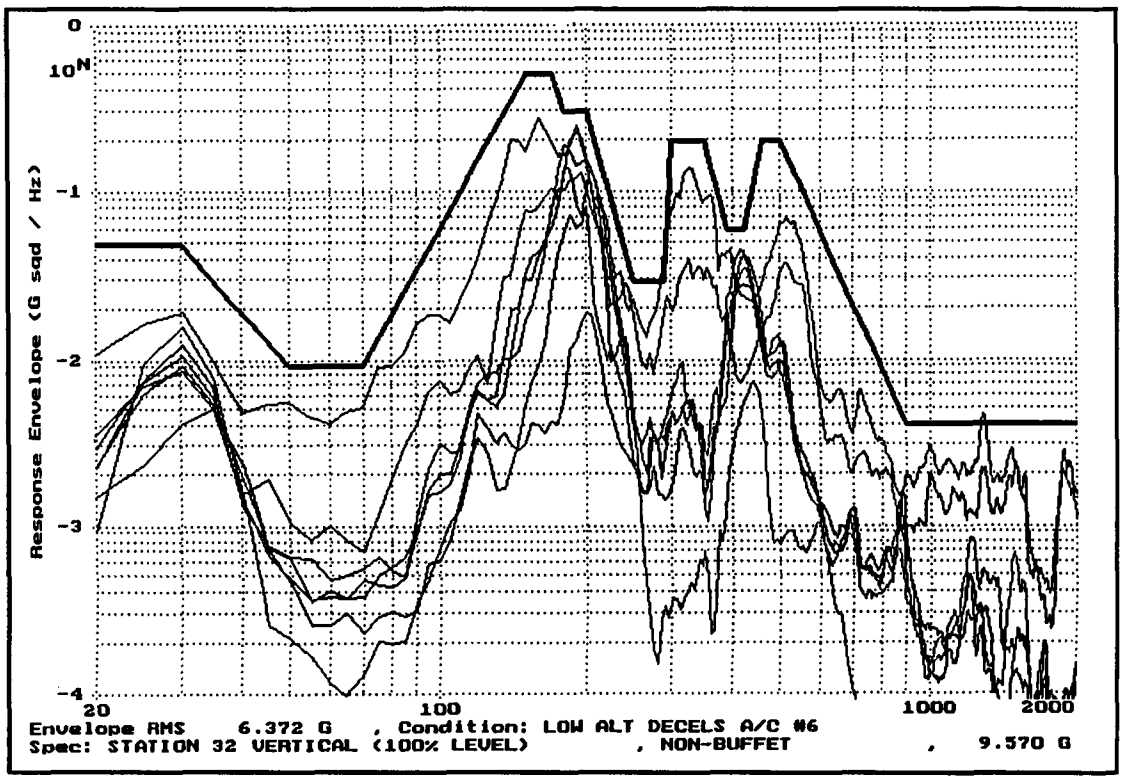

Figure 2-7 Typical Vibration Envelope

CHAPTER 3

EQUIPMENT MISSION PROFILES

The equipment's mission profile describes the various environmental conditions that the equipment will see during typical use, and usually resembles that of its platform. The equipment is mounted to its platform during its mission phase, consequently, it experiences the very same environments as its platform. During the mission phase, the platform subjects the equipment to a very severe vibration environment. This vibration environment is both random in occurrence and in magnitude; therefore, it is entirely non-deterministic and must be dealt with measurements taken during actual aircraft flight in conjunction with using a probabilistic methodology.

Description

A military platform carries the equipment used in this study on three different kinds of missions: these are the training, the alert, and the combat missions. Both the alert and combat missions may be characterized as either being very long and benign, or being very short and intense. Both of these missions rarely consist of more than one air-to-air engagement, and are usually flown with "live" missiles.

Live missiles contain warheads, and their electronic systems must be fully capable of guiding them to their respective targets with a high degree of reliability. Constant exposure to vibration eventually results in fatigue failures within the electronic subsystems. These failures could prevent the missiles from being launched or even guide properly to their respective targets.

Training missions usually consist of three to four air-to-air engagements and are usually flown without live missiles. Each engagement may contain as many as ten maneuvers. The vibration levels generated by the platform or by the aerodynamic turbulence during these maneuvers are very severe.

The worst possible combination, from the stand point of assessing and predicting vibration damage, is to use the alert aircraft with live missiles for training missions. Using these aircraft for training missions is not a problem in itself. The problem is that the ground crews rotate a small set of missiles among the few alert aircraft, which constantly exposes these missiles to a very severe vibration environment. This results in a small group of missiles accumulating a substantial amount of fatigue damage in a period of time which is short in comparison with that which results from alert and combat missions.

Because of the above complications, it is necessary to make some special assumptions for training missions in order to simplify the vibration and the structural analyses. First, the equipment's lifetime is limited to 450 hours. Second, the composition of the training mission or "profile" (Table 3-1) remains the same from one training mission to the next. Third, the equipment remains at the same location on the platform throughout its 450 hour lifetime. Finally, the equipment must not experience a structural failure within this time period.

Estimated Mission Profile

The equipment's mission profile defines the environmental conditions that exist during its field use. It guides the field test program in measuring the equipment's responses to its vibration environment. Since the platform carries the equipment, the equipment will experience the same flight conditions as its platform, and subsequently the same vibration environments.

The equipment's mission profile is adapted from the platform's mission profile. The different segments within the estimated mission profile are shown in Table 3-1. Altitude is plotted as a function of time in the plot shown in Fig. 3-1. A major deficiency with this type of plot is that the air combat maneuver (ACM) segment in the estimated mission profile is undefined. The estimated mission profile (Table 3-1) contains no description of the events, number of events, or even the flight conditions of the maneuvers that occur within the ACM segment.

Air Combat Maneuver (ACM) Segment

The air combat maneuver (ACM) segment contains a multitude of events that may produce very severe vibration levels. These events may consume a significant portion of the equipment's fatigue life. It is important then to define the events within the ACM segment in order to assess the amount of fatigue damage.

The ACM segment contains all those maneuvers that a pilot uses to obtain a tactical advantage over an adversary. This segment contains high G turns, decelerations, dives, climbs, and other types of maneuvers. The pilot usually initiates high G turns and decelerations with rapid throttle movements. Subsequently, these maneuvers produce severe vibration levels that greatly exceed those levels from steady state flight, or from slow throttle movements.

During the equipment's design and development phase, the equipment's procuring agency conducted numerous meetings with the platform user, the platform manufacturer, the platform engine manufacturer, and the equipment manufacturer. These meetings provided the forum to define the types of maneuvers, the number of maneuvers, and also the different maneuver environments. Subsequently, these forums enabled the equipment's procuring agency to estimate the content of the platform's ACM segment.

Some of the typical contributions based upon information provided from the various different sources are summarized in Table 3-2. The equipment's procuring agency in this case has concluded that a total of fifteen maneuvers were preceded with rapid throttle movements or "throttle chops". These maneuvers consisted of ten high G turns of 5 seconds duration each, and five decelerations of 10 seconds duration each. In addition, ten percent of the total maneuver time was estimated as being spent at low altitude.

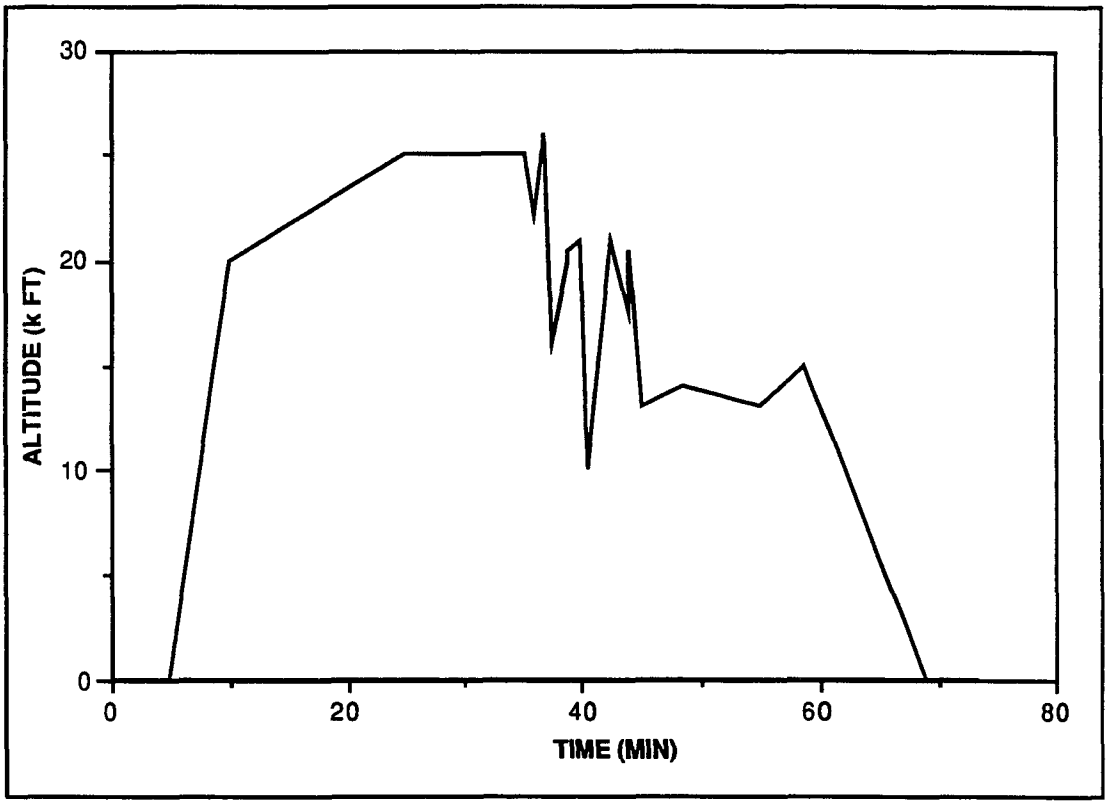

Figure 3-1 Estimated Mission Profile (Gallagher 1987, p. 50)

Table 3-1 Estimated Mission Profile Summary (Gallagher 1987, p. 51)

MISSION SEGMENT	DURATION (min)	ALTITUDE (kft)
1 Taxi	1 to 5	0
2 Takeoff	0.1	0 to 2
3 Climb	5	2 to 20
4 Cruise	10 to 20	20 to 25
5 Loiter/Vector	10 to 30	25
6 ACM	5 to 10	10 to 25
7 Return to Base	10 to 20	15
8 Descend	7 to 8	15 to 2
9 Land	0.1	2 to 0
10 Taxi	1 to 5	0

Table 3-2 Contributions by Different Sources Used to Define the Estimated ACM segment

EVENT	CONTRIBUTION	SOURCE
MISSION DURATION	78 minutes	Equipment manufacturer
ACM SEGMENT DURATION	12.7 minutes	Sidewinder Fatigue Load Spectrum
NUMBER OF THROTTLE CHOPS	15	F-15 System Project Office
MANEUVER DURATION	5 to 10 seconds	Instrument Measurement Vehicle Vibration Data Base

Aircraft buffet normally accounts for 42 seconds of the 12.7 minutes in the ACM segment. Buffet is a unique oscillatory condition that is due to unsteady separation of the turbulent boundary layer from the platform's wings and tail surfaces at high angles-of-attack. Aircraft buffet primarily occurs at high altitudes (18,000 to 30,000 ft), with high Mach numbers (0.7 to 1.0), in high G turns (5 to 9 Gs), and at high angles-of-attack (8 to 20 degrees). Aircraft buffet is not specifically analyzed nor is it used in this study, except as to complete the definition of the equipment's mission profile.

The remaining time in the air combat maneuver segment is allocated to sustained maneuvers. Sustained maneuvers are those that occur at both high and low altitudes, at low Gs (1 to 3 Gs), and at low angles-of-attack (2 to 5 deg). These are usually turns and they are not typically preceded by rapid throttle movements. Once again, for the estimated ACM segment as defined in Table 3-3, 10% of the total sustained maneuver time was estimated as being spent at low altitudes.

Table 3-3 Summary of Events Within an Estimated ACM Segment (Johnson, Stuart, and Topham 1989)

EVENT	NUMBER	TOTAL EXPOSURE PER	
		MISSION (sec)	LIFETIME (hrs)
* Windup Turns	(5 sec each)		
HI	9	45.0	4.3
LO	1	5.0	0.5
* Decelerations	(10 sec each)		
HI	4.5	45.0	4.3
LO	0.5	5.0	0.5
* Sustained Maneuver			
HI	N/A	660.0	63.5
LO	N/A	66.0	6.5
Buffet	N/A	42.0	4.0
* Note: 10% of time spent at low altitude			

Actual Mission Profile

As is the usual case, the platform manufacturer's data base on platform usage was not available in time to influence the results of the estimated mission profile. The platform's manufacturer currently uses this type of data to monitor the cumulation of fatigue damage in certain critical platform structures. The particular data base used in the present study had not been edited by the platform's manufacturer for use in his fatigue monitoring program; therefore, the equipment's procuring agency requested these computer tapes for possible mission analysis (McDonnell Douglas1989).

These computer tapes contained a total of 350 hours of unedited platform mission data. There are approximately 250 different missions in this data base, representing a comprehensive cross section of the different missions in which the platform is currently used. The present study restricted its analysis to those training missions where live missiles were carried by the platform. This quickly enabled a tractable problem to be presented for the present study, by reducing the number of missions available for analysis from 250 to 13.

The 13 training missions were analyzed for similarities. Perhaps not surprisingly, the 13 missions were essentially the same. Therefore, one mission was selected at random. This mission is described by the plots contained in Appendix A and is summarized below in Table 3-4. The platform's altitude is plotted as a function of time in Fig. 3-2 for comparison with the estimated mission

profile shown in Fig. 3-1. It is obvious the actual mission profile contains substantially more maneuvers, and it is not as benign as the estimated profile would suggest

Table 3-4 Summary of an Actual Mission

MISSION SEGMENT	DURATION (min)	ALTITUDE (kft)	MACH #	AIR SPEED (Knots)	AOA (deg)	Nz (G)	Nx (G)
1 Taxi	5.0	0	0	0	2	1	0
2 Takeoff	1.0	0 to 2	0 to 0.5	0 to 350	2	1	0.4
3 Climb	3.5	2 to 20	0.5 to 0.75	350	4	1.3	0.3 to 0.2
4 Cruise	14.0	20	0.8	370	2	1	0 to 0.1
5 ACM	21.7	12 to 28	0.4 to 1.0	180 to 520	2 to 20	1 to 7	-0.2 to 0.8
6 Cruise	5.0	18	0.5	230	2	1	0
7 Descend	6.7	18 to 5	0.5	230 to 300	3	1	0
8 Cruise	10.8	5 to 3	0.5	300	2	1	0
9 Pattern	3.0	3 to 1.5	0.5 to 0.2	330 to 130	15	4	-0.1 to 0.6
10 Landing	0.5	1.5 to 0	0.2	130	10	1	0
11 Taxi	5.0	0	0	0	2	1	0

Information gleaned from previous field tests with the equipment being carried on its platform was used to identify the various events within the ACM segment. The ACM segment shown in Appendix A is the result of expanding the time scale within the ACM segment shown in Fig. 3-2. The ACM segment is readily identified by the rapid changes in altitude that occur over short time intervals starting at 18 minutes and lasting through to 40 minutes into the mission. Numerous different parameters were plotted against time to observe their respective changes during different maneuvers. This study overlaid a number of these plots on the same graph, and attempted to identify the various different events within the ACM segment. The results of this effort are summarized in Table 3-5.

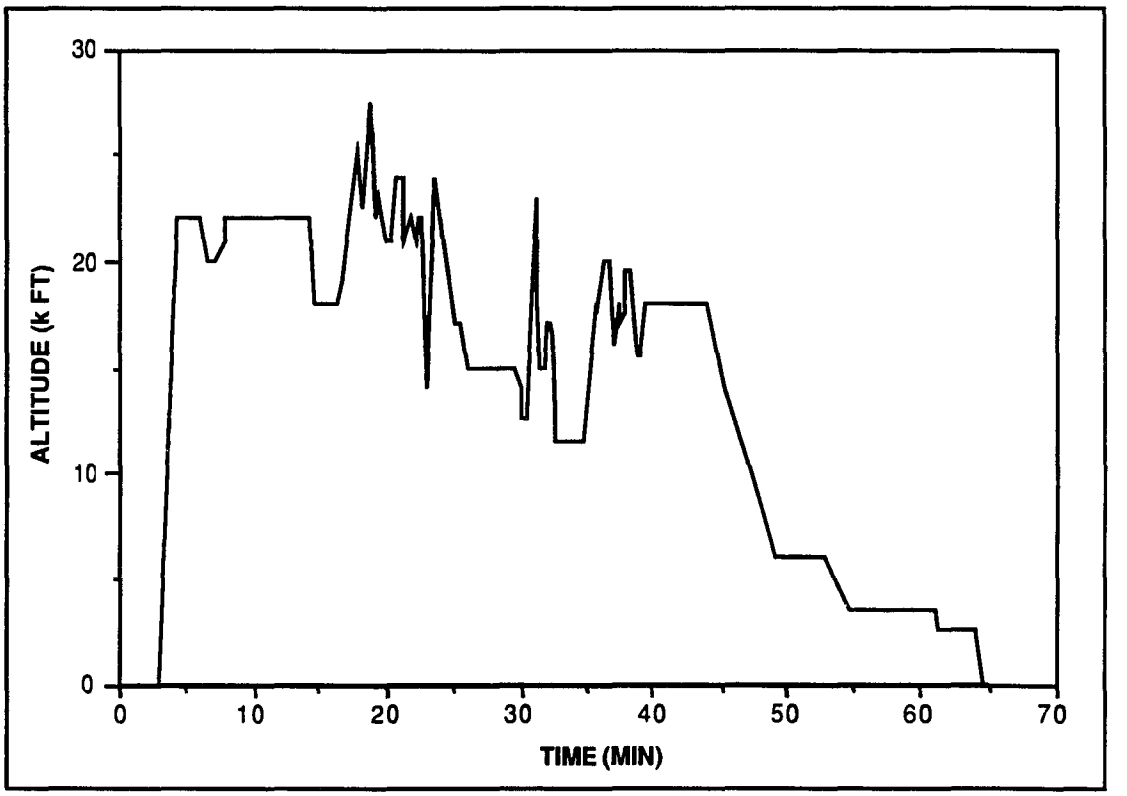

Figure 3-2 Actual Mission Profile (Scheidter 1989)

Table 3-5 Summary of Events Within an Actual ACM Segment

EVENT	NUMBER	TOTAL EXPOSURE PER	
		MISSION (sec)	LIFETIME (hrs)
Windup Turns	(11 sec each)		
HI	23.5	258.5	25.5
LO	2.5	27.5	2.7
Decelerations			
HI	N/A	N/A	N/A
LO	N/A	N/A	N/A
Sustained Maneuver			
HI	N/A	423.0	41.7
LO	N/A	47.0	4.6
Buffet	N/A	22.0	2.2

Mission Profile Analysis

The present study compared Table 3-1 to Table 3-4, and in the process validated the times allocated to each of the various segments in the estimated mission profile. However, there were major differences in the maneuver content between the ACM segment shown in Table 3-3 for the estimated mission profile, and the ACM segment shown in Table 3-5 for the actual mission profile. The ACM segment from the actual mission profile, when compared to the estimated profile, contains:

1. Substantially more maneuvers
2. Longer maneuvers
3. No decelerations
4. Two thirds of the sustained maneuver time
5. Twenty seconds of low altitude maneuvers

This study could not substantiate the assumption that 10% of the platform's maneuver time occurred at low altitude. If the 10% assumption was applied to the actual mission profile, it would increase the low altitude maneuver time by a factor of 2.7 over what was actually observed. Yet, this assumption is the basis for the duration used with the 100% vibration response envelope described in Chapter 4 and shown in Fig. 4-2.

This chapter has attempted to show that the equipment experiences essentially the same mission profiles and environment as its platform. We have also shown that the platform's mission profile guides the field tests used to measure the equipment's response to its field vibration environment. The next chapter uses the estimated mission profile (Table 3-3) to develop the equipment's laboratory vibration envelopes and test times.

CHAPTER 4

LABORATORY VIBRATION LEVELS AND TEST TIMES

Determining laboratory vibration envelopes and test times for a given piece of equipment requires extensive field testing with a specially equipped measurement vehicle. This vehicle is usually an instrumented prototype that contains either dummy sub-systems, or is an instrumented early production version of the equipment. The instrumented measurement vehicle is carried by the platform during field tests. It is equipped with its own instrumentation system, and measures and records its own responses to the platform's maneuvers at different environmental conditions for future data analysis.

Assumptions

In order to establish the necessary information for quantifying vibration envelope, the equipment's manufacturer measures, records, and processes the equipment's vibration responses to its platform's field environment. A multitude of different equipment locations and components were instrumented and their vibration responses measured and recorded for future analysis. For the specific case analyzed in the present study, the data was recorded, processed, and stored by the manufacturer in a computerized vibration data base for data analysis. This data base is the basis for the present study's analysis.

The data base contains over 12,000 processed vibration response levels. It contains vibration responses from different locations on the equipment structure, and from different electronic components within the equipment itself. It is an unclassified data base, and can be obtained with permission from: ASD/YMEA, Eglin AFB, FL 32542. Since, the data base contains a vast amount of vibration data, some assumptions must be used to simply both the vibration analysis and the subsequent structural analysis. First, this study will restrict the vibration analysis to the equipment's vertical (z) axis. Even with this restriction, the problem is still complex and requires further simplification.

There are a number of different vibration envelopes for each of the different stations (locations) on the equipment's vertical axis. Each equipment station has its own unique set of vibration envelopes. The current methodology is to attempt to excite the test item so as to achieve to vibration envelope at a number of different stations. Yet, it is intuitively obvious that the equipment does not simultaneously respond to all vibration envelopes simultaneously. With this in mind, this study will confine its analysis to one station on the equipment's vertical axis.

Laboratory Vibration Levels

This study will arbitrarily select equipment station 32 for its own vibration analysis. Station 32 is a critical joint between the forward guidance section and the rear guidance section. The joint between these two sections maintains an inert gas under pressurization within the rear guidance section. There are a total of six different vibration envelopes that are available for the station 32 vertical, and they are presently used to control the equipment's responses during laboratory tests.

These six envelopes essentially describe two entirely different vibration environments. Three of these envelopes encompass the equipment's response to a unique vibration condition called buffet. Buffet is an extremely transient environment. The nature and severity of buffet suggests that the equipment's manufacturer should have processed the data as a nonstationary random process; however, the data was processed as a stationary process. Due to this fact, this study will not consider buffet vibration in its analysis.

The three remaining envelopes describe the equipment's responses to both transient and steady state events. It could be implied that all events other than the steady state are transient, hence, a nonstationary random processes. In essence this is true. The procedure commonly used in the test community is to look at an event's G_{RMS} time history. A time history like the one shown in Fig. 4-1, is assumed as stationary over a small time sample of about 6 seconds.

The vibration envelope shown in Fig. 4-2 is called the "100% vibration envelope"; its boundaries are such that it captures all the equipment's vibration responses to numerous different events. It describes for all practical purposes

two vibration events (high G turns and decelerations) that occur at low altitude on the forward and rear platform locations. The platform can carry a total of four missiles on its fuselage, and they are carried in tandem on each side, hence, the term "forward and rear platform locations".

The 100% vibration envelope is used in both the equipment's and in its section's laboratory tests. The equipment's manufacturer compared the vibration levels from numerous different events and environmental conditions to one another. They found that as the dynamic pressure decreased (primarily altitude), the shape of the 100% vibration envelope adequately defined other events but at a lower G_{RMS} levels. Therefore, they multiplied the the 100% vibration envelope's G_{RMS} level (Fig. 4-2) by 0.75 and 0.65, respectively. Together, the 100% and 75% envelopes completely define the high dynamic pressure (low altitude) vibration events. The 65% envelope defines those vibration events from: the low G maneuvers at high and low altitudes; high G maneuvers at high altitude; and steady state events at both high and low altitudes.

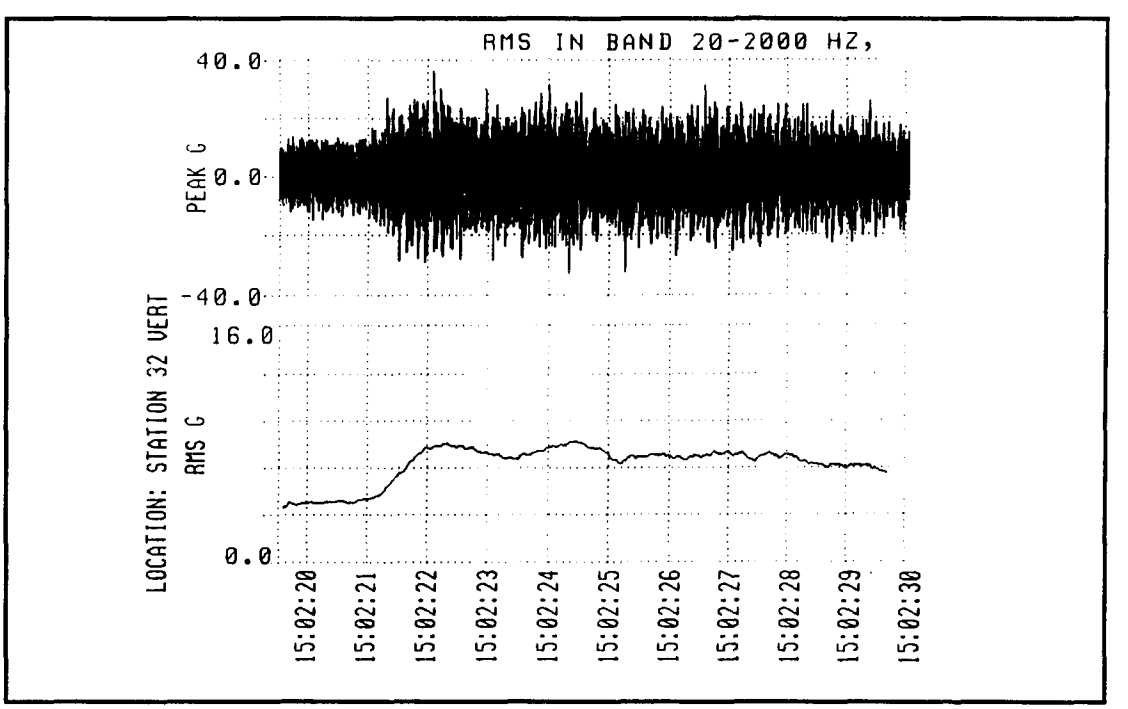

Figure 4-1 Acceleration Time History

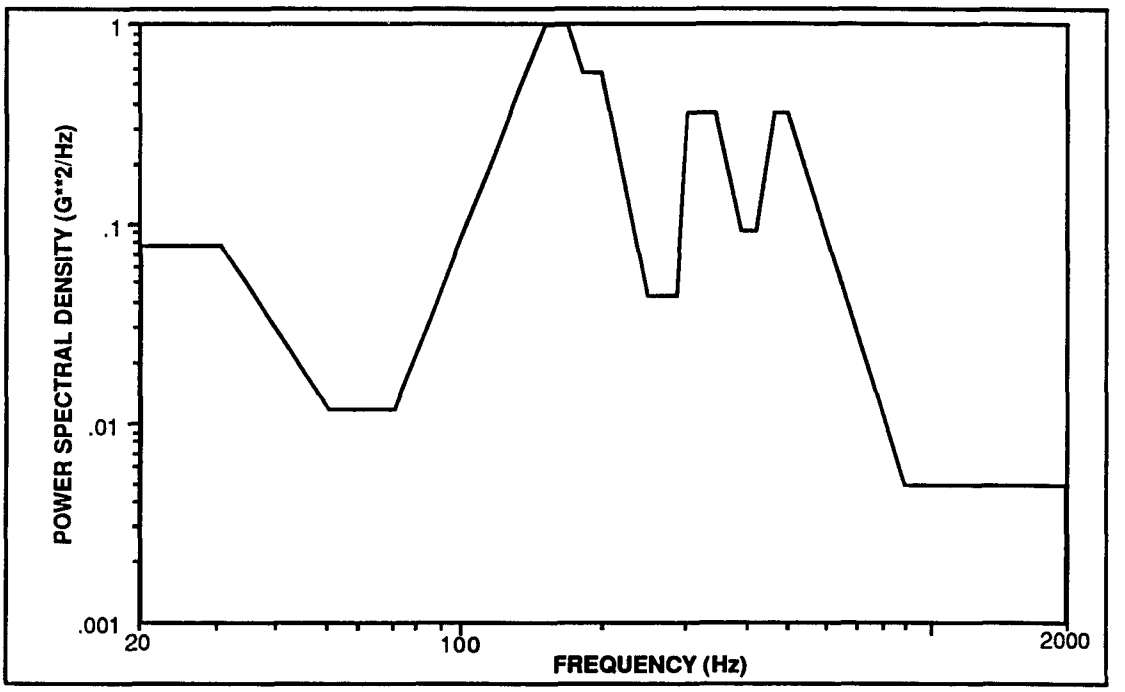

Figure 4-2 100% Laboratory Vibration Test Envelope

For the particular piece of equipment studied in this thesis, the equipment's manufacturer used the vibration data in Fig. 4-3 to build the 100% vibration response envelope shown in Fig. 4-2. Each trace shown in Fig. 4-3 corresponds to an unique response recorded for a specific location on the platform, during a specific event, and for a specific environmental condition. Figure 4-3 shows the wide variation, described by the envelope boundaries, in both frequency bandwidth and in the acceleration power spectral densities at the equipment's resonance frequencies. These variations are due to enveloping together the equipment's vibration responses from different locations on its platform, different vibration events, and from different environmental conditions.

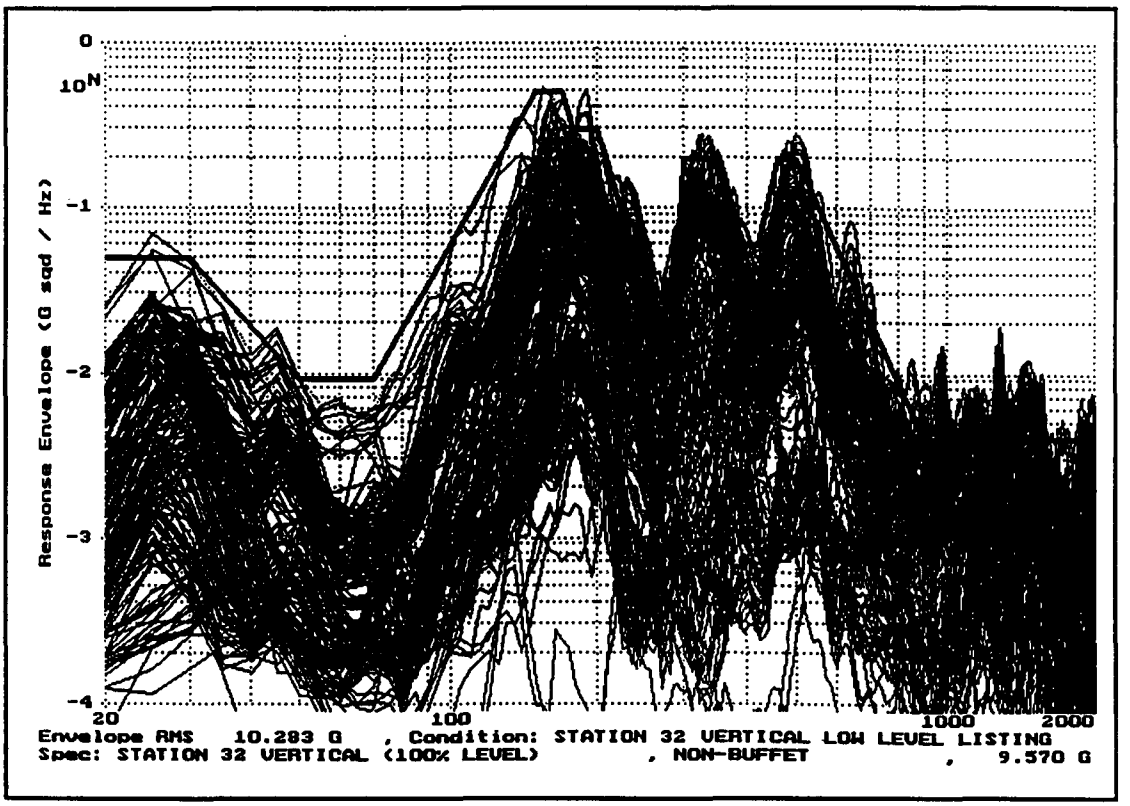

Figure 4-3 Field Vibration Data Envelope

One of the objectives of the present study was to sort all the vibration data contained in Fig. 4-3. First, the data was sorted by each of the equipment's possible locations on its platform. Second, the data was sorted by each of the different type of vibrations events. Finally, the data was sorted by each of the different environmental conditions. The results of this sorting effort are discussed in the following paragraphs and are available in Appendix B.

The vibration analysis reveals that both the low altitude high G turns and decelerations contain similar vibration spectra. The vibration spectra for both events are similar for the same equipment locations on the platform. The data also shows that the 100% vibration response envelope does not capture the high frequency content in either event ($f > 1000$ Hz). However, this is not particularly important since fatigue, the basic focus of the present study, is a low frequency ($f < 300$ Hz) phenomenon.

The equipment's responses to both vibration events were grouped by its location on the platform. The envelope in Fig. 4-4 is for low altitude high G turns and decelerations with the equipment attached to the forward location on the platform. The envelope in Fig. 4-5 is for the same events as those in Fig. 4-4, but this time with the equipment attached to the rear location on the platform. If one was to overlay Fig. 4-4 and Fig. 4-5 together on the same graph and envelope the peaks, it would result in the envelope shown in Fig. 4-2.

The three vibration envelopes shown in Fig. 4-2, Fig. 4-4, and Fig. 4-5 form the basis for this study, which will use them in a simulated equipment test to evaluate how vibration envelopes affect fatigue damage. A simulated section test will also be run using Fig. 4-2. The results from the section test will be compared with those results obtained by using Fig. 4-2 alone in the equipment test, to evaluate how different boundary conditions affect fatigue damage.

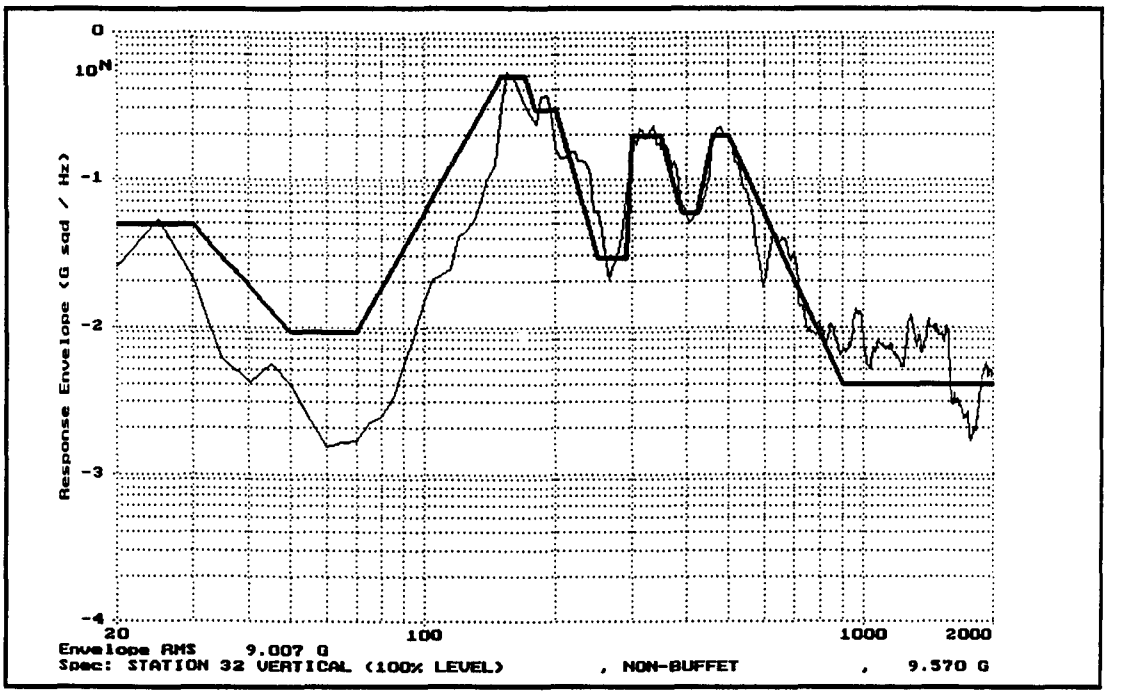

Figure 4-4 Fwd Deceleration and High G Turn Envelope

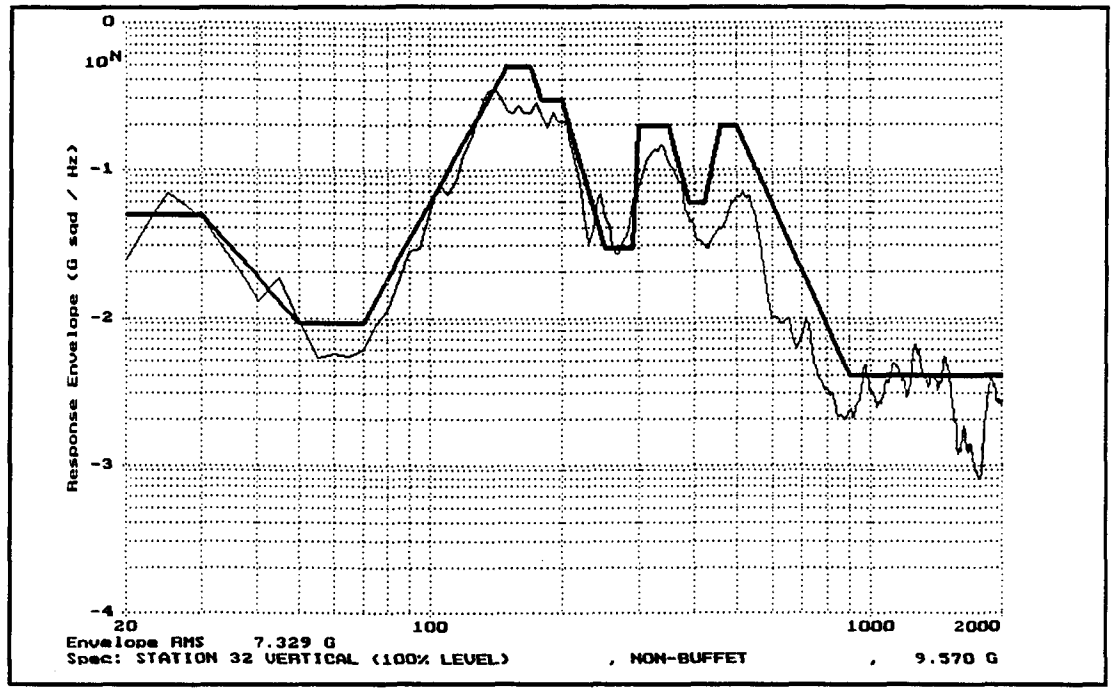

Figure 4-5 Rear Deceleration and High G Turn Envelope

Laboratory Test Durations

Fatigue analysis requires that the laboratory test durations be known in advance in order to calculate the cumulative fatigue damage. The equipment's manufacturer used a statistical analysis of the platform's usage data to derive the test durations for each of the vibration envelopes. The data for the present study was correlated with the estimated mission profile to arrive at the times shown Table 4-1. The envelope shown in Fig. 4-2 essentially accounts for half the total low altitude windup turn/deceleration (WUT/decel) time shown in Table 4-1. The 75% vibration response envelope accounts for the remaining half of the total low altitude WUT/decel time. This amounts to 0.5 hours of testing with Fig. 4-2, and 0.5 hours of testing at 75% of envelope level shown in Fig. 4-2.

The present study study applied the same rationale to the actual mission profile (Tables 3-4 and 3-5) to derive laboratory test durations that corresponded to a 450 hour lifetime. The knowledge gained earlier allowed us to associate spectral shapes with each of the different vibration events. In addition, our knowledge in the platform parameters that changed during these events was crucial in our development of Table 4-2. The 100% vibration response

Table 4-1 Estimated Use During a 450 Hour Lifetime (Johnson, Stuart, and Topham 1989)

MISSION SEGMENT	TIME (min)	PERCENT MISSION	* 450 HRS
Taxi/Takeoff	10.8	13.85	62.34
Cruise	56.6	70.00	315.00
ACM	12.6	16.15	72.68
WUT	0.2	0.26	1.17
Decel	1.5	1.92	8.64
Sustained Maneuvers	10.3	13.21	59.45
Buffet	0.7	0.90	4.04

envelope shown in Fig. 4-2 accounts for half the total low altitude WUT/decel time shown in Table 4-2. The 75% vibration response envelope would account for the remaining half of the total low altitude WUT/decel time. This amounts to 1.35 hours of laboratory vibration with Fig. 4-2, and 1.35 hours of laboratory vibration with 75% of the envelope level shown Fig. 4-2.

Table 4-2 Actual Use During a 450 Hour Lifetime

MISSION SEGMENT	TIME (min)	PERCENT MISSION	* 450 HRS
Taxi	10.0	13.16	59.22
Takeoff	1.5	1.97	8.87
Cruise	51.7	68.03	306.12
ACM	13.0	17.11	77.00
WUT/Decel	4.8	6.32	28.44
Decel	0.0	0.00	0.00
Sustained Maneuvers	7.8	10.26	46.17
Buffet	0.4	0.53	2.39

Vibration Analysis

The actual mission profile (Fig. 3-2) discussed in Chapter 3 shows that very little time is spent at the low altitude WUT/decel conditions. The specific numerical assumption that the platform spends 10% of its total ACM time at low altitude is just that, an assumption. The vibration spectra that makes up the envelope in Fig. 4-2 is a compilation of vibration spectra from different equipment locations on the platform, different vibration events, and different environmental conditions. It is also apparent from vibration data contained in Appendix B, that there is a wide variation of vibration responses even among those events that produce the most severe vibration levels.

This wide variation in vibration responses indicates a lack of knowledge about the equipment's most severe vibration environment. It is a significant weakness in the current method of applying the estimated mission profile to determine test envelopes and test times. Our analysis, thus far, shows that the estimated mission profile does not adequately define the events at the most severe vibration conditions. This implies that the equipment may be excited at its resonant frequencies for an unrealistic length of time, thereby, producing extremely high internal forces, moments, and stresses within the its structure. Consequently, the results from either the equipment or the section test could easily be misinterpreted: this conclusion is one of the major results of the present study.

CHAPTER 5

STRUCTURAL MODELS

The equipment's dynamic response to a vibration environment is either measured directly or it can be modeled analytically. The size of the equipment, the amount of available space, and environmental conditions usually dictate the choice of instrumentation for a measurement approach. The chief reasons for the accelerometers widespread use are its small sizes, ease of installation, and the availability of high speed digital data acquisition techniques. Consequently, the equipment's vibration response to a dynamic environment is easily and readily measured.

A basic drawback to a measurement approach is that instrumentation used to measure the equipment's internal loads is often bulky. This instrumentation must be installed on the equipment and the whole system calibrated together. Calibrating an instrumented loads vehicle is an extremely difficult and time consuming task, because any number of external load combinations can produce the same internal loads.

Strain gauges and load cells are generally used to measure static loads, however, they are not very effective for measuring dynamic loads. On the other hand, accelerometers are ideally suited to measure dynamic responses. Yet, accelerometers have their own set of limitations, and cannot be used to measure internal loads. In the case where accelerometers are the only source of information, the internal loads can be deduced analytically through the use of finite element computer models, coupled with accelerometer measurements.

Engineers conduct vibration tests on the basis of attempting to match shaker table results with the equipment's field vibration response envelopes. Often the equipment is tested on the shaker table in sections with support conditions that are entirely different from those used in the field environment. These compromises are often made to accommodate using available test facilities; this procedure may expose the equipment to very severe laboratory

vibration test levels. In order to understand what these compromises mean with respect to fatigue damage from laboratory tests, the present study has used finite element methods to model the equipment's response to different vibration levels and different support conditions.

Finite Element Models

For the particular piece of equipment chosen as the focus of this study, the equipment's manufacturer has developed a finite element model which is used in the present study. The model was written for modal and static structural analyses for the equipment in an unsupported state (Hughes Aircraft Company 1986, pp. A1 - A6). In the following paragraphs we will describe the application of this model used to calculate the structural loads due to different vibration levels and to different support conditions. The finite element model was run on a VAX computer using a commercial version of MacNeal-Schwendler Corporation's (MSC's) NASTRAN structural analysis program.

We have used the equipment's finite element model as the foundation to build two distinct models. The first model simulates the assembled equipment mounted to its platform or to a shaker table; the second simulates the conditions that exist when the equipment's forward section is mounted directly to a shaker table. Together, these models were used to determine the equipment's natural frequencies, mode shapes, transmissibilities, and structural loads in response to various vibration inputs.

The same procedures were used in both models in order to determine the structural loads due to different vibration levels and to different support conditions. An analytical modal analysis was conducted on each model in both its unsupported and supported states. These frequencies and their associated mode shapes were compared to those from the modal test data. The models were subsequently adjusted to match the first two frequencies and the mode shapes from the modal tests.

The effort to iteratively adjust the finite element models to predict the first couple of frequencies and their modes completed, the next task was to determine the transmissibilities. A 1 G^2/Hz acceleration was applied at the base of each model's support structure to obtain the transmissibilities. Each model's

response to the 1 G^2/Hz excitation produced its own unique transmissibility. These transmissibilities were in turn used to determine the vibration inputs required to produce the desired response at a particular control point on the equipment. Finally, both models were excited by these new inputs, and the internal structural loads tabulated for subsequent use in the fatigue analysis.

Equipment Finite Element Models

Finite element analysis is treated in several excellent textbooks (See for example, Finite Element Analysis Fundamentals by Gallagher 1975), and the reader is referred to these works for specific details. The discussion that follows applies to unique aspects regarding the equipment's finite element analysis. The equipment's response to different vibration spectra and support conditions were determined with a low frequency finite element model. Usually, the skin and the component frequencies of the equipment are high relative to the structural frequencies. Consequently, these frequencies are not easily excited, therefore, the equipment's manufacturer ignored them in the process of building the equipment's finite element model.

The equipment's finite element model is composed of the following parameters which are abbreviated in the input file as concentrated masses "CONM2", rigid elements "RBE2", beam elements "CBAR", and springs "CELAS2". The material and physical properties required for each of the parameter introduced above, is entered as a "record" or on a "card" in building the equipment's finite element model.

The finite element models may contain as many cards as necessary to define the structural and dynamic properties. The masses (element nodes) and springs represent the equipment's internal components and were lumped together to form a linear array. The beam elements represent the equipment's skin and various structural members. The beam elements are used to connect the linear array of masses together to form the model's structure.

The original equipment finite element model did not contain any form of attachment to the platform or even its support structure. Therefore, the support structure and the attachments with the equipment were simulated in the finite element model with rigid "RBE2" elements. The support structure consists of grid

points 126, 129, 132, and 133, respectively. The RBE2 elements connect grid points 126, 129, and 132 to base of the structure at grid point 133.

The RBE2 elements were also used to connect grid points 10, 16, and 22 on the model's centerline to its attachments at grids points 124, 127, and 130, respectively. The connections and the stiffnesses between the model's attachments and its support structure are incorporated in the CELAS2 cards. These cards connected grid points 124, 125, 127, 128, 130, and 131 which are on the surface of the equipment model to grid points 126, 129 and 132 on the support structure. Grid point 133 was used to excite the equipment model during each of the numerous computer runs. The equipment model and its support structure are show graphically in Fig. 5-1. The equipment model's input file and control deck for the 100% vibration response at station 32 vertical used in the NASTRAN analysis is listed in Appendix C.

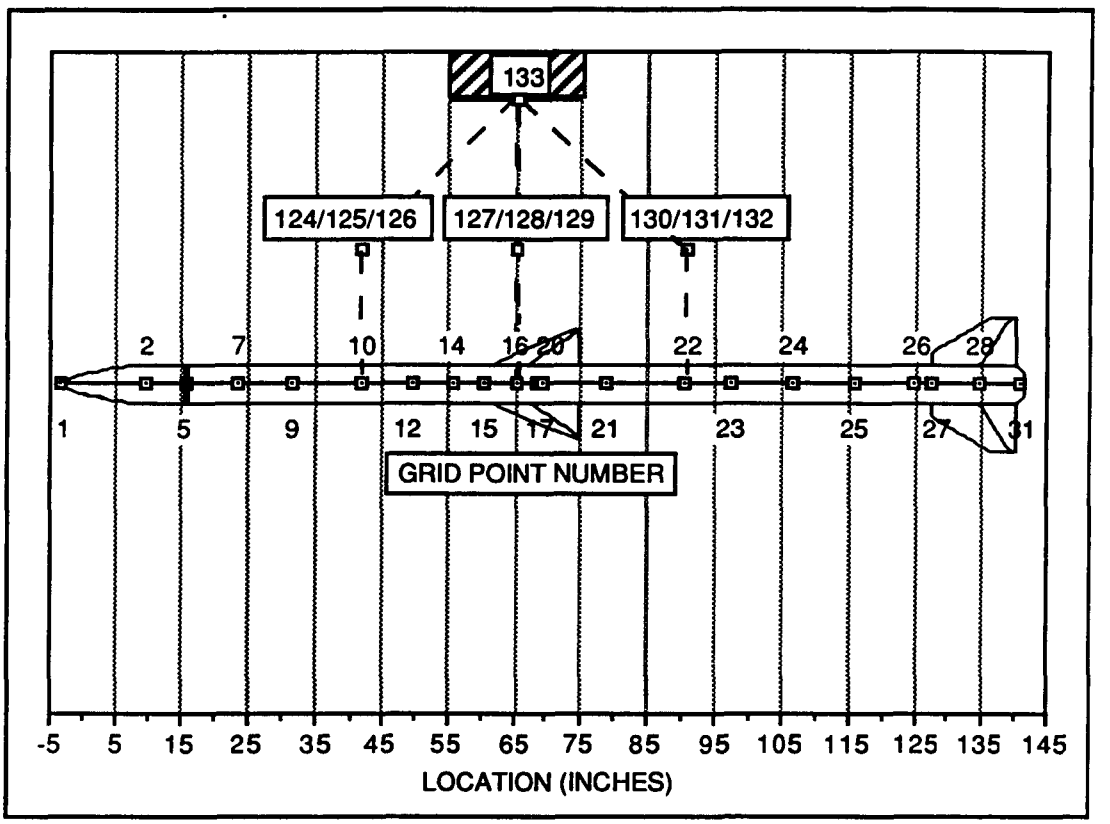

Figure 5-1 Equipment Finite Element Model

The section model and its support structure are shown in Fig. 5-2. This is a model of the equipment's forward section from grid point 1 through 14. The support structure consists of two large yokes that attach the section directly to the shaker table. These yokes attach to the equipment's guidance section at grid points 9 and 14 respectively. The guidance section's support structure consists of grid points 22, 23, and 24, which are connected together with RBE2 cards. The stiffnesses between the section and its support structure are incorporated in the CELAS2 cards. These cards connect grid points 20 and 21 on the section model to grid points 22 and 23 on its support structure. Both the $1G^2/Hz$ white noise input and the other vibration inputs were applied to grid point 24 to produce the model's transmissibility and the 100% vibration response envelope (Fig. 4-2) at grid point 9.

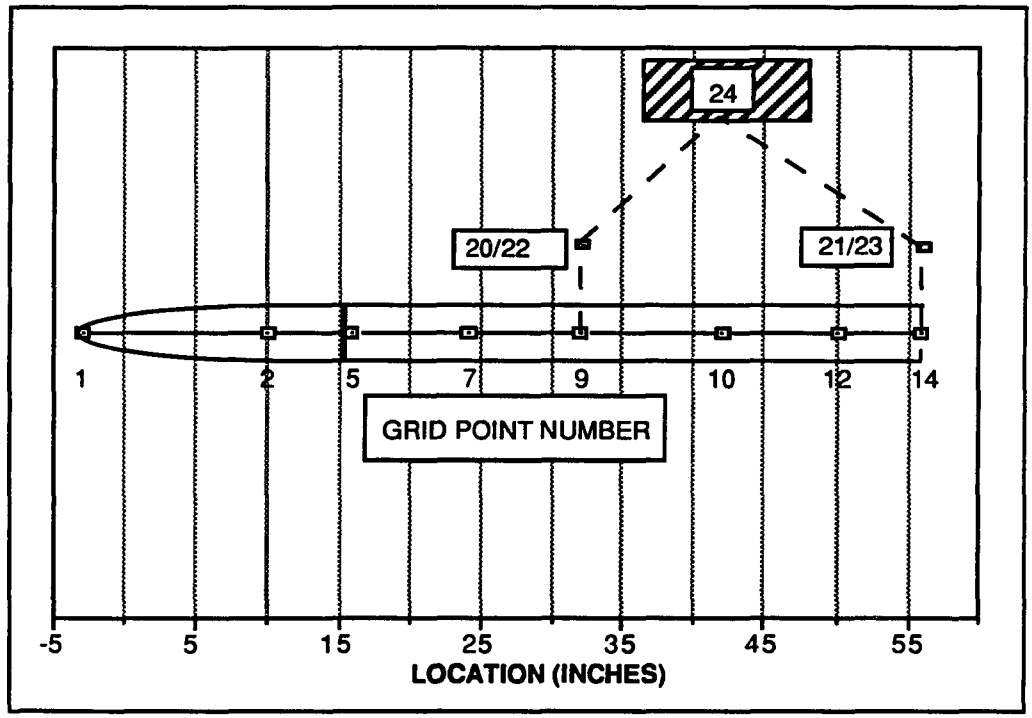

Figure 5-2 Equipment Section Finite Element Model

Structural Analysis

The structural analysis began with a modal analysis on both models. This analysis was run on both the equipment model and on the section model in their respective unsupported and supported states. The results are summarized in Table 5-1, and are shown in Fig. 5-3A, Fig. 5-3B, Fig. 5-4A and Fig. 5-4B. These figures show that there are considerable differences between the two models in their respective unsupported and supported states.

The results from the modal analysis were compared to actual modal analysis test data. This comparison was necessary to validate the analytical results and to ensure that the models were dynamically correct. Unfortunately, modal data was only available for the equipment model. Modal data was not available for the section in either its unsupported or its supported states. Therefore, the modes and frequencies for the section model were estimated, since, there was no way to validate the model without any modal data.

Table 5-1 Equipment Resonant Frequencies

DESCRIPTION	NATURAL FREQUENCY		MODE SHAPES
	PREDICTED (Hz)	MEASURED (Hz)	(FIG)
UNSUPPORTED EQUIPMENT			5-3A
FIRST BENDING	38.3	39	
SECOND BENDING	90.5	95	
THIRD BENDING	137.3	138	
SUPPORTED EQUIPMENT			5-3B
FIRST BENDING	32.4	29.4	
SECOND BENDING	36.6	39.1	
THIRD BENDING	130	102	
UNSUPPORTED EQUIPMENT SECTION			5-4A
FIRST BENDING	131	N/A	
SECOND BENDING	193.4	N/A	
THIRD BENDING	206.9	N/A	
SUPPORTED EQUIPMENT SECTION			5-4B
FIRST BENDING	88.4	N/A	
SECOND BENDING	154.1	N/A	
THIRD BENDING	198.8	N/A	

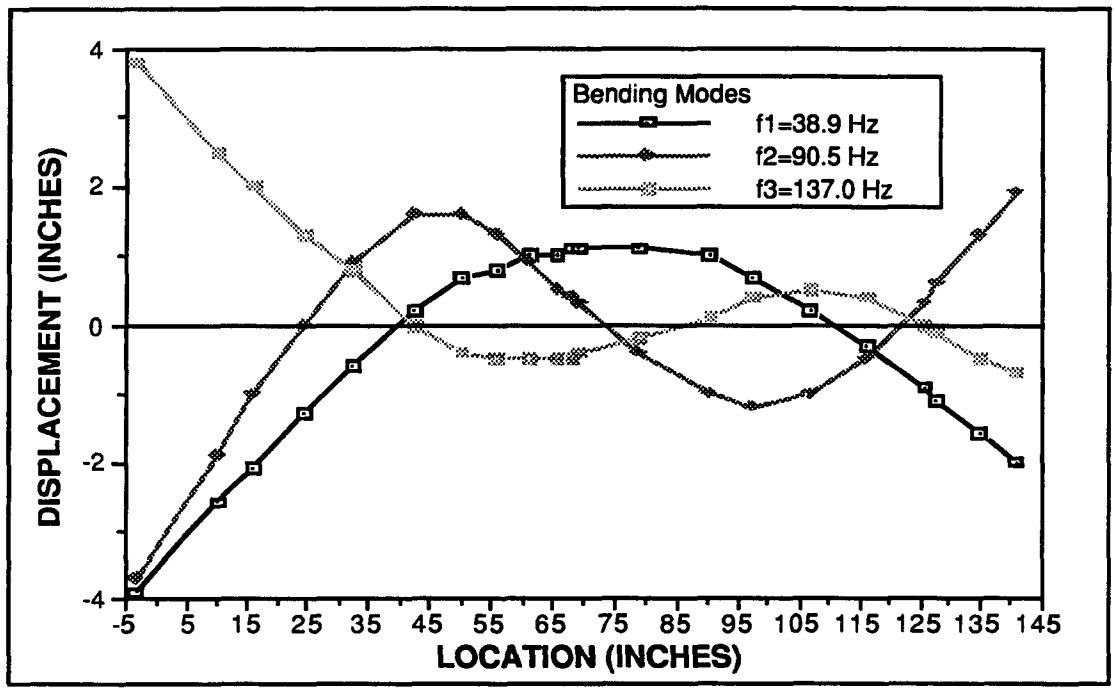

Figure 5-3A Unsupported Equipment Mode Shapes

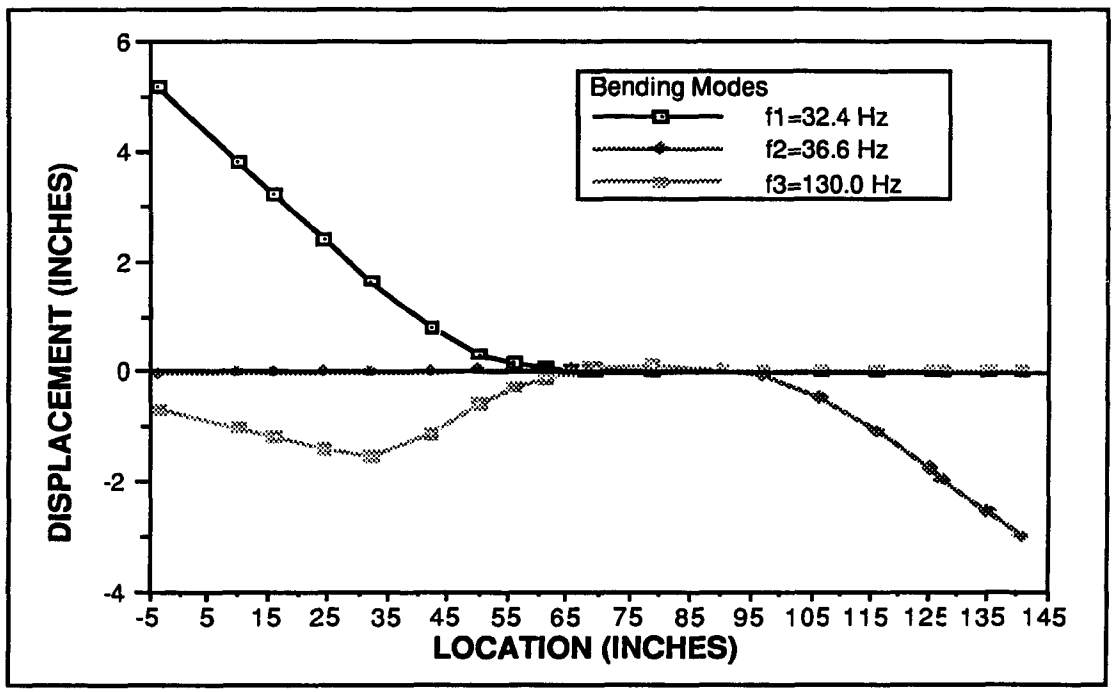

Figure 5-3B Supported Equipment Mode Shapes

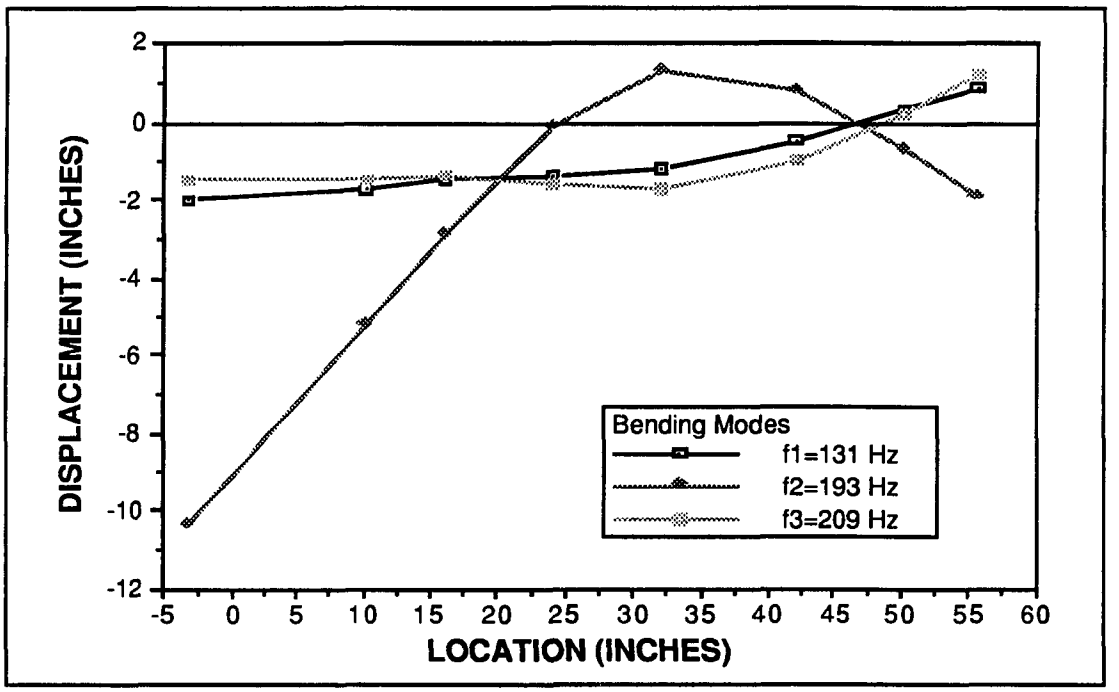

Figure 5-4A Unsupported Section Mode Shapes

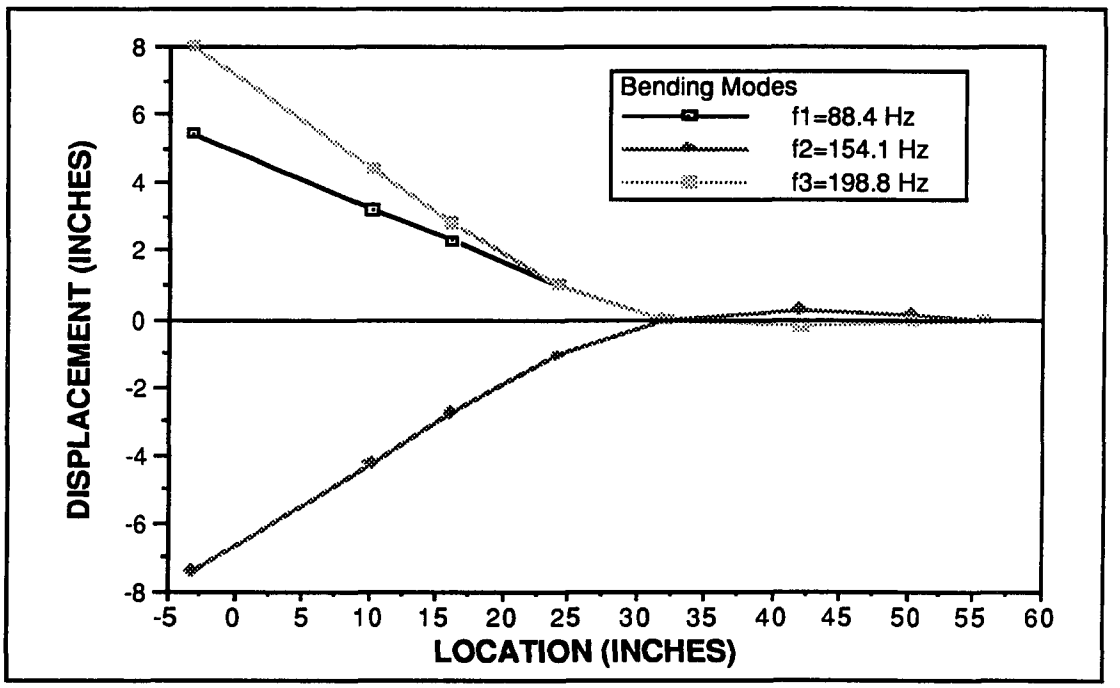

Figure 5-4B Supported Section Mode Shapes

The data contained in Table 5-1 shows that the analytical unsupported equipment model's modes and frequencies closely approximate those from the modal tests. The analytical modal analysis also shows the supported equipment model closely simulates the dynamic characteristics of the equipment when attached to its support structure. However, the lack of any modal data for the section model is a potential liability that leaves the finite element results in an unsubstantiated state.

Upon completion of the modal analysis, the next step was to determine the unique transmissibilities associated with both supported models. A 1 G^2/Hz white noise base excitation was applied to both models over a frequency range of 20 to 500 Hz. The transmissibilities from both NASTRAN models were produced as a function of frequency. These were used in turn to determine the vibration inputs necessary to produce each of the desired responses at the same control point on both models. The results of this analysis are shown in Fig. 5-5 and in Fig. 5-6 for the supported equipment model and the supported section model, respectively.

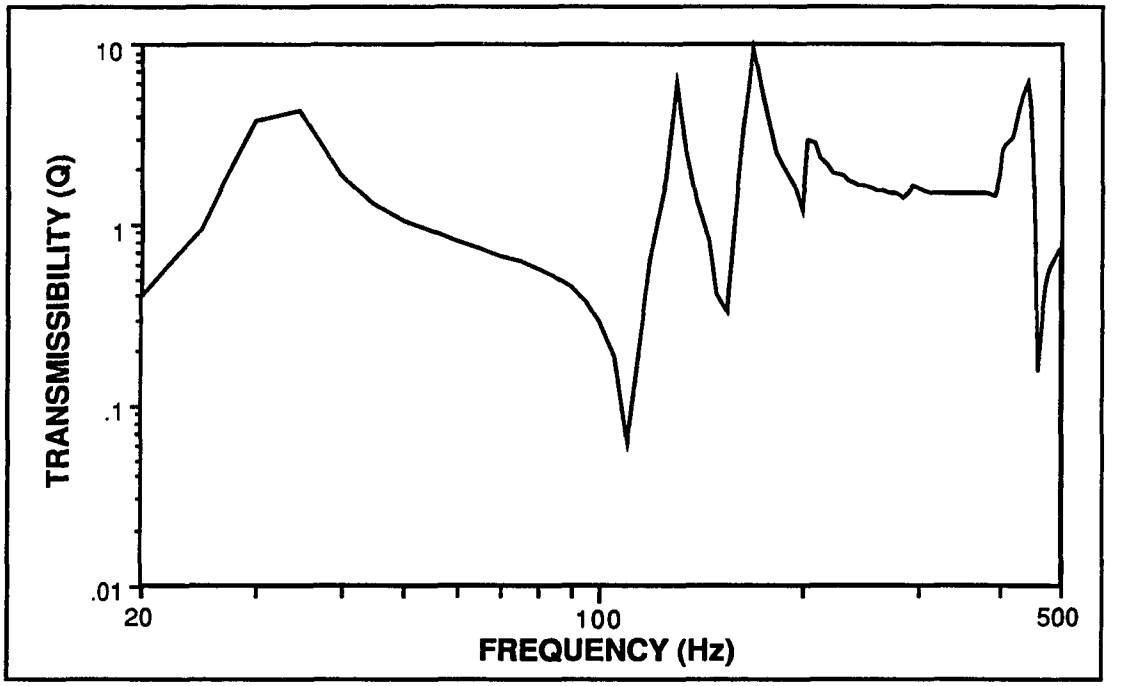

Figure 5-5 Transmissibility Curve for the Supported Equipment Model

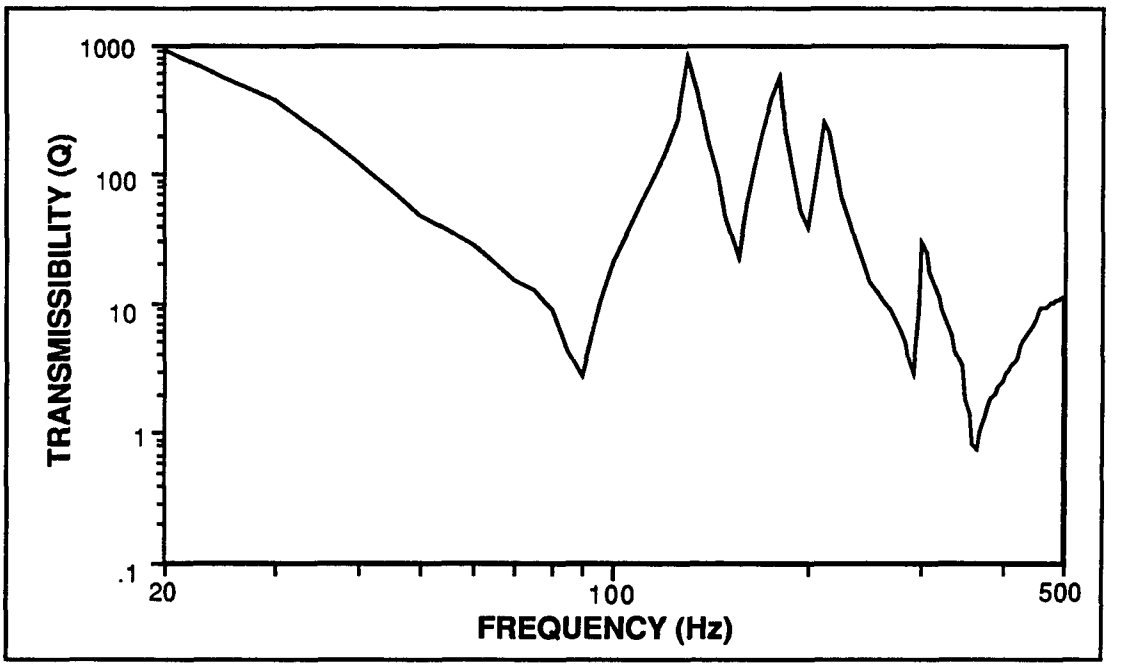

Figure 5-6 Transmissibility Curve for the Supported Section Model

The results contained in Fig. 5-5 and Fig. 5-6 are the transmissibility curves for the supported equipment model and the supported section model. These were used to determine the vibration input levels required to excite both models to match the vibration responses shown earlier in Fig. 4-2, Fig. 4-4, and Fig. 4-5. The formula for the vibration output is defined by

$$P_{out} = Q^2 * P_{in}$$

where P_{out} = Power Spectral Density (G^2/Hz) out

P_{in} = Power Spectral Density (G^2/Hz) in

Q^2 = Transmissibility (unitless)

The vibration input is then defined as

$$P_{in} = \frac{P_{out}}{Q^2}$$

This equation was used to derive the vibration inputs like the one shown in Fig. 5-7 for the 100% vibration response envelope (Fig. 5-8). This process was repeated for each of the three remaining vibration envelopes developed in the present study. The response envelopes, the transmissibilities, and the vibration inputs used in this study to generate the results shown in Table 5-2 are all contained in Appendix D for both the supported equipment model and the supported section model.

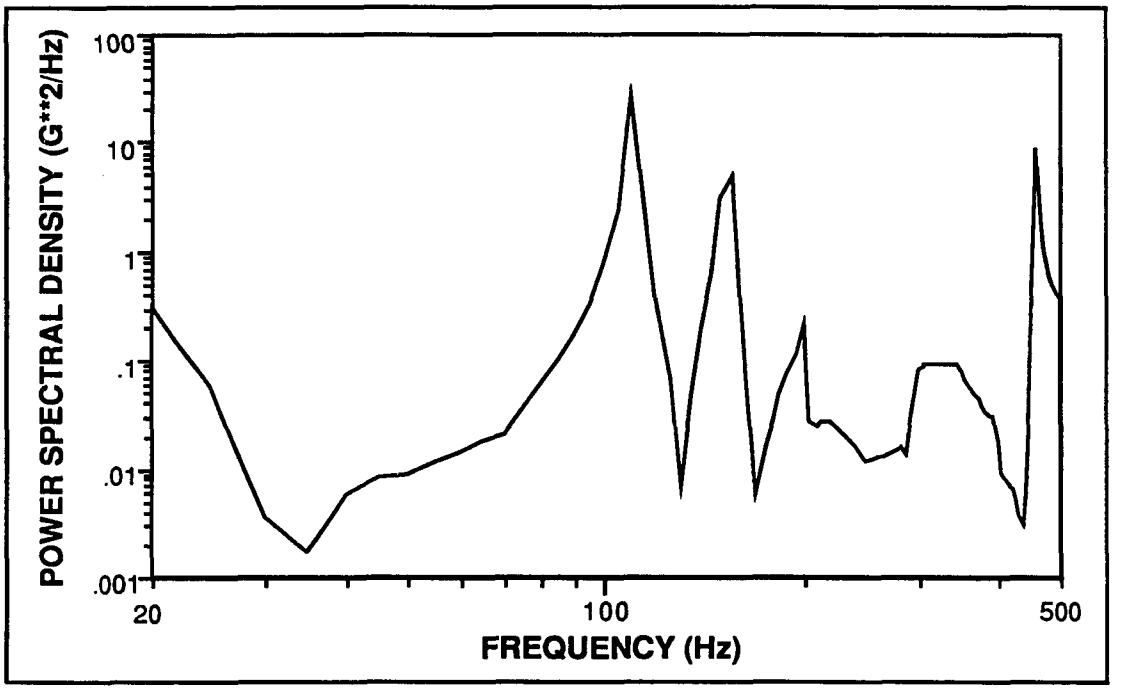

Figure 5-7 Vibration Input Curve for the 100% Vibration Envelope

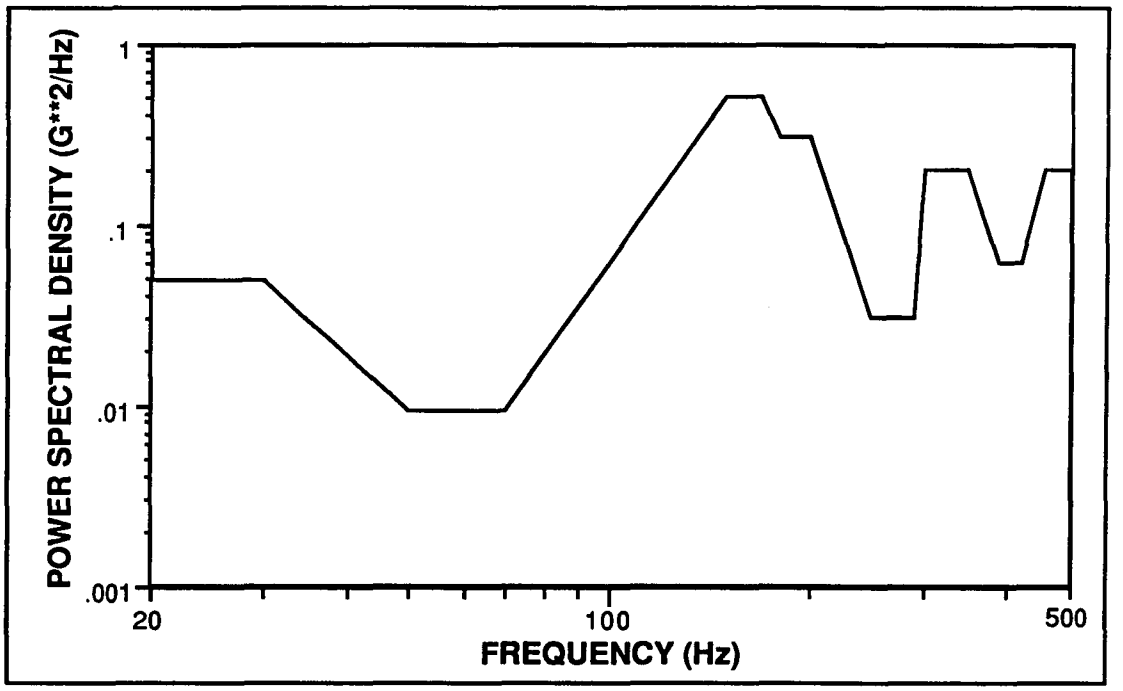

Figure 5-8 100% Vibration Test Envelope

Table 5-2 Structural Analysis Data Summary

TYPE OF TEST	TEST TIME	1 ST FREQ	BENDING MOMENT	SHEAR FORCE	BENDING STRESS	ACCEL
	(MIN)	(Hz)	RMS (IN-LBF)	RMS (LBF)	RMS (PSI)	RMS (G)
EQUIPMENT TEST TO FIG. 4-2 (100% TEST ENVELOPE)	30	32.4	5590	234	2360	8.37
SECTION TEST TO FIG. 4-2 (100% TEST ENVELOPE)	30	88.4	1.01E+08	50900	5429000	8.34
EQUIPMENT TEST TO FIG. 4-4 (FWD TEST ENVELOPE)	30	32.4	4160	191	1760	7.74
EQUIPMENT TEST TO FIG. 4-5 (AFT TEST ENVELOPE)	30	32.4	4460	192	1890	6.65

The results from the structural analysis are summarized in Table 5-2, and are contained in Appendix E. The responses at station 32 (grid point 9) for each of the different vibration inputs were compared to those shown in Fig. 4-2, Fig. 4-4, and Fig. 4-5. The results in Table 5-2 are for element 4B which connects grid points 7 and 9 together. These results were compared with those from element 5A which connects grid points 9 and 10 together. The internal loads were higher in element 4B than in element 5A. The values shown in Table 5-2 are the RMS values for the bending moments, the shear forces, the bending stresses, and the accelerations.

The summary in Table 5-2 shows the 100% vibration response envelope does indeed produce higher internal forces than either of the two vibration events that effectively define this envelope. Yet, neither of these events produce bending moments quite as high as the 100% vibration envelope does by itself. The section test results show it we were able to produce the 100% vibration response envelope at grid point 9. However, these particular results are in great error. The results show the bending moment to be1 X 10^6 in-lb_f, which far exceeds the material properties of Ti-6AL-4V, and indicates the section would have experienced a catastrophic failure.

The error in the section model's results can be attributed to the unavailability of modal test data. The yokes that attach the section to the shaker table need to be changed to permit the same degrees-of-freedom to exist in the test as in the actual hardware. Obviously, the constraints and stiffnesses used in the section model are incorrect. Without any modal data or other test data such as bending moments, it is almost impossible to determine the correct support conditions.

The results contained in Table 5-2 also show that the same 100% vibration response envelope was reached in both the equipment and in the section model analytical tests. Vibration testing is often conducted on the premise that matching the vibration response envelopes at a given location constitutes dynamic similarity. Yet, while the section results are invalid, they nevertheless show that the same vibration response levels were attained in both tests, but the internal structural forces were quite different.

The stresses shown in Table 5-2 are dependent on the geometry of the beam elements (CBAR) within both models. The actual stresses in any component other than these beam elements must be determined from the bending moment within the element. The stresses in the equipment's skin are used in this study to demonstrate how fatigue damage varies with different vibration levels and boundary conditions.

The equipment's structure is essentially a 7 inch diameter hollow cylindrical beam built in five sections. All the sections are joined together with screws. The number and diameter of these screws varies depending upon each section's location. The two sections at station 32 (grid point 9) are joined together with eleven screws. This joint must withstand large dynamic loads without catastrophic failure. For simplicity, only those stresses in the equipment's skin will be determined for use in the fatigue analysis.

Example Calculations

The eleven holes in the circumference of the equipment's skin will cause localized stress concentrations. Therefore, an appropriate stress concentration factor must be determined. Figure 5-9 is used to determine the appropriate stress concentration factor for a joint with the following geometric parameters

$d = 0.1925$ in
$b = 1.9200$ in
$h = 0.1925$ in

Therefore

$h/b = 0.2607$ $\qquad$ $d/b = 0.1003$

These ratios when used in Fig. 5-9 result in a stress concentration factor of

$K_t = 7.45$ to 7.25

For simple beam bending in which plane cross sections remain plane, stress is given by the following equation

$$S_b = Mc/I$$

where S_b = Bending stress (psi)
M = Bending moment (in-lb_f)
I = Moment of inertia of cross section (in^4)
c = Distance form neutral axis to surface (in)

The moment of inertia for a hollow cylinder is

$$I = (\pi)\,[d_o^4 - d_i^4]/64$$

$$I = (\pi)\,[6.816^4 - 6.713^4]/64$$

$$I = 3.13\ in^4$$

where d_o = Outside Diameter (in)

d_i = Inside Diameter (in)

The maximum stress in the skin is then

$$S_{max} = K_t\, S_b$$

$$S_{max} = (7.45)[(5590)(3.40)/(6.26)]$$

$$S_{max} = 22350\ psi$$

Since no mean load is applied to the equipment, it is assumed that each cycle results in a complete reversal so that

$$R = S_{max} / S_{min} = -1$$

The structural analysis has provided most of the information necessary to determine the cumulative fatigue damage. The maximum stress levels were calculated for each of the four cases discussed in this chapter. The next chapter applies these results to determine the number of cycles to failure for each of the 1σ, 2σ, and 3σ stress levels.

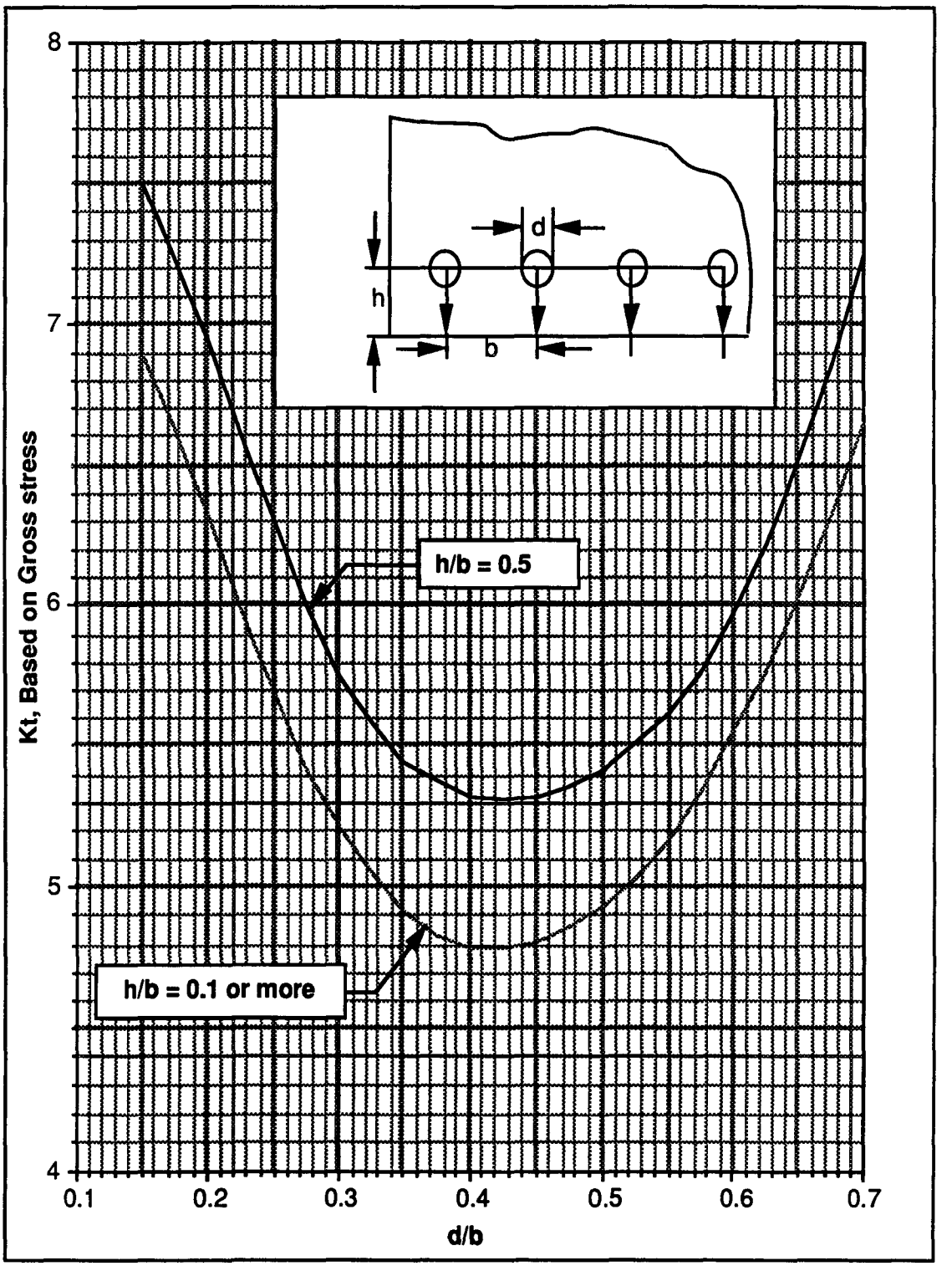

Figure 5-9 Stress Concentration Factors for Screw Joints (Smith 1989)

CHAPTER 6

CUMULATIVE FATIGUE DAMAGE

The structural analysis does not account for the effects the equipment's frequencies and exposure times have on the fatigue life. Therefore, another means must be used to determine the effects that repetitive exposure to a dynamic environment has on the equipment's fatigue life. Cumulative fatigue damage theory (See Curtis, Tinling and Abstein 1971, pp. 80 - 88; Fackler 1972, pp. 5 - 33; Fisher 1988, pp. 42-34 - 42-35; and Steinberg 1988, pp. 409 - 411) provides the means to account for the combined effects of stress, frequency, and duration of the vibration.

Cumulative fatigue damage theory is used to evaluate the combined effects that different load levels, frequencies, and exposure times have on fatigue life. The theory is first used to evaluate the effects of enveloping vibration data versus not enveloping the vibration data. The theory is also used to evaluate the differences in fatigue life due to using the same vibration envelope for two different tests with different support conditions. The cumulative fatigue damage theory provides the means to evaluate the combined effects of vibration levels and durations on fatigue life.

Fatigue Damage Theory

Fatigue damage theory is a subject in itself. This chapter presents only the theory necessary to comprehend the subject matter as it relates to this study. Additional information is readily available from the sources listed above and they are contained in this study's reference section.

The equipment's fatigue life is strongly influenced by the loads acting upon its external structure. These loads essentially deform and produce unique stress patterns within the equipment's structure. A load may be one of the following (Fackler 1972, p. 6):

1. Single
2. Sequential
3. Superpositioned
4. Superpositioned Random
5. Random

Any one of these loads independently or in combination will contribute to the equipment's cumulative fatigue damage. At some point enough fatigue damage accumulates to cause a structural failure.

S-N Curves

Cumulative fatigue damage is dependent on experimentally determined S-N curves (endurance curves). These curves are available for numerous different types of materials, various combinations of loads, temperatures, geometries, and imperfections. Any of these conditions may affect the material's properties, and consequently reduce the material's fatigue life by changing the slope of the S-N curve, or by lowering the curve altogether.

Coupons are made from these materials and are exposed to alternating sinusoidal stresses. Eventually, most of the coupons will develop signs of fatigue, thereby indicating a finite fatigue life for that particular stress level. Next, the stress level is changed and the process repeated with a new coupon until it too experiences failure. These results are plotted on log-log graph paper as shown in Fig. 6-1. Finally, a best fit curve is drawn through the data to define the material's fatigue life.

There are usually large amounts of data scatter in the number of cycles to failure for any given stress level. This scatter may range from as low as 10 to 1 to as high as 100 to 1 (Fackler 1972, p. 11). The fatigue curve is plotted in terms of mean stress versus the number of cycles to failure. At low cycles the

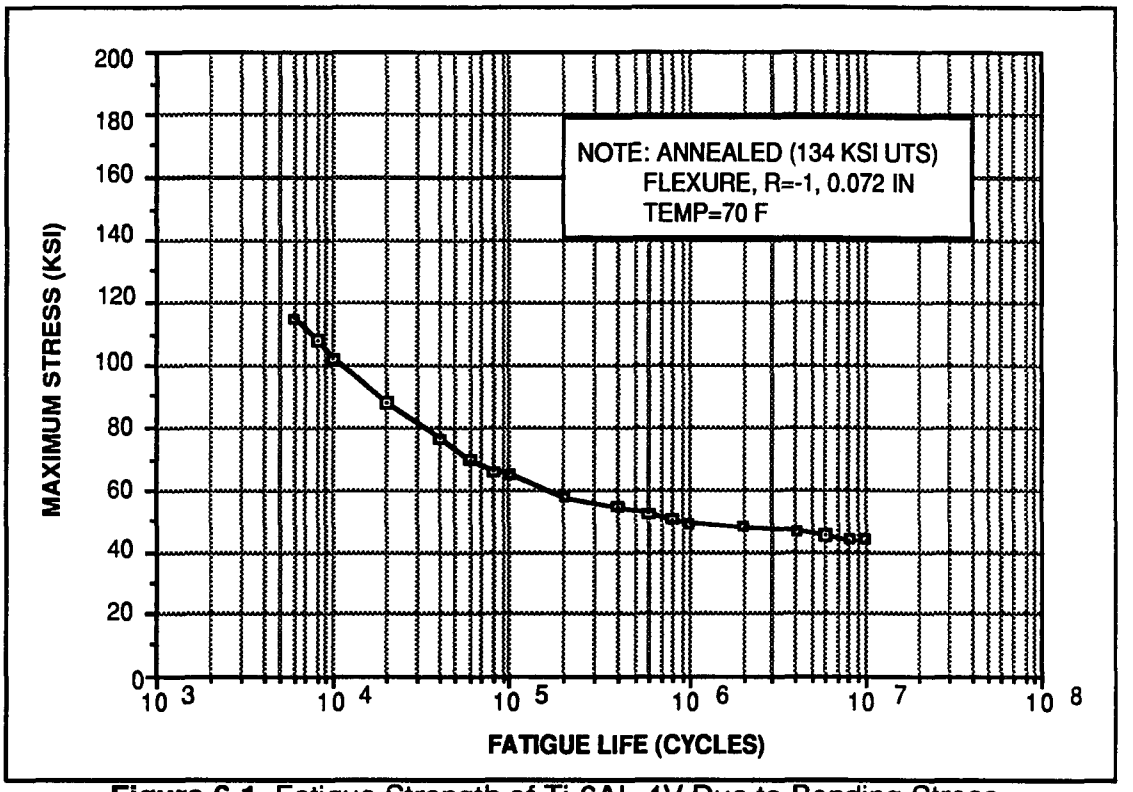

Figure 6-1 Fatigue Strength of Ti-6AL-4V Due to Bending Stress (DOD 1991)

curve approaches the material's static properties, while at high cycles the curve approaches the materials endurance limit. The endurance limit defines a certain stress level that will not cause failure regardless of the number of cycles consumed. If the material has no discernible endurance limit is assumed to have a fatigue life of $1x10^7$ cycles.

Other factors such as loads, temperatures, and material imperfections also affect the material's S-N curves. Either one or more of these conditions may raise or lower the fatigue curve, and also may change the slope of the fatigue curve. However, the vast majority of S-N curves available in the literature are for materials at room temperatures, with no surface imperfections, and with zero mean stresses.

Miner's Rule

Miner's rule (See Fackler 1972, pp. 5 - 33) is perhaps the most widely used method for determining cumulative fatigue damage. Miner's rule is relatively simple to use, and its results are comparable to those obtained from using complicated and more sophisticated methods (Fackler 1972, p. 11).

Miner's rule sums the material's fractions of life consumed at each different load condition. This theory assumes the following:

1. Fatigue damage is proportional to absorbed work.
2. Absorbed work is proportional to the ratio of the applied stress cycles divided by the number of fatigue cycles at the same stress level.
3. Damage to cause a failure is a constant.
4. Damage is a function of load.
5. Damage is independent of load sequence.

Miner rule predicts failure when the sum, D, of the ratios of the applied stress cycles divided by the number of cycles to failure is equal to 1.0 (Fackler 1972, p. 11).

$$D_m = \sum_{\infty}^{i} \frac{n_i}{N_i}$$

where D_m = Normalized damage index

n_i = Number of cycles consumed at a load condition

N_i = Number of cycles to failure at load condition

Miner's rule is graphically illustrated in Fig. 6-2. This figure clearly shows that the damage is independent of the applied stress. It also shows that equal damage can be achieved from numerous different stress levels. Finally, it shows that the damage is independent of the sequence in which the various stresses are applied.

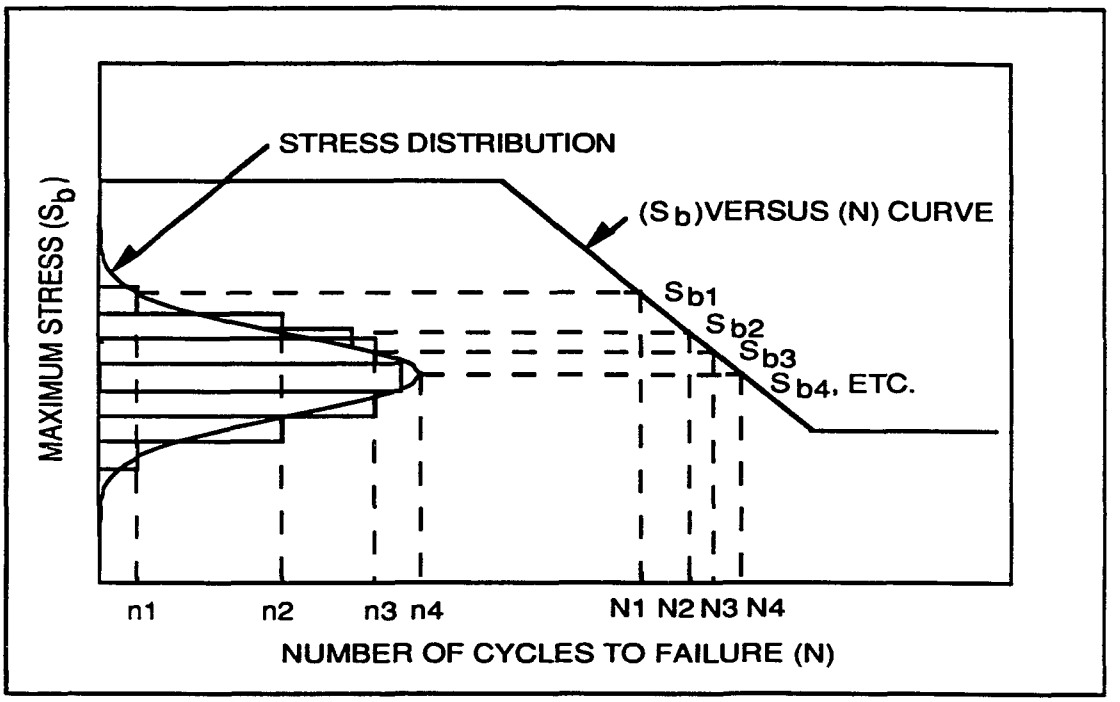

Figure 6-2 Cumulative Linear Fatigue Damage (Fisher 1988, p. 42-35)

Miner's rule usually predicts failure at a damage index of D = 1.0. Yet, many researchers have shown that there are significant deviations from D = 1.0. The most common explanation for these deviations is that the load, the load sequence, and the random variation in loads all tend to influence the damage index (Fackler 1972, p. 11). Therefore, the normalized damage index is usually taken as:

1. D < 0.3 life critical component
2. D < 0.7 non life critical components
3. D = 1.0 for comparative purposes

The S-N curve shown earlier in Fig. 6-1 is for Ti-6Al-4V and it is applicable for bending stresses only. The bending stresses were derived from each of the four vibration events that were run in the structural analysis. The stresses are on the vertical axis in Fig. 6-1. The intercept with the material's fatigue curve defines the number of cycles to failure (N_i) along the horizontal

axis at that stress level. The actual number of cycles (n_i) that were consumed during the event are readily determined from the equipment's resonant frequencies and the time (t) spent in the event that produced the stress level.

The number of cycles resulting in complete stress reversals are determined from the equipment's resonant frequencies. Random vibration simultaneously excites all the resonant frequencies in multiple degrees-of-freedom systems. Fatigue damage is directly related to those frequencies that have the highest transmissibilities, and the lowest amount of structural damping (Steinberg 1988, p. 258).

However, fatigue damage is primarily caused by exciting the equipment's fundamental frequency, which also has the largest displacement. This assumption is used in this study to simplify the fatigue analysis. The number of cycles (n_i) at resonance are:

$$n_i = (f_n) * t$$

where n_i = Number of cycles consumed at a stress condition

f_n = Fundamental frequency (Hz)

t = Time (Sec)

The above relationship is used to calculate the number of cycles at resonance for each supported model. It is also used to determine the number of cycles at 1σ, 2σ, and 3σ stress levels in the next section.

Example Calculations

Problem: Find the fatigue damage at the resonant frequency for the equipment due to the 100% vibration test envelope (Fig. 4-2) for the following:

Material = Ti-6AL-4V
Stress = 22.35 ksi
Frequency = 32.4 Hz
Time = 30 min

Solution: The number of fatigue cycles generated during the 30 minute test for the 1σ, 2σ, and 3σ events are:

$$n_1 = (32.4)(30)(60)(0.6830) = 39838 \text{ cycles}$$
$$n_2 = (32.4)(30)(60)(0.2710) = 15805 \text{ cycles}$$
$$n_3 = (32.4)(30)(60)(0.0433) = 2525 \text{ cycles}$$

The bending stress due to random vibration for the 1σ, 2σ, and 3σ levels are:

$$S_{b1} = (22.35)(1\sigma) = 22.35 \text{ ksi}$$
$$S_{b2} = (22.35)(2\sigma) = 44.70 \text{ ksi}$$
$$S_{b3} = (22.35)(3\sigma) = 67.05 \text{ ksi}$$

The number of cycles to failure at each of the above stresses were obtained from Fig. 6-1:

$$N_1 = (1 \times 10^7)$$
$$N_2 = (1 \times 10^7)$$
$$N_3 = (3 \times 10^5)$$

Following Miner's rule, the total fatigue damage due to a 30 minute vibration test is as follows:

$$D_m = \sum_{\infty}^{i} \frac{n_i}{N_i} = \frac{n_1}{N_1} + \frac{n_2}{N_2} + \frac{n_3}{N_3} + \ldots$$

$$D_m = \sum_{\infty}^{i} \frac{39838}{1 \times 10^7} + \frac{15805}{1 \times 10^7} + \frac{2525}{3 \times 10^5}$$

$$D_m = 1.4 \times 10^{-2}$$

Fatigue Analysis Results

The previous section demonstrated the procedure used to determine fatigue damage. These procedures were used to calculate the cumulative fatigue damage for the equipment's response to three different vibration levels, and for the equipment's and the section's response to the same vibration level. The results from the fatigue analysis are summarized in Table 6-1.

Table 6-1 shows the 100% vibration envelope (Fig. 4-2) produces four times more fatigue damage than the equipment attached its platform's forward location (Fig. 4-4), and three times more fatigue damage than the equipment attached to its platform's rear location (Fig. 4-5). Finally, the 100% vibration response envelope produced twice the fatigue damage obtained by summing the cumulative fatigue damage from Fig. 4-4 and Fig. 4-5 sequentially together.

The fatigue damage from the section test could not be calculated, since the section model did not produce realistic internal loads. The results suggest the structure failed despite achieving the 100% vibration response envelope at grid point 9 (Fig. 4-2). While the analytical equipment section test did not produce believable results, it did demonstrate one of the objectives of this study: the same vibration test level was attained in both the equipment test and the section test, yet there were considerable differences in the internal structural loads.

Table 6-1 Fatigue Damage Calculations for Station 32 Vertical

ITEM/K	(0-P)	Sb	Sb (MEAN)	Sb (MAX)	Sb (MIN)	R	Nl	ni	Dm
	(KSI)	(KSI)	(KSI)	(KSI)	(KSI)		(CYCLES)	(CYCLES)	
		(1)*(2)		(4)+(3)	(4)-(3)	(6)/(5)	(REF FIG. 6-2)		(9)/(8)
EQUIPMENT (FIG. 4-2)									
K=1	22.35	22.35	0	22.35	-22.35	-1	1.00E+07	39838	3.98E-03
K=2	22.35	44.7	0	44.7	-44.7	-1	1.00E+07	15805	1.58E-03
K=3	22.35	67.05	0	67.05	-67.05	-1	7.00E+04	2525	3.61E-02
SECTION (FIG. 4-2)								TOTAL Dm =	4.20E-02
K=1	4088.00	4088	0	4088	-4088	-1	N/A	108693	N/A
K=2	4088.00	8176	0	8176	-8176	-1	N/A	43122	N/A
K=3	4088.00	12264	0	12264	-12264	-1	N/A	6889	N/A
EQUIPMENT (FIG. 4-4)								TOTAL Dm=	N/A
K=1	16.91	16.91	0	16.91	-16.91	-1	1.00E+07	39838	3.98E-03
K=2	16.91	33.82	0	33.82	-33.82	-1	1.00E+07	15805	1.58E-03
K=3	16.91	50.73	0	50.73	-50.73	-1	6.00E+05	2525	4.21E-03
EQUIPMENT (FIG. 4-5)								TOTAL Dm=	1.00E-02
K=1	18.10	18.1	0	18.1	-18.1	-1	1.00E+07	39838	3.98E-03
K=2	18.10	36.2	0	36.2	-36.2	-1	1.00E+07	15805	1.58E-03
K=3	18.10	54.3	0	54.3	-54.3	-1	3.00E+05	2525	8.42E-03
								TOTAL Dm=	1.40E-02

CHAPTER 7

CONCLUSIONS AND RECOMMENDATIONS

The purpose of this study was (1) to determine and compare the fatigue damage from two different vibration events to an envelope of these events, and (2) to determine and compare the fatigue damage from using the same vibration envelope in an equipment test to that in a section test. These two goals were achieved, although the results from the section test were in error. Nevertheless, these results demonstrated that achieving the same vibration response level in the equipment test and the section test does not imply the internal loads are the same. A brief overview of this study, its most significant results, its conclusions, and its recommendations are discussed below.

The laboratory vibration test times and levels are derived from the equipment anticipated and its actual usage. The equipment's usage is often dictated by its platform. The equipment used in this study is mounted to its platform and subjected to some very severe vibration levels. Therefore, an estimate of the platform's mission profile was compared to that from an actual mission profile. It is the platform's mission profile that defines the various vibration events and subsequent exposure times for the equipment.

The equipment's mission profile provided a description of the two worst vibration events that essentially define the 100% vibration response envelope. The mission profile also defined the corresponding exposure times associated with each event that were subsequently used to define the test duration for the 100% laboratory vibration response envelope. The estimated mission profile was compared to an actual mission profile to determine if its description of the segments, events, and times were appropriate.

The mission profile provided the means to scope the search of an extensive computerized vibration data base. The vibration data was analyzed by event and by the equipment's location on its platform. The vibration data from the two worse vibration events were compared. These envelopes were for the

equipment mounted to its platform's forward and rear locations, and together they essentially defined the 100% vibration response envelope.

The structural analysis used two finite element models, one was of the equipment attached to a shaker table, while the other was of a section attached to a shaker table. An analytical modal analysis was run on both models. The analytical results were compared to the modal data, and the models adjusted in order to achieve the dynamic similarity. Modal data for the section was not available for comparison in either the supported or unsupported states. A 1 G^2/Hz excitation was applied to both models in their supported states to produce their respective transmissibility curves. Vibration inputs were determined from the desired responses and the transmissibility curves. Finally, the vibration inputs were used to excite the finite element models to produce the desired responses at station 32 (grid point 9).

The structural analysis was run on both the equipment model and the section model in their respective supported states. The NASTRAN structural analysis produced results in terms of bending moments, shear forces, bending stresses, and finally accelerations. The stresses in the equipment's skin were calculated based upon the geometry of the equipment's cross section. These stresses were used in conjunction with the appropriate fatigue curve for the material in question to determine the cumulative fatigue damage. The results were compared to ascertain the differences in fatigue damage between the two events that together essentially defined the 100% vibration test envelope. The 100% vibration test envelope was also used in the supported section model and those results were compared to those from using the 100% vibration envelope in the supported equipment model.

Significant Results

As a direct result of this study, the following significant results were obtained:

1. An accurate definition of the equipment's intended usage is critical to produce accurate and realistic vibration test levels and test times.
2. Assumptions about the equipment's usage quickly out weigh most of the benefits derived from a detailed mission analysis.

3. Assumptions and estimates should be validated and changes made to analytical models to reflect new information when it becomes available.
4. As expected, vibration envelopes produce higher internal loads in the equipment that either of the two vibration events that essentially make up the envelope.
5. As expected, the same vibration levels may be attained in two different tests with different boundary conditions, however, the internal loads are considerably different.
6. Modal tests for the equipment under various boundary conditions are required in order to validate the dynamic characteristics of the analytical models.

Recommendations

It is recommended that the following measures should be undertaken to build upon the results obtained in this study:

1. Determine the structural and dynamic characteristics of the support structures used in both the equipment and the sections tests.
2. Conduct a modal tests on the section model in both its supported and its unsupported states.
3. Validate all assumptions about the equipment's vibration environments prior to using them to design its laboratory tests.
4. Do not spend the effort trying to define the equipment's vibration environments if assumptions are going to be made later about the most severe vibration events.
5. Investigate using other properties such as bending moment or strain as a means of achieving dynamic similarity between different vibration environments and different vibration tests.
6. Conduct a detailed structural analysis on the equipment to predict the actual forces acting upon it versus assuming a single point excitation.
7. Conduct a structural analysis on the equipment mounted to its platform or shaker table, and simultaneously excite both the forward and rear ends.

APPENDIX A

ACTUAL MISSION PROFILE DATA

The plots contained in this appendix are derived from an actual training mission. This actual mission profile was discussed in Chapter 3, and subsequently summarized in Table 3-4. The present study used a combination of different sources to define the various mission segments. The first graph in this appendix shows the platform's altitude as a function of time. The time scale used in this graph must be divided by 10 to arrive at "seconds". This scale is due to the software program used to graph the mission data automatically selected the values to insert into the scales.

The definition of each of the mission segments requires some priory knowledge about the function and operation of the platform. The definition of the various segments is broken down so as to group similar portions together as they occur in sequence. The actual mission profile shows a few more occurrences, i.e., cruise, descend, cruise, descend, etc., than the author listed in Table 3-4. This is because the author took the liberty to group similar segments together to simplify the analysis.

The graphs following the overall mission profile are expansions of the air combat maneuver (ACM) segment defined as starting at 800 seconds and ending at approximately 2100 seconds into the mission. The time scale used in each of these graphs covers a span of 400 seconds. The ACM segment starts at 800 seconds on the first graph, increments 400 seconds with each succeeding graph, and ends on the last graph at 2400 seconds. In order to identify the various different types of platform maneuvers, three platform parameters were graphed simultaneously as a function of time, they are altitude (H), Mach number (M), and normal acceleration (N_Z). These graphs were used in conjunction with two other platform parameters that were also graphed as a function of time, they are angle-of-attack (AOA) and longitudinal acceleration (N_X).

These graphs were used to determine a) the type of maneuvers, and b) the length of the maneuvers. All maneuvers in the ACM segment were grouped by average normal acceleration (N_Z) and time; and by the average peak normal acceleration and time. This allowed us to arrive at a total of 778 seconds (13 minutes) of actual maneuver time. Next, the maneuvers were identified and

sorted by one of three categories, a) decreasing Mach number turns, b) constant Mach number turns, and c) increasing Mach number turns. Those decreasing Mach number turns that occurred at approximately the same altitude for the duration of the maneuver were labeled as windup turns (WUTs). This definition accounted for 288 seconds (4.8 minutes) of the total maneuver time. Of these, several occurred above 18,000 feet, at an AOA that exceeded 8 degrees, and between a Mach number of 0.9 to 0.7. These conditions have been associated with buffet, which accounted for a total of 24 seconds (0.4 minutes) of the total maneuver time. The other maneuvers were categorized as sustained maneuvers, which accounts for 468 seconds (7.8 minutes).

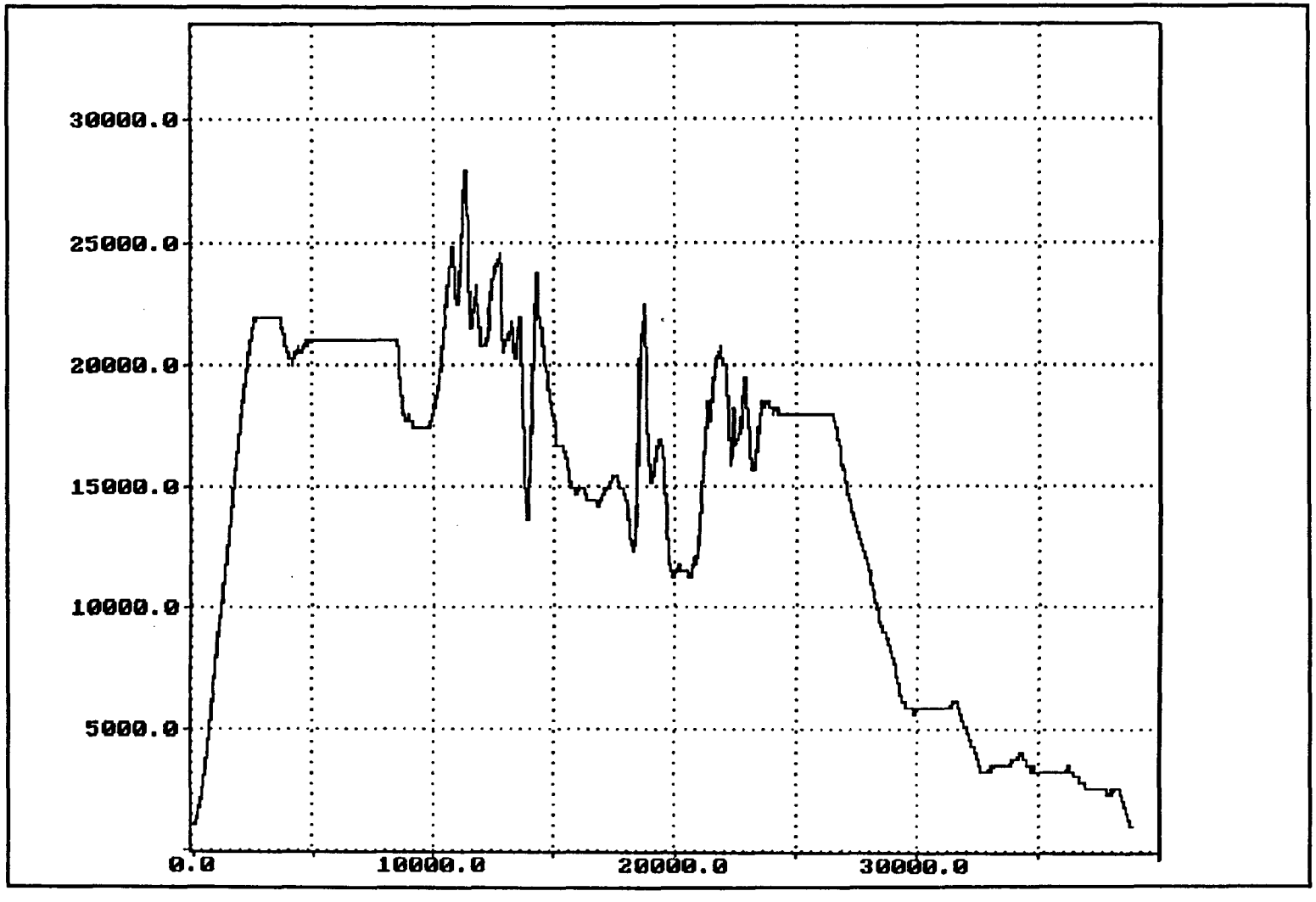

FIGURE A-1 Actual Mission Profile Overview

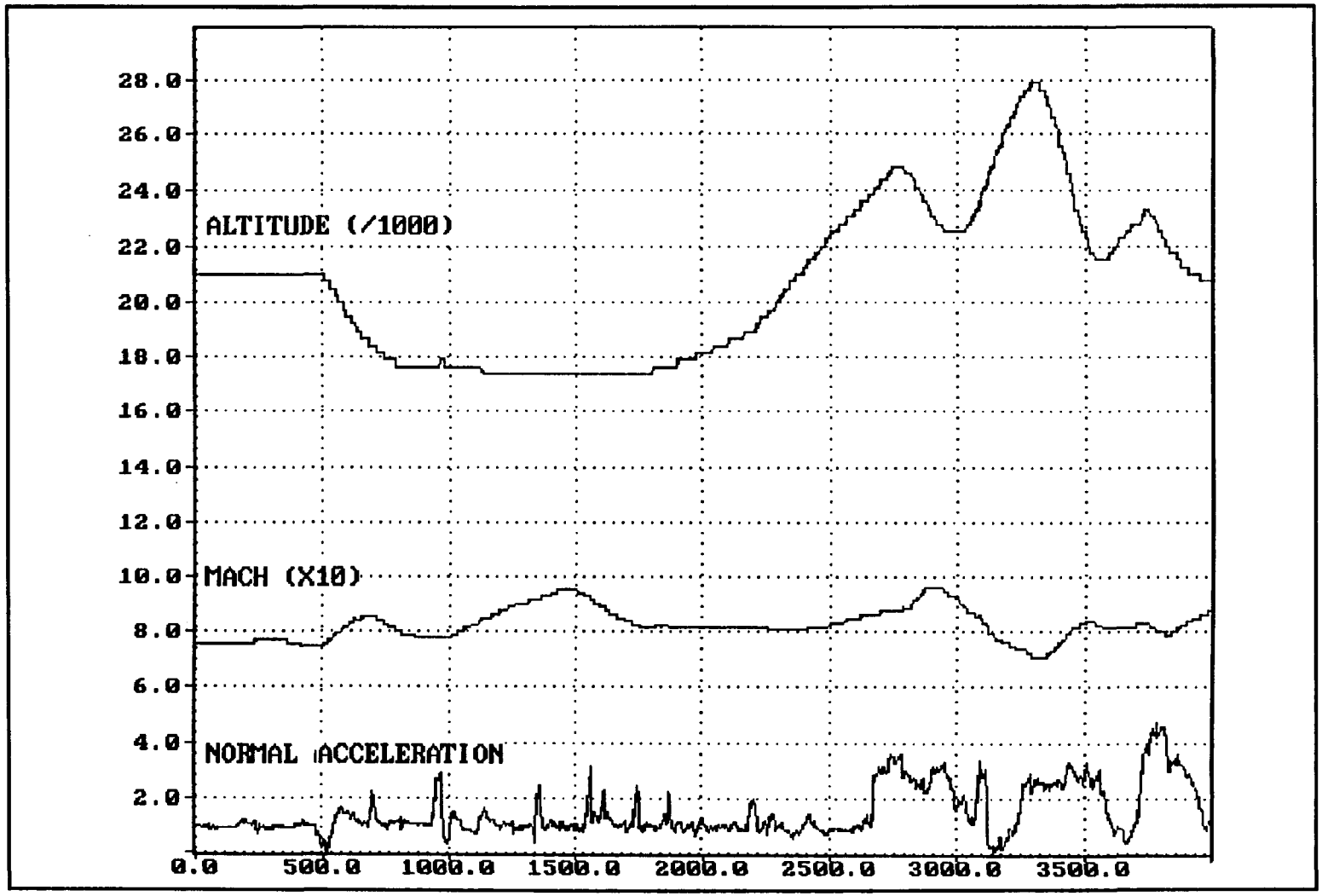

FIGURE A-2 Altitude, Mach, and Normal Acceleration Versus Time During an ACM Segment

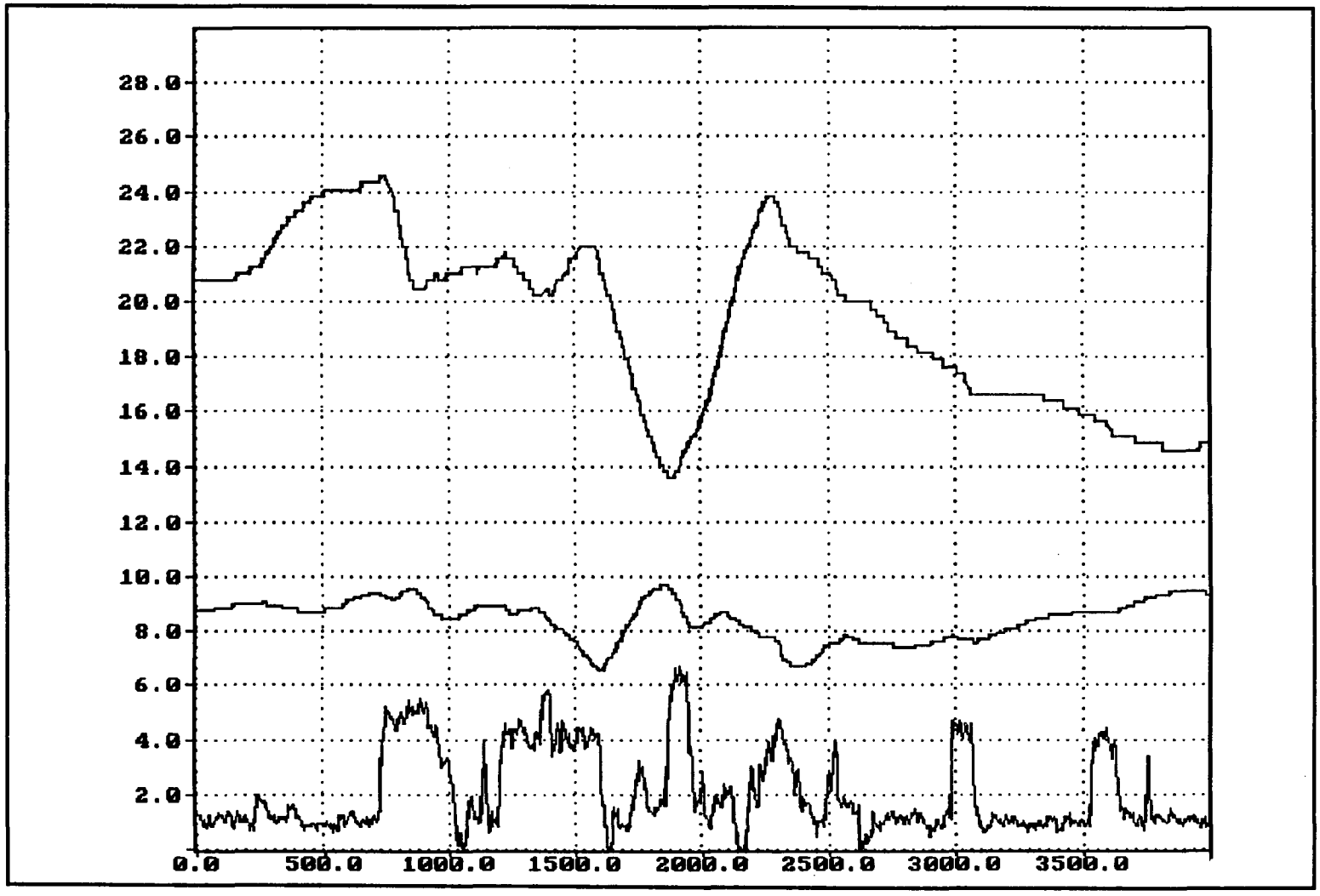

FIGURE A-2 Continued

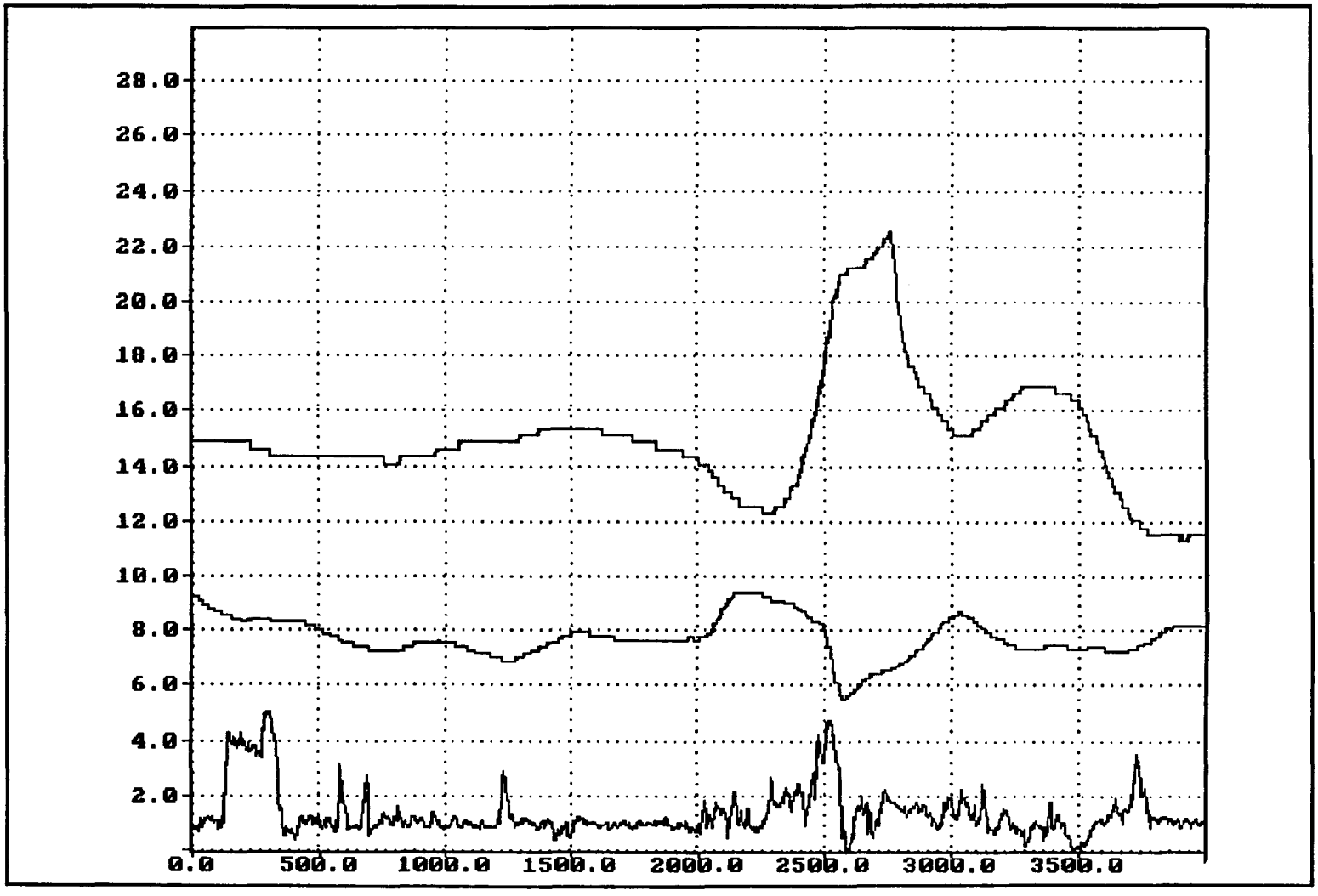

FIGURE A-2 Continued

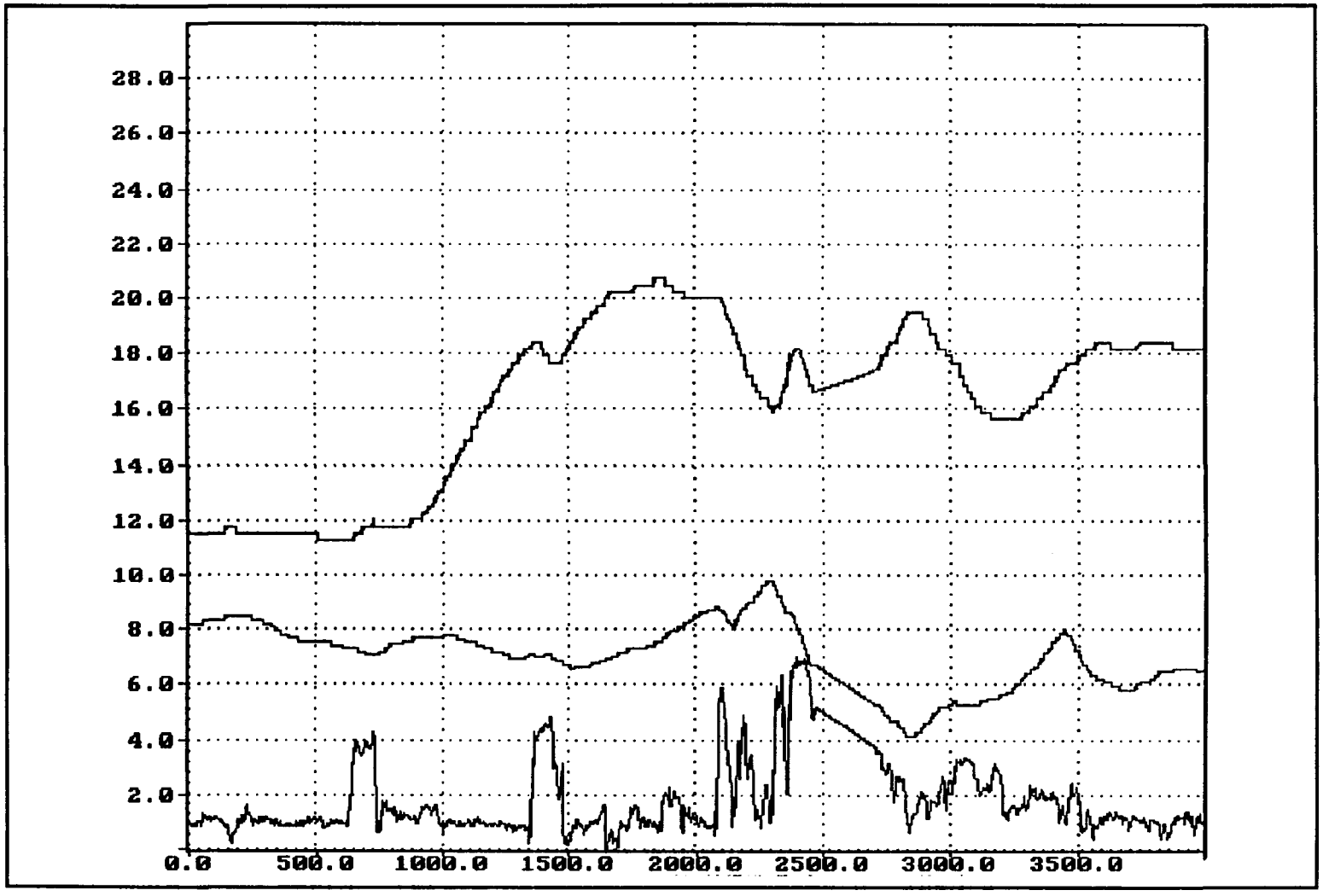

FIGURE A-2 Continued

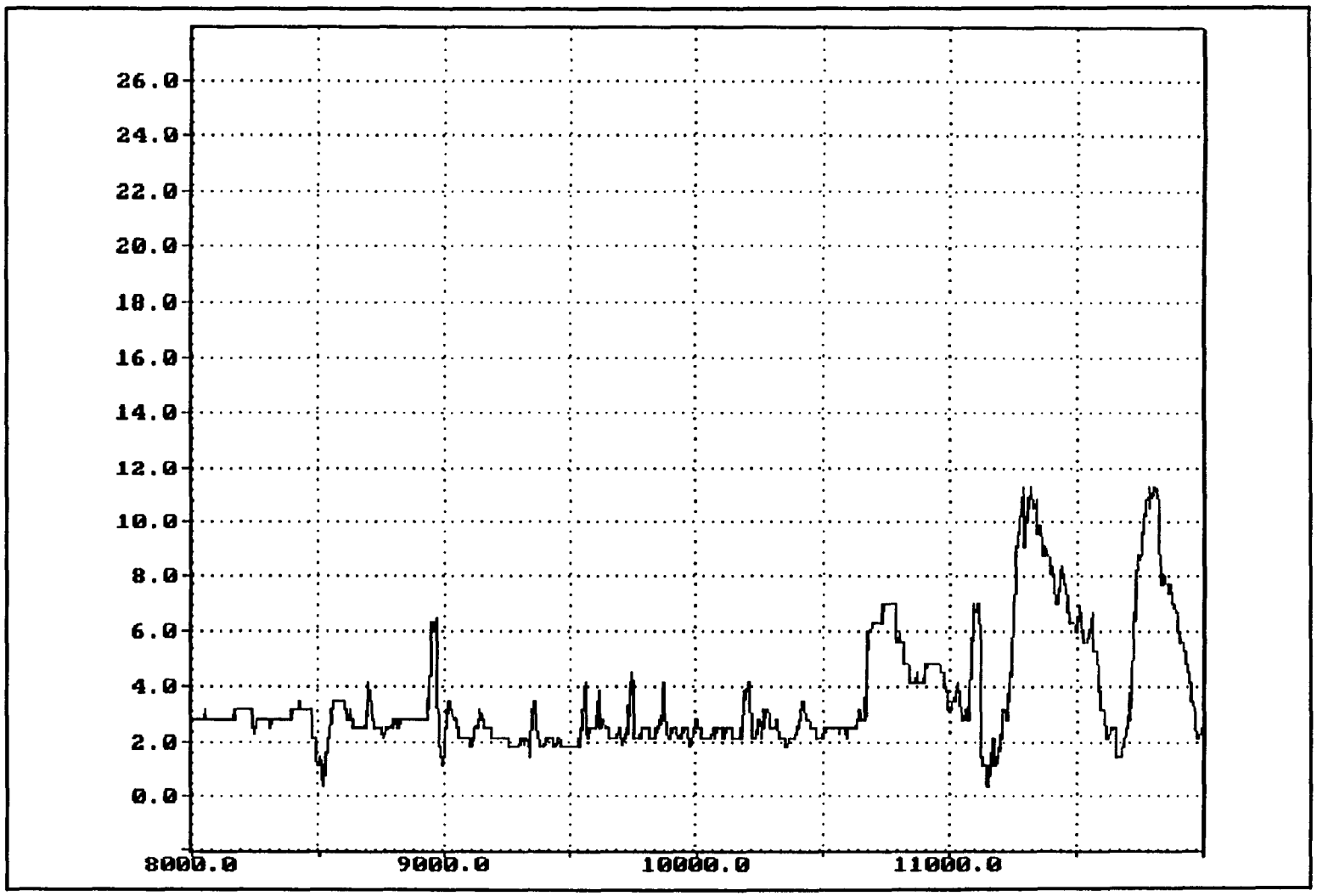

FIGURE A-3 Angle-of-Attack Versus Time During an ACM Segment

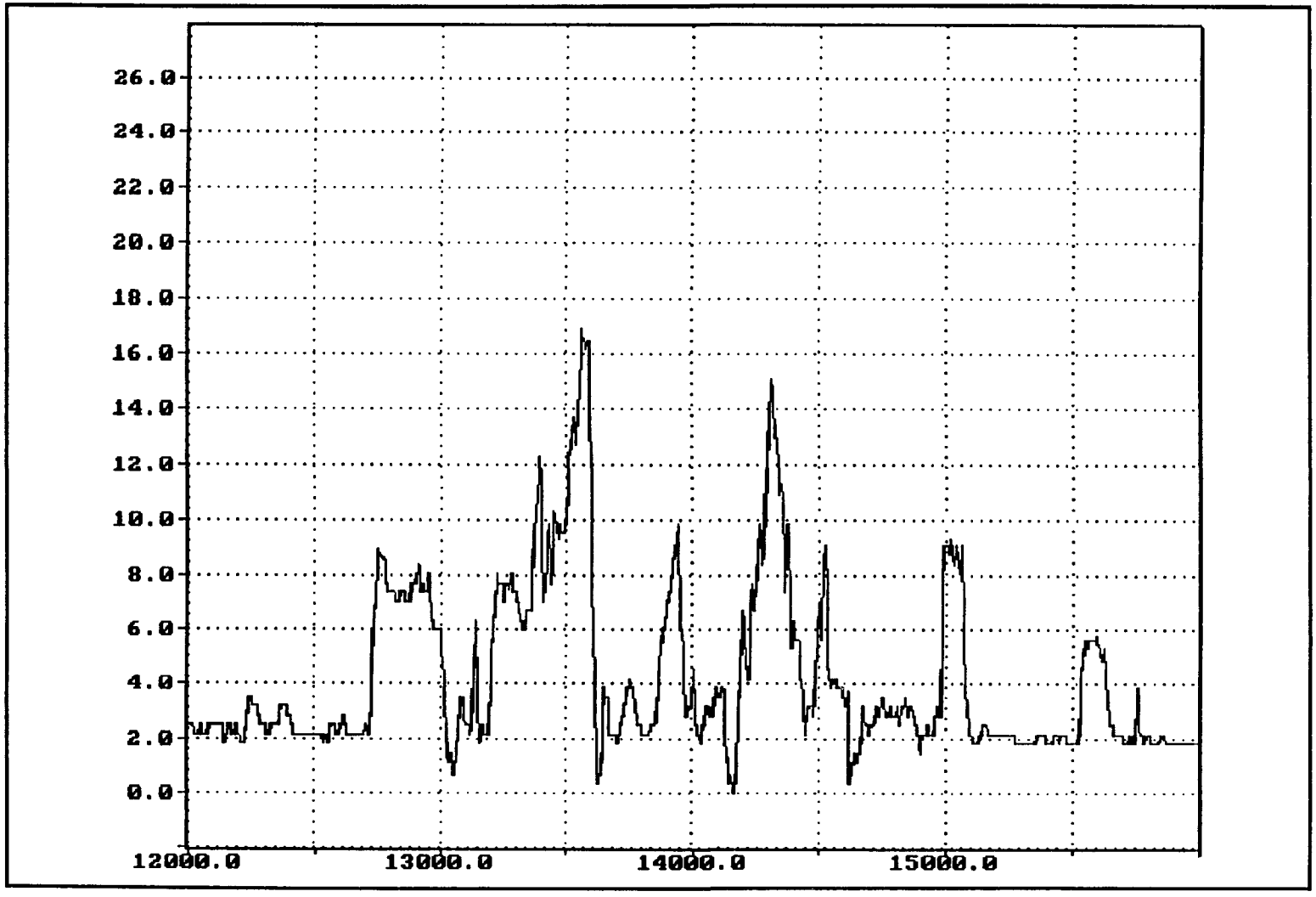

FIGURE A-3 Continued

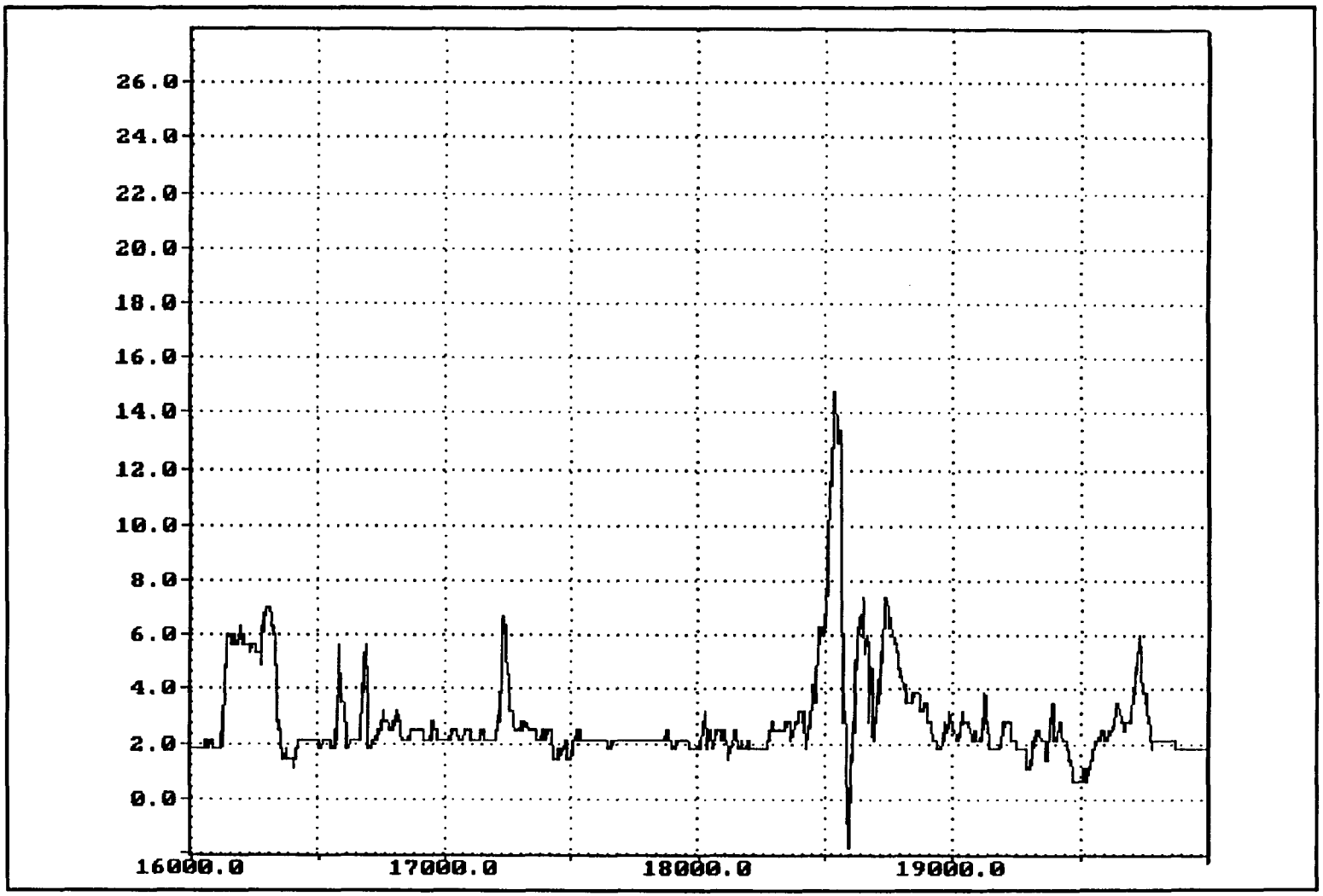

FIGURE A-3 Continued

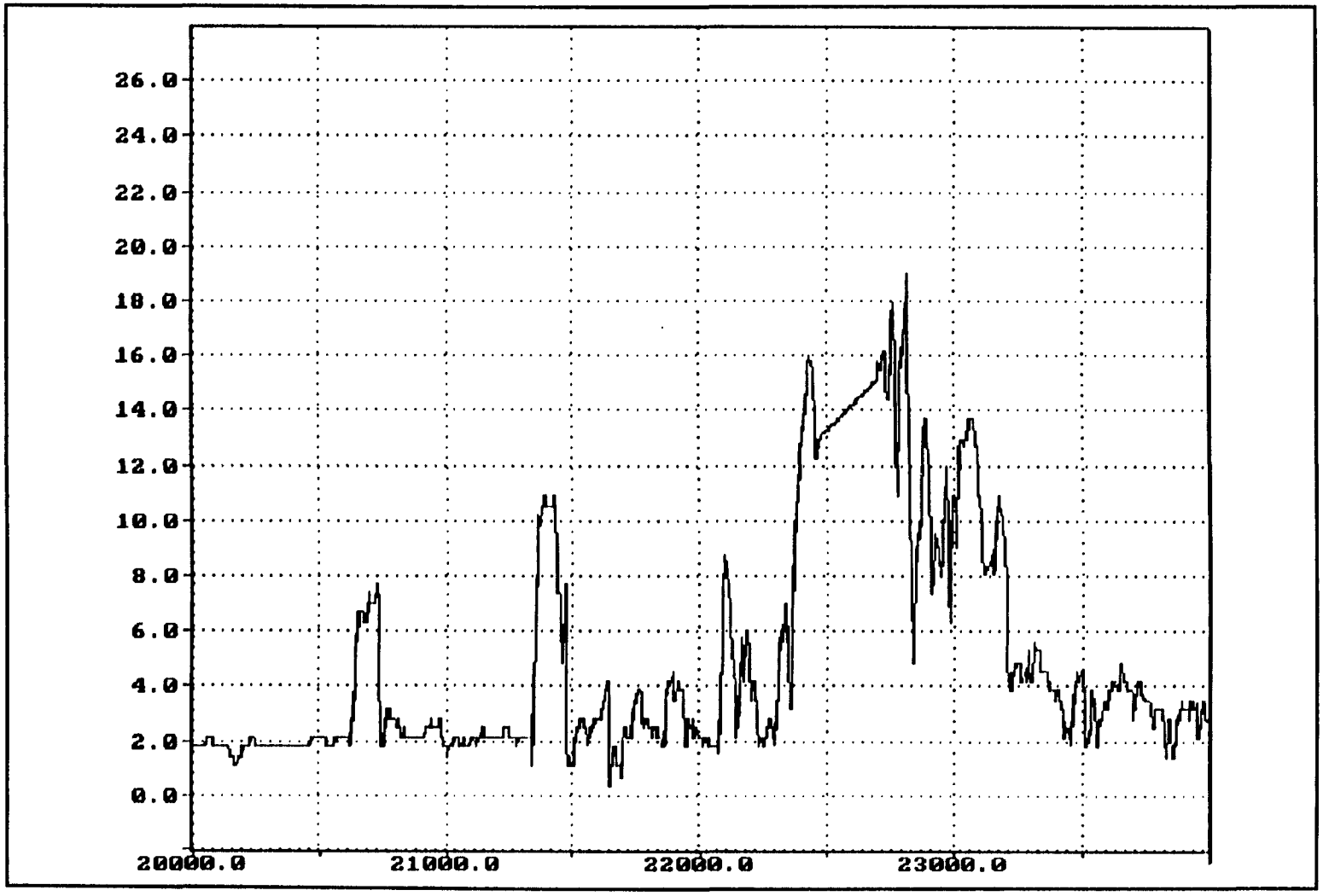

FIGURE A-3 Continued

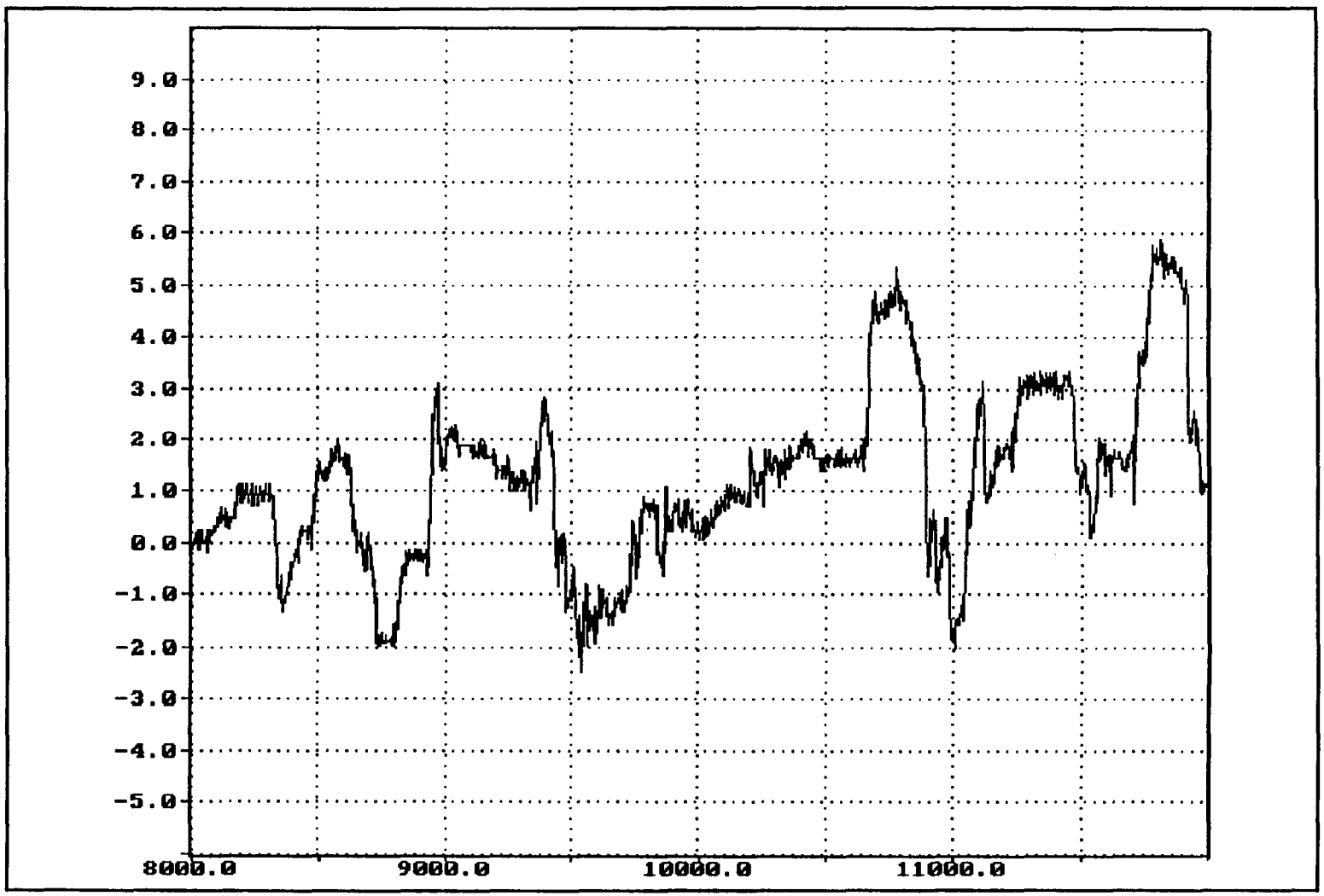

FIGURE A-4 Longitudinal Acceleration Versus Time During an ACM Segment

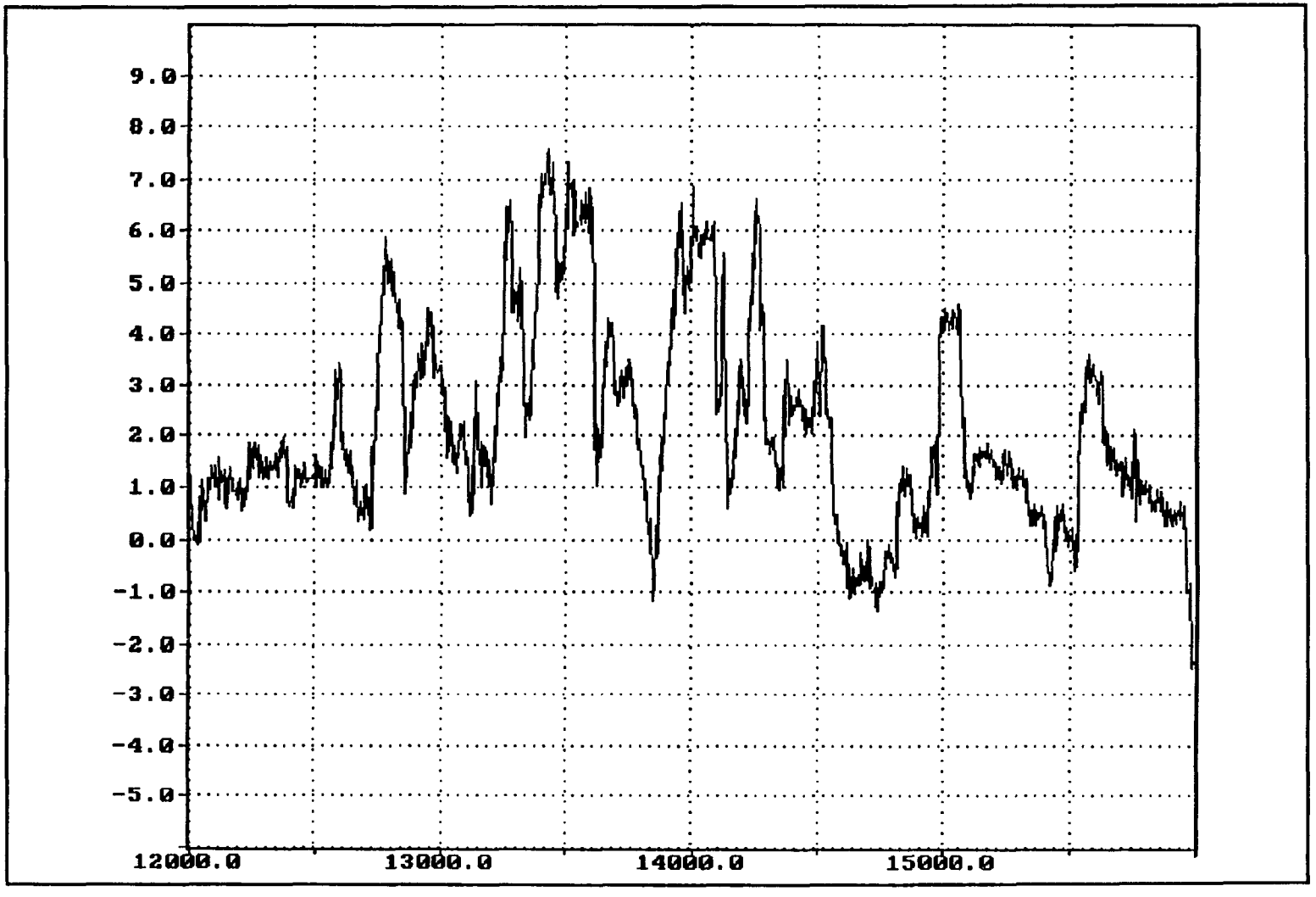

FIGURE A-4 Continued

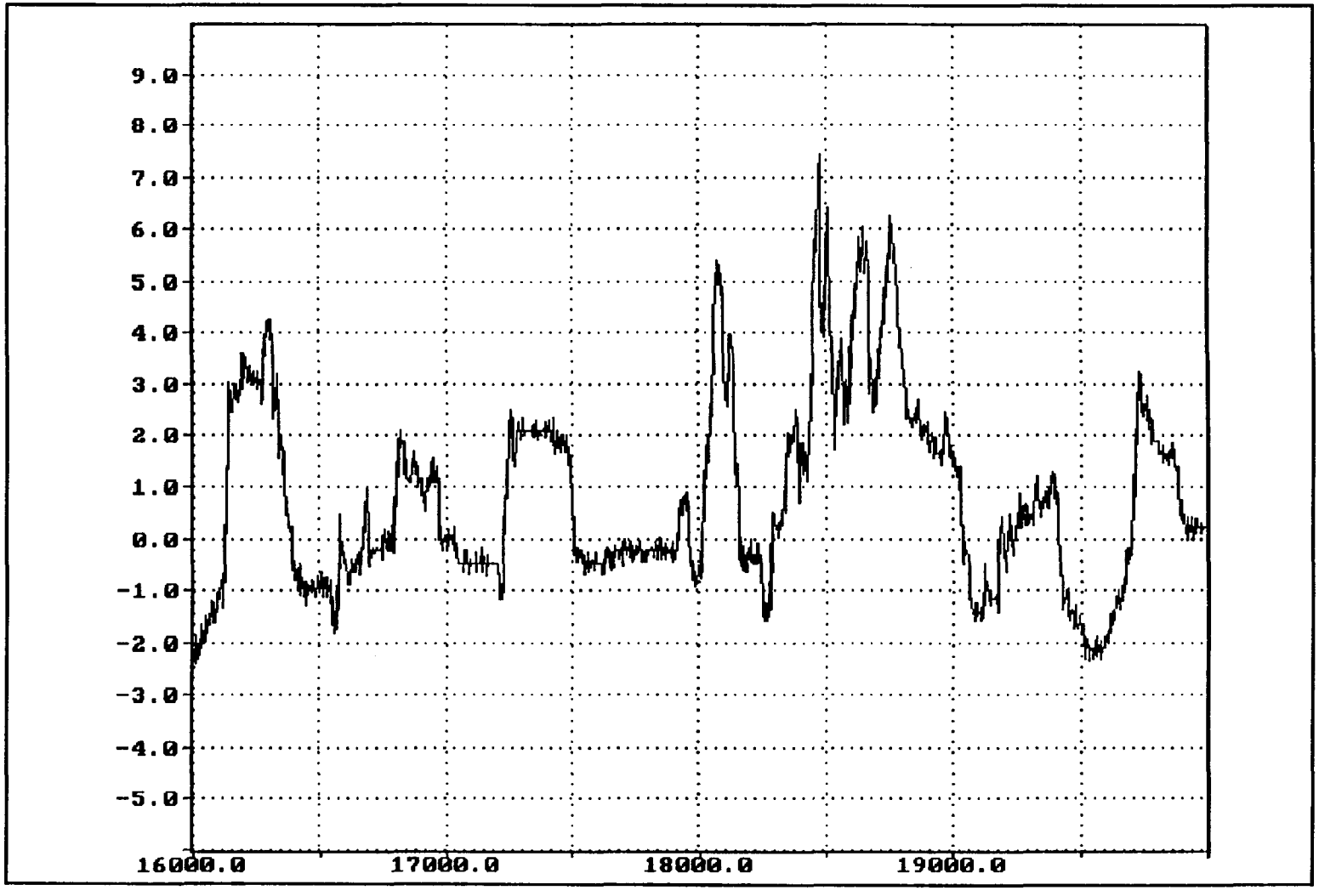

FIGURE A-4 Continued

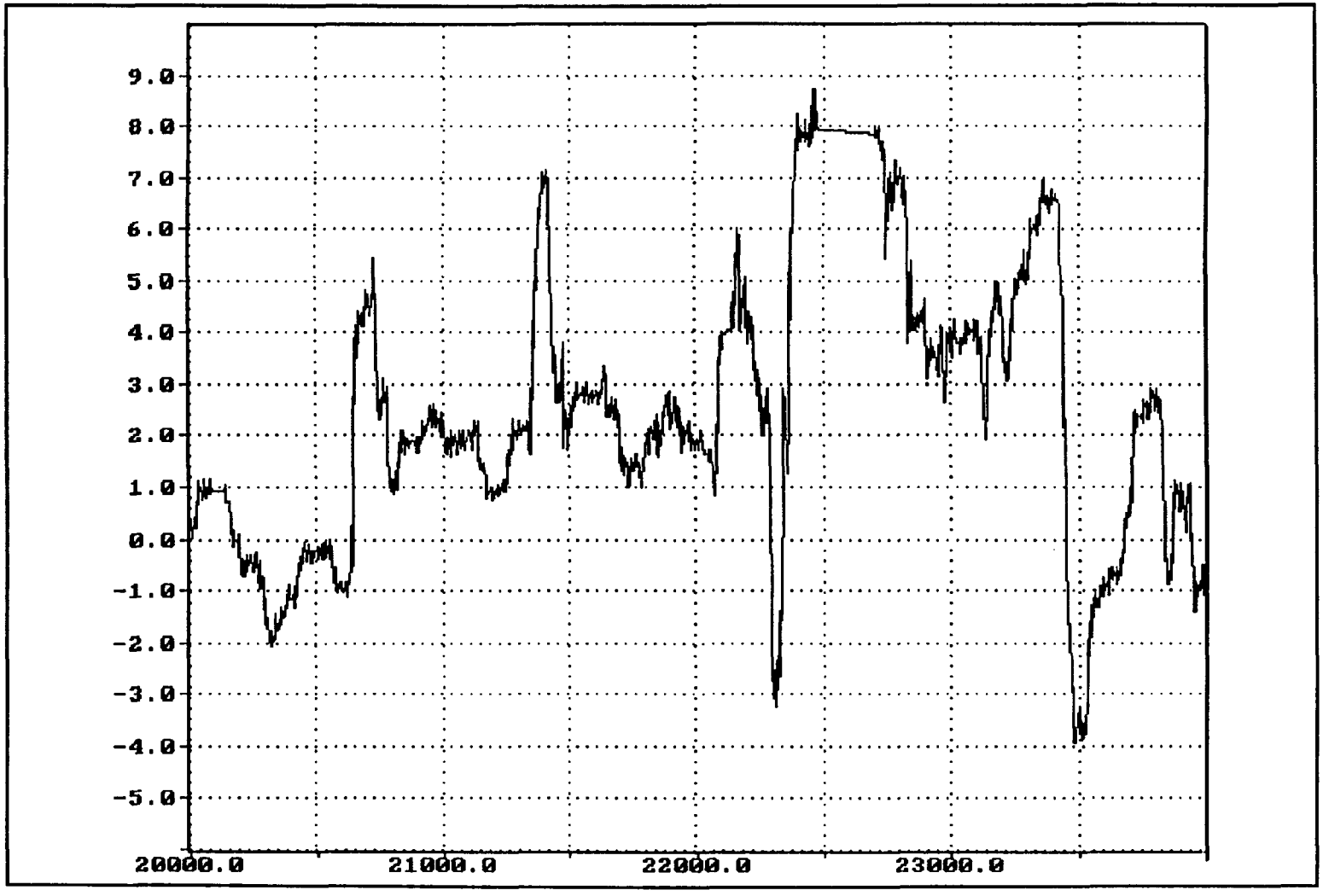

FIGURE A-4 Continued

APPENDIX B

VIBRATION EVENTS AND ENVELOPES

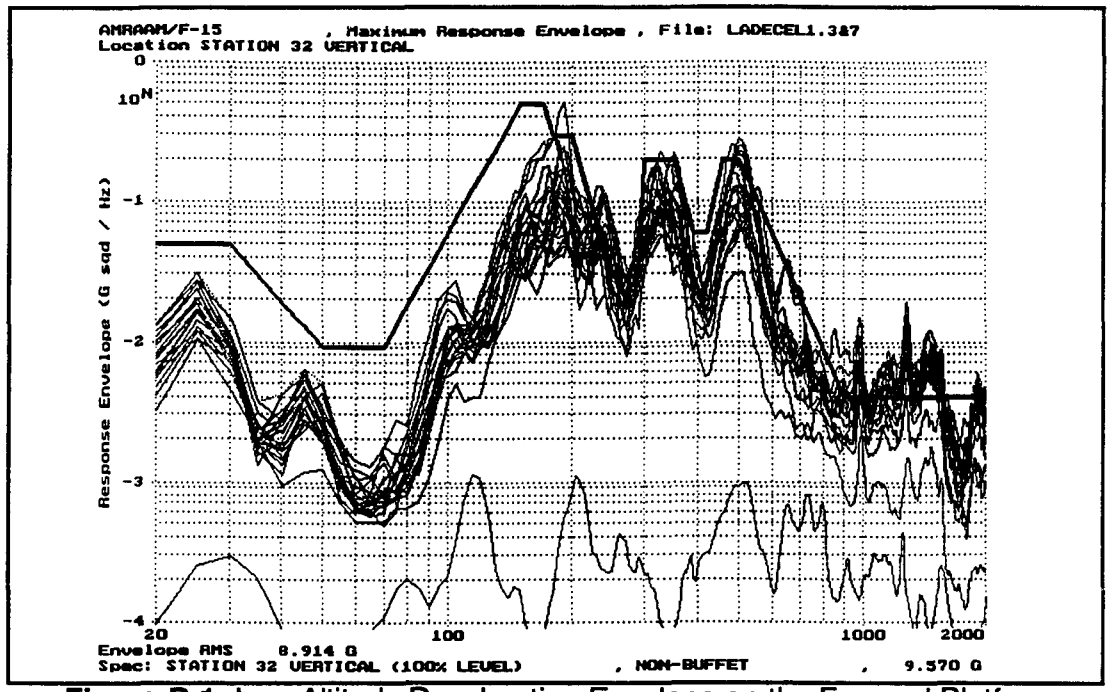

Figure B-1 Low Altitude Deceleration Envelope on the Forward Platform Location for Station 32 Vertical

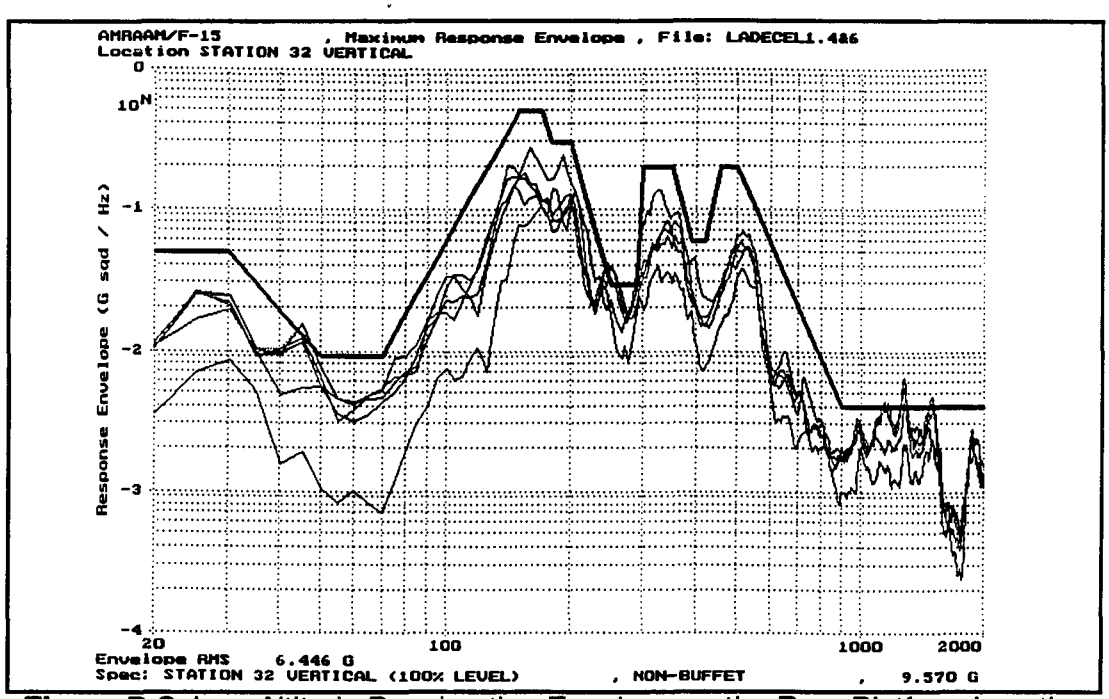

Figure B-2 Low Altitude Deceleration Envelope on the Rear Platform Location for Station 32 Vertical

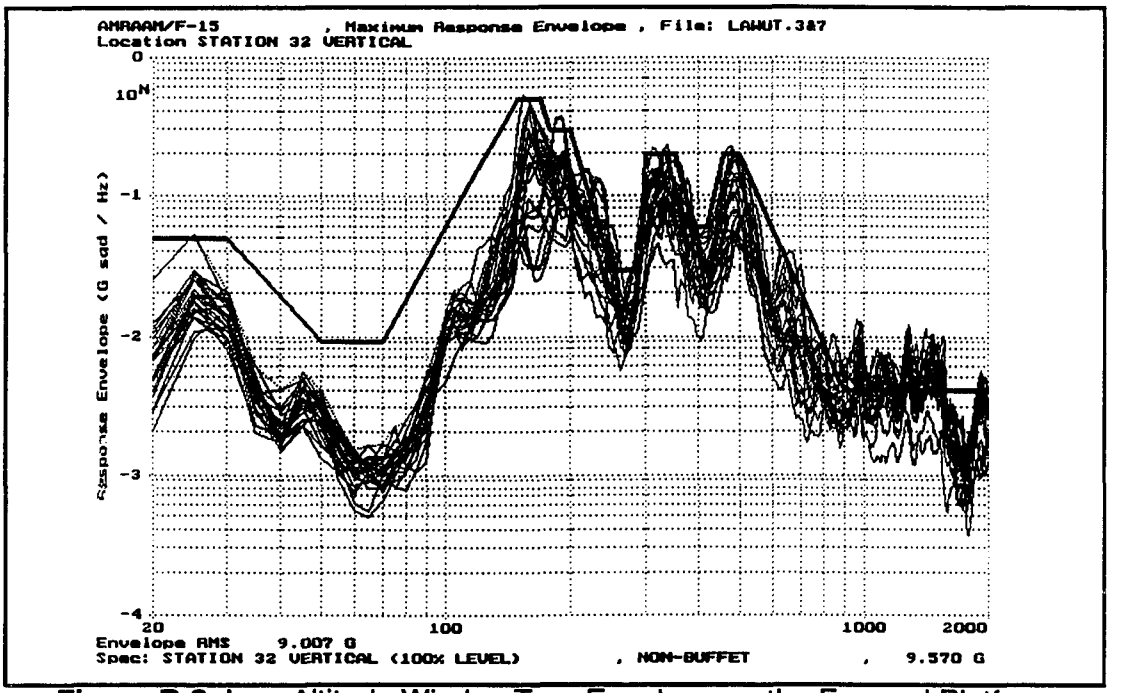

Figure B-3 Low Altitude Windup Turn Envelope on the Forward Platform Location for Station 32 Vertical

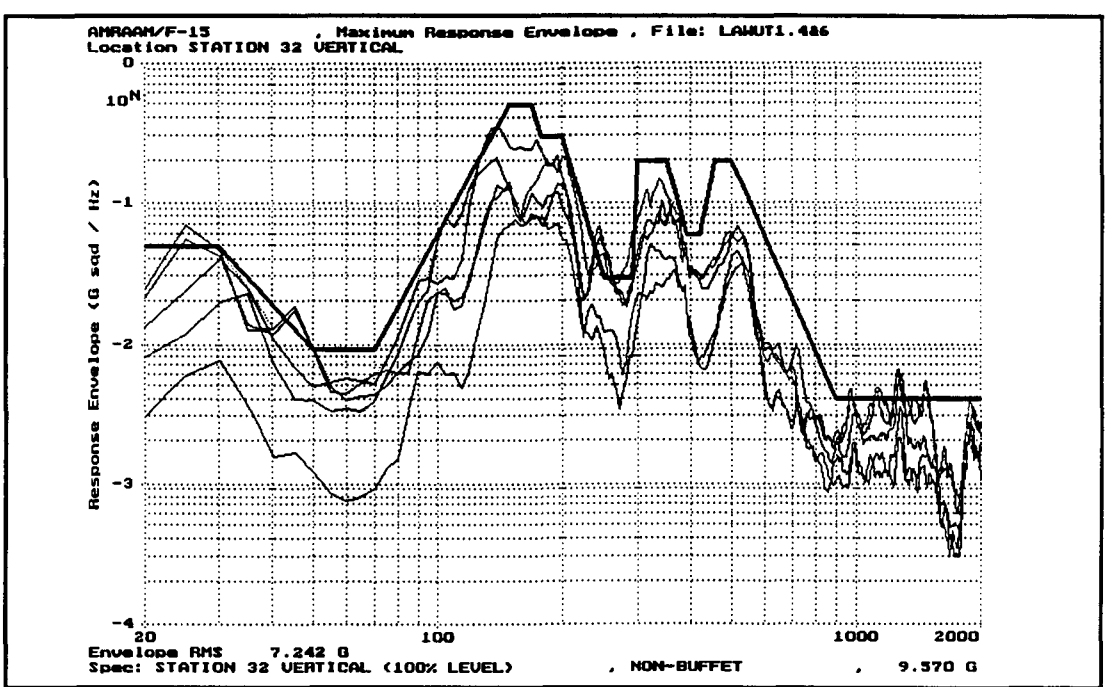

Figure B-4 Low Altitude Windup Turn Envelope on the Rear Platform Location for Station 32 Vertical

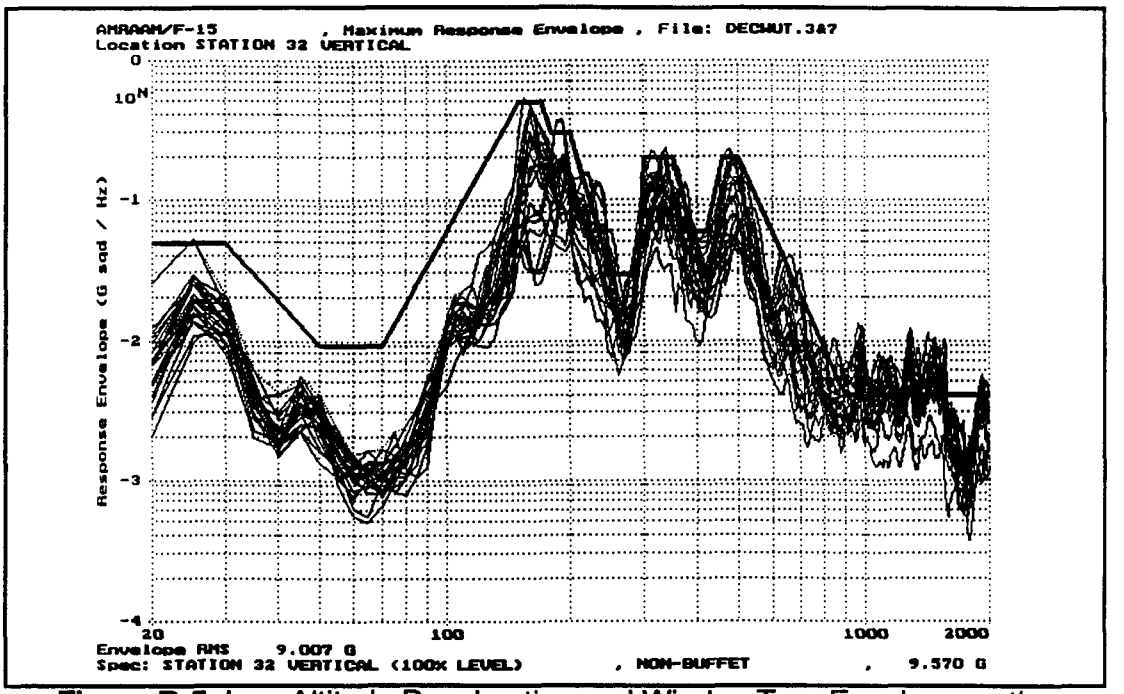

Figure B-5 Low Altitude Deceleration and Windup Turn Envelope on the Forward Platform Location for Station 32 Vertical

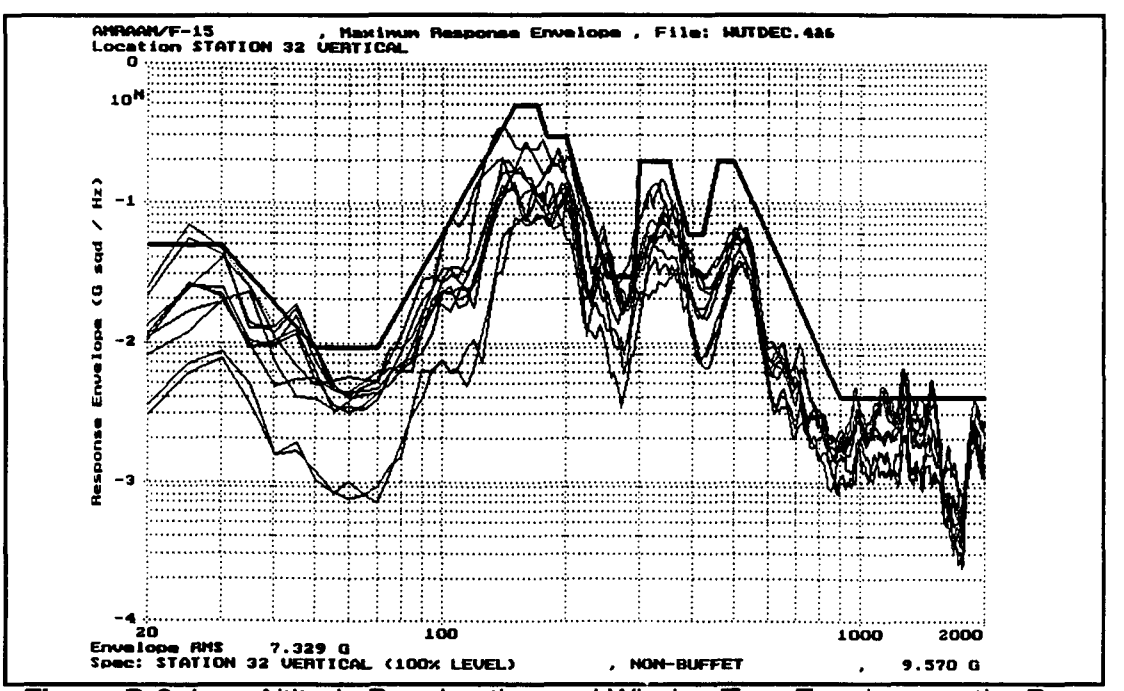

Figure B-6 Low Altitude Deceleration and Windup Turn Envelope on the Rear Platform Location for Station 32 Vertical

APPENDIX C

EQUIPMENT FINITE ELEMENT MODEL

This study assumes that the reader is familiar with NASTRAN and the techniques necessary to run a dynamic analysis. The two finite element models used in the course of this study to produce the results discussed in Chapter 5 now follow. The first listing contains the control cards and the input file for the supported equipment model that was used to produce the 100% vibration response envelope at station 32 vertical. The second listing contains the control cards and the input file for the supported section model that was also used to produce the 100% vibration response envelope at station 32 vertical. In order to run these models, one requires access to a commercial version of MSC NASTRAN. Essentially, only the vibration inputs (shown in Appendix D) need to be changed in both the equipment and the section models to obtain the appropriate responses at station 32 vertical (also shown in Appendix D).

Supported Equipment Model Listing for 100% Vibration Envelope

```
COMMAND=> TYPE LAU32VHF.DAT
ID AMRAAM, TEST
SOL 30
TIME 10
CEND
$
SUBTITLE = RANDOM ANALYSIS OF THE AMRAAM MOUNTED ON A LAU-106
$
$   THE MASS MOMENT OF INERTIA AND SHEAR AREA COEFFICIENTS ARE ADDED
$
SPC = 10
METHOD = 100
RANDOM = 110
FREQ = 120
LOADSET = 130
SDAMPING = 13
$
SET 31 = 5,9,10,14,16,21,22,27 $ ACCELEROMETERS AT 16,32,42,55,66,78,90,127
SET 41 = 2,3,4,5,6,7,8,9,10,12,13,14,18,19
$
LABEL= UNIT ACCELERATION IN THE Z PLANE. 32VH PSD. GRID 133
DLOAD = 1
$
SKIPON
DISPLACEMENT(SORT2,PHASE) = 31
FORCE(SORT2,PHASE) = 41
STRESS(SORT2,PHASE,VONMISES) = 41
SKIPOFF
$
OUTPUT(XYPLOT)
CSCALE = 1.8
PLOTTER NAST
XGRID = YES
YGRID = YES
XLOG = YES
YLOG = YES
$
$   ACCELERATION PSD OUTP
$
XTITLE = FREQUENCY (HERTZ)
YTITLE = ACCELERATION PSDF
XYPLOT ACCE PSDF /1(T3)/2(T3)/3(T3)/4(T3)/5(T3)/6(T3)/7(T3)
XYPLOT ACCE PSDF /8(T3)/9(T3)/10(T3)/11(T3)/12(T3)/13(T3)/14(T3)
XYPLOT ACCE PSDF /15(T3)/16(T3)/17(T3)/19(T3)/20(T3)/21(T3)
XYPLOT ACCE PSDF /22(T3)/23(T3)/24(T3)/25(T3)/26(T3)/27(T3)
XYPLOT ACCE PSDF /28(T3)/31(T3)/133(T3)
XYPRINT ACCE PSDF /1(T3)/2(T3)/3(T3)/4(T3)/5(T3)/6(T3)/7(T3)
XYPRINT ACCE PSDF /8(T3)/9(T3)/10(T3)/11(T3)/12(T3)/13(T3)/14(T3)
XYPRINT ACCE PSDF /15(T3)/16(T3)/17(T3)/19(T3)/20(T3)/21(T3)
XYPRINT ACCE PSDF /22(T3)/23(T3)/24(T3)/25(T3)/26(T3)/27(T3)
XYPRINT ACCE PSDF /28(T3)/31(T3)/133(T3)
$
$   FORCE PSD OUTPUT
$
YTITLE = BENDING MOMENT A2 FORCE PSDF
```

```
XYPLOT ELFORCE PSDF /2(3)/3(3)/4(3)/5(3)/6(3)/7(3)/8(3)/9(3)
XYPLOT ELFORCE PSDF /10(3)/12(3)/13(3)/14(3)/18(3)/19(3)/20(3)
XYPRINT ELFORCE PSDF /2(3)/3(3)/4(3)/5(3)/6(3)/7(3)/8(3)/9(3)
XYPRINT ELFORCE PSDF /10(3)/12(3)/13(3)/14(3)/18(3)/19(3)/20(3)
YTITLE = BENDING MOMENT B2 FORCE PSDF
XYPLOT ELFORCE PSDF /2(5)/3(5)/4(5)/5(5)/6(5)/7(5)/8(5)/9(5)
XYPLOT ELFORCE PSDF /10(5)/12(5)/13(5)/14(5)/18(5)/19(5)/20(5)
XYPRINT ELFORCE PSDF /2(5)/3(5)/4(5)/5(5)/6(5)/7(5)/8(5)/9(5)
XYPRINT ELFORCE PSDF /10(5)/12(5)/13(5)/14(5)/18(5)/19(5)/20(5)
YTITLE = SHEAR 2 FORCE PSDF
XYPLOT ELFORCE PSDF /2(7)/3(7)/4(7)/5(7)/6(7)/7(7)/8(7)/9(7)
XYPLOT ELFORCE PSDF /10(7)/12(7)/13(7)/14(7)/18(7)/19(7)/20(7)
XYPRINT ELFORCE PSDF /2(7)/3(7)/4(7)/5(7)/6(7)/7(7)/8(7)/9(7)
XYPRINT ELFORCE PSDF /10(7)/12(7)/13(7)/14(7)/18(7)/19(7)/20(7)
$
$   STRESS PSD OUTPUT
$
YTITLE = BENDING STRESS END A PSDF
XYPLOT STRESS PSDF /2(2)/3(2)/4(2)/5(2)/6(2)/7(2)/8(2)/9(2)
XYPLOT STRESS PSDF /10(2)/12(2)/13(2)/14(2)/18(2)/19(2)/20(2)
XYPRINT STRESS PSDF /2(2)/3(2)/4(2)/5(2)/6(2)/7(2)/8(2)/9(2)
XYPRINT STRESS PSDF /10(2)/12(2)/13(2)/14(2)/18(2)/19(2)/20(2)
YTITLE = BENDING STRESS END B PSDF
XYPLOT STRESS PSDF /2(12)/3(12)/4(12)/5(12)/6(12)/7(12)/8(12)/9(12)
XYPLOT STRESS PSDF /10(12)/12(12)/13(12)/14(12)/18(12)/19(12)/20(12)
XYPRINT STRESS PSDF /2(12)/3(12)/4(12)/5(12)/6(12)/7(12)/8(12)/9(12)
XYPRINT STRESS PSDF /10(12)/12(12)/13(12)/14(12)/18(12)/19(12)/20(12)
$
BEGIN BULK
$
$.....1..... $.....2..... $.....3..... $.....4..... $.....5..... $.....6..... $.....7..... $.....8..... $.....9..... $.....10.....
$
CBAR    1       1       1       2       19
CBAR    2       2       2       5       19
CBAR    3       3       5       7       19
CBAR    4       3       7       9       19
CBAR    5       13      9       10      19
CBAR    6       13      10      12      19
CBAR    7       13      12      14      19
CBAR    8       5       14      15      19
CBAR    9       5       15      16      19
CBAR    10      6       16      17      19
CBAR    11      6       17      20      19
CBAR    12      7       20      21      19
CBAR    13      7       21      22      19
CBAR    14      7       22      23      19
CBAR    15      7       23      24      19
CBAR    16      7       24      25      19
CBAR    17      7       25      26      19
CBAR    18      8       26      27      19
CBAR    19      9       27      28      19
CBAR    20      9       28      31      19
CBAR    21      10      4       6       19
CBAR    22      11      6       8       19
CBAR    23      11      8       9       19
CBAR    24      12      9       11      19
CBAR    25      12      11      12      19                                      CB25
CB25            56
CBAR    26      12      12      13      19                                      CB26
CB26    56
```

```
CBAR     27        12        13        14        19
CELAS2   41        15566.0 53          6         3
CELAS2   42        4330.8  3 3       4         3
CELAS2   43        5814.4  3 4       4         4
CELAS2   44        10.0+5  3 5       4         5
CELAS2   45        4330.8  3 2       4         2
CELAS2   46        10.0+5  3 6       4         6
CELAS2   47        15566.0 52          6         2
$
$.....1..... $.....2..... $.....3..... $.....4..... $.....5..... $.....6..... $.....7..... $.....8..... $.....9..... $.....10.....
$
$ONM2    EID       GRID      CID       MASS      X1        X2        X3                  ONM2
$ONM2    I11       I12       I22       I31       I32       I33
CONM2    1         1         0         0
CONM2    2         2         0         6.6                                             M2
M2       53.742    208                 208
CONM2
M3       14.983
CONM2    4         4         0         0.50302                                         M4
M4       4.076
CONM2    5         5         0         1.06023                                         M5
M5       8.633
CONM2    6         6         0         6.7201                                          M6
M6       54.72
CONM2    7         7         0         1.74988                                         M7
M7       14.245              20.1                20.1
CONM2    8         8         0         14.40605                                        M8
M8       117.305
CONM2    9         9         0         18.2817                                         M9
M9
CONM2    10        10        0         3.8786                                          M10
M10      51.582              70.3                70.3
CONM2    11        11        0         12                                              M11
M11      97.713
CONM2    12        12        0         11.84782                                        M12
M12      96.489              75.5                75.5
CONM2    13        13        0         2.74857                                         M13
M13      22.381
CONM2    14        14        0         11.56973                                        M14
M14      94.209              70.9                70.9
CONM2    15        15        0         15.85802                                        M15
M15      129.126             96.1                96.1
CONM2    16        16        0         9.23033                                         M16
M16      75.16               40.6                40.6
CONM2    17        17        0         2.38858                                         M17
M17      19.45
CONM2    20        20        0         18.02666                                        M20
M20      146.786             79.3                79.3
CONM2    21        21        0         28.82384                                        M21
M21      234.705             328                 328
CONM2    22        22        0         26.89761                                        M22
M22      219.02              307                 307
CONM2    23        23        0         25.30467                                        M23
M23      206.405             153                 153
CONM2    24        24        0         26.99207                                        M24
M24      219.785             227                 227
CONM2    25        25        0         27.13995                                        M25
M25      220.992             309                 309
CONM2    26        26        0         13.67676                                        M26
M26      111.366             115                 115
```

```
CONM2   27      27      0       15.56258                                        M27
M27     126.722
CONM2   28      28      0       18.70046                                        M28
M28     152.275         157             157
CONM2   31      31      0       4.89278                                         M31
M31     39.841          31.5            31.5
$
$.....1..... $.....2..... $.....3..... $.....4..... $.....5..... $.....6..... $.....7..... $.....8..... $.....9..... $.....10.....
$
$       TELEMETRY MODEL
$
CONM2   91      20      -1      1.075   71.04   3.5355  3.5355          M91
M91     2.093           7.8                     7.8
CONM2   92      20      -1      1.075   71.04   -3.5355 3.5355          M92
M92     2.093           7.8                     7.8
CONM2   93      20      -1      1.075   71.04   3.5355  -3.5355         M93
M93     2.093           7.8                     7.8
CONM2   94      20      -1      1.075   71.04   -3.5355 -3.5355         M94
M94     2.093           7.8                     7.8
CONM2   95      28      -1      2.715   134.06  4.0305  4.0305          M95
M95     8.71            31.32                   31.32
CONM2   96      28      -1      2.715   134.06  -4.0305 4.0305          M96
M96   8 8.71            31.32                   31.32
CONM2   97      28      -1      2.715   134.06  4.0305  -4.0305         M97
M97   8 8.71            31.32                   31.32
CONM2   98      28      -1      2.715   134.06  -4.0305 -4.0305         M98
M98   8 8.71            31.32                   31.32
$
$       SELECT APPROPRIATE FREQUENCY RANGE
$
EIGR    100     MGIV    20      500                                             EIGR10
EIGR10  MASS
$
$.....1..... $.....2..... $.....3..... $.....4..... $.....5..... $.....6..... $.....7..... $.....8..... $.....9..... $.....10.....
$
GRID    1       0       -3.20   0       0
GRID    2       0       10.12   0       0
GRID    3       0       13.55   0       0
GRID    4       0       13.55   0       0
GRID    5       0       16.20   0       0
GRID    6       0       16.20   0       0
GRID    7       0       24.12   0       0
GRID    8       0       24.12   0       0
GRID    9       0       32.03   0       0
GRID    10      0       42.00   0       0
GRID    11      0       41.17   0       0
GRID    12      0       50.31   0       0
GRID    13      0       52.98   0       0
GRID    14      0       55.65   0       0
GRID    15      0       61.15   0       0
GRID    16      0       65.70   0       0
GRID    17      0       68.58   0       0
GRID    19      0       68.58   6.4     0                       123456
GRID    20      0       69.60   0       0
GRID    21      0       78.90   0       0
GRID    22      0       90.63   0       0
GRID    23      0       97.50   0       0
GRID    24      0       106.80  0       0
GRID    25      0       116.10  0       0
GRID    26      0       125.40  0       0
```

```
GRID    27      0       127.90  0       0
GRID    28      0       134.89  0       0
GRID    31      0       140.67  0       0
MAT1    64      16.0+6          0.290   0
MAT1    177     29.0+6          0.318   0
MAT1    4140    29.0+6          0.318   0
MAT1    6061    10.0+6          0.333   0
MAT1    9606    18.0+6          0.260   0
$
$       ELIMINATE NULL COLUMNS IN MASS AND STIFFNESS MATRICES
$
PARAM   ASING   1
PARAM   AUTOSPC YES
$
PARAM   GRDPNT  0
$
$        DEFINE MULTIPLICATION FACTOR TO CONVERT WEIGHT INTO MASS
$
PARAM   WTMASS  0.00259
$
$.....1..... $.....2..... $.....3..... $.....4..... $.....5..... $.....6..... $.....7..... $.....8..... $.....9..... $.....10.....
$
PBAR    1       9606    3.14    6.28    6.28    12.56                           P01A
P01A    2.474874 2.474874 -2.47487 2.474874 -2.47487 -2.47487 2.474874 -2.47487 P01B
P01B    0.5306  0.5306
PBAR    2       9606    5.12    26.96   26.96   53.92                           P02A
P02A    2.474874 2.474874 -2.47487 2.474874 -2.47487 -2.47487 2.474874 -2.47487 P02B
P02B    0.5306  0.5306
PBAR    3       64      0.9832  5.8452  5.8452  11.6904                         P03A
P03A    2.474874 2.474874 -2.47487 2.474874 -2.47487 -2.47487 2.474874 -2.47487 P03B
P03B    0.5306  0.5306
PBAR    4       177     0.9946  5.296   5.296   10.592                          P04A
P04A    2.474874 2.474874 -2.47487 2.474874 -2.47487 -2.47487 2.474874 -2.47487 P04B
P04B    0.5306  0.5306
PBAR    5       4140    8.3     45.16   45.16   90.32                           P05A
P05A    2.474874 2.474874 -2.47487 2.474874 -2.47487 -2.47487 2.474874 -2.47487 P05B
P05B    0.5306  0.5306
PBAR    6       4140    4.25    24.36   24.36   48.72                           P06A
P06A    2.474874 2.474874 -2.47487 2.474874 -2.47487 -2.47487 2.474874 -2.47487 P06B
P06B    0.5306  0.5306
PBAR    7       4140    1.3946  8.3862  8.3862  16.7724                         P07A
P07A    2.474874 2.474874 -2.47487 2.474874 -2.47487 -2.47487 2.474874 -2.47487 P07B
P07B    0.5306  0.5306
PBAR    8       177     0.9746  5.296   5.296   10.592                          P08A
P08A    2.474874 2.474874 -2.47487 2.474874 -2.47487 -2.47487 2.474874 -2.47487 P08B
P08B    0.5306  0.5306
PBAR    9       177     5       9       9       18                              P09A
P09A    2.474874 2.474874 -2.47487 2.474874 -2.47487 -2.47487 2.474874 -2.47487 P09B
P09B    0.5306  0.5306
PBAR    10      6061    1       2       2       4                               P10A
P10A    2.474874 2.474874 -2.47487 2.474874 -2.47487 -2.47487 2.474874 -2.47487 P10B
P10B    0.5306  0.5306
PBAR    11      6061    0.4     0.66    0.66    1.32                            P11A
P11A    2.474874 2.474874 -2.47487 2.474874 -2.47487 -2.47487 2.474874 -2.47487 P11B
P11B    0.5306  0.5306
PBAR    12      6061    0.7854  2.454   2.454   4.908                           P12A
P12A    2.474874 2.474874 -2.47487 2.474874 -2.47487 -2.47487 2.474874 -2.47487 P12B
P12B    0.5306  0.5306
PBAR    13      64      1.0004  5.5629  6.1393  11.702                          P13A
P13A    2.474874 2.474874 -2.47487 2.474874 -2.47487 -2.47487 2.474874 -2.47487 P13B
```

```
P13B    0.5306  0.5306
$
$       ALLOW Z TRANSLATION, Y ROTATION
$
SPC1    10      1246    1       THRU    9
SPC1    10      1246    11      THRU    15
SPC1    10      1246    17      20      21
SPC1    10      1246    23      THRU    28
SPC1    10      1246    31
$
$       LAUNCHER
$
$       Hook and swaybrace grid points
$
GRID    124     0       42      0       3.5
GRID    125     0       42      0       3.5
GRID    126     0       42      0       3.5
GRID    127     0       65.7    0       4.398
GRID    128     0       65.7    0       4.398
GRID    129     0       65.7    0       4.398
GRID    130     0       90.63   0       4.371
GRID    131     0       90.63   0       4.371
GRID    132     0       90.63   0       4.371
$
$       Connect model to hook and swaybrace points
$
RBE2    140     124     235     10
SPC1    10      146     10      124
RBE2    141     127     123456  16
RBE2    142     130     234     22
SPC1    10      156     22      130
$
$       Ejection launcher
$
GRID    133     0       65.7    0       7.5
RBE2    143     133     3       126     129     132
SPC1    10      12456   126     129     132     133
$
$       Concentrated mass at grid point 133
$
CONM2   100     133     0       1.0+8
$
$       Springs between launcher, swaybrace, and hooks
$
CELAS2  1       3.70+4  125     2       124     2
CELAS2  2       1.25+4  126     2       125     2
CELAS2  3       1.44+6  129     1       127     1
CELAS2  4       1.44+6  128     2       127     2
CELAS2  5       9.99+6  129     3       127     3
CELAS2  6       1.56+5  129     4       127     4
CELAS2  7       1.56+5  129     5       127     5
CELAS2  8       1.18+5  129     6       127     6
CELAS2  9       4.00+4  129     2       128     2
CELAS2  10      6.01+5  131     2       130     2
CELAS2  11      4.79+6  132     3       130     3
CELAS2  12      5.73+6  131     4       130     4
CELAS2  13      4.00+4  132     2       131     2
CELAS2  14      6.40+5  132     4       131     4
$
$       Constraints for intermediary series spring grid points
```

```
$
SPC1     10        13456     125       128
SPC1     10        1356      131
$
$        FREQUENCY RESPONSE ANALYSIS (WHITE NOISE BASE EXCITATION)
$
PARAM    NEWSEQ 3
PARAM    COUPMA!
$
$        FREQUENCY SELECTION
$
FREQ1    120       20        5         96
$
$        STRUCTURAL DAMPING
$
TABDMP1,13 ,,,,,,,,+DAMP          $ 3% DAMPING FOR ALL FREQUENCIES
DAMP,0.0,0.0,1.0,0.03,500.0,0.03,501.0,0.0,DAMP2
DAMP2,ENDT
$
$        APPLIED LOADING
$
LSEQ     130       10        1
RLOAD1   1         10                            150
DAREA    10        133       3         1.0+8
TABLED1,150,,,,,,,,TABD
TABD,0.0,1.0,500.0,1.0,1000.0,1.0,ENDT
$
$        RANDOM ANALYSIS DATA
$
RANDPS,110, 1, 1,1.,,140
TABRND1,140,,,,,,,,TR1A
TR1A     20        0.31312   25        0.05587   30        0.00355   35        0.00170   TR1B
TR1B     40        0.00575   45        0.00804   50        0.00861   55        0.01146   TR1C
TR1C     60        0.01428   65        0.01721   70        0.02044   75        0.03481   TR1D
TR1D     80        0.05859   85        0.09961   90        0.17396   95        0.32633   TR1E
TR1E     100       0.71475   105       2.33285   110       26.93140  115       2.55711   TR1F
TR1F     120       0.37974   125       0.06449   130       0.00660   135       0.04635   TR1G
TR1G     140       0.19462   145       0.64793   150       3.07731   155       4.77448   TR1H
TR1H     160       0.39335   165       0.04421   170       0.00571   175       0.01553   TR1I
TR1I     180       0.02846   185       0.04842   190       0.07303   195       0.11106   TR1J
TR1J     200       0.21333   205       0.02732   210       0.02376   215       0.02675   TR1K
TR1K     220       0.02606   225       0.02377   230       0.02099   235       0.01821   TR1L
TR1L     240       0.01566   245       0.01344   250       0.01147   255       0.01198   TR1M
TR1M     260       0.01246   265       0.01294   270       0.01344   275       0.01403   TR1N
TR1N     280       0.01480   285       0.01572   290       0.01321   295       0.03020   TR1O
TR1O     300       0.08184   305       0.08516   310       0.08740   315       0.08896   TR1P
TR1P     320       0.09007   325       0.09085   330       0.09137   335       0.09168   TR1Q
TR1Q     340       0.09182   345       0.09179   350       0.09164   355       0.07797   TR1R
TR1R     360       0.06643   365       0.05674   370       0.04863   375       0.04190   TR1S
TR1S     380       0.03642   385       0.03220   390       0.02903   395       0.02898   TR1T
TR1T     400       0.01764   405       0.00924   410       0.00827   415       0.00774   TR1U
TR1U     420       0.00674   425       0.00625   430       0.00513   435       0.00370   TR1V
TR1V     440       0.00300   445       0.00577   450       0.02305   455       0.28412   TR1W
TR1W     460       8.59468   465       1.72981   470       1.00254   475       0.74025   TR1X
TR1X     480       0.59765   485       0.50754   490       0.44605   495       0.40188   TR1Y
TR1Y     500       0.36892   ENDT
RANDT1,110,100,0.,,1
$
ENDDATA
```

Supported Section Model Input File Listing

```
COMMAND=> TYPE SECST32VHF.D.
ID AMRAAM, TEST
SOL 30
TIME 10
CEND
$
SUBTITLE = RANDOM ANALYSIS ON THE AMRAAM SECTION W/ SHAKER TABLE
$
$   THE MASS MOMENT OF INERTIA AND SHEAR AREA COEFFICIENTS ARE ADDED
$
SPC = 10
METHOD = 100
RANDOM = 110
FREQ = 120
LOADSET = 130
SDAMPING = 13
$
SET 31 = 5,9,14   $ ACCELEROMETERS AT 16,32
SET 41 = 2,3,4,5,7,23,24,27
$
LABEL= UNIT ACCELERATION IN THE Z PLANE. 32VH PSD. GRID 24
DLOAD = 1
$
SKIPON
DISPLACEMENT(SORT2,PHASE) = 31
FORCE(SORT2,PHASE) = 41
STRESS(SORT2,PHASE,VONMISES) = 41
SKIPOFF
$
OUTPUT(XYPLOT)
CSCALE = 1.8
PLOTTER NAST
XGRID = YES
YGRID = YES
XLOG = YES
YLOG = YES
$
$   ACCELERATION PSD OUTPUT
$
XTITLE = FREQUENCY (HERTZ)
YTITLE = ACCELERATION PSDF
XYPLOT ACCE PSDF /1(T3)/2(T3)/3(T3)/4(T3)/5(T3)/6(T3)/7(T3)
XYPLOT ACCE PSDF /8(T3)/9(T3)/10(T3)/11(T3)/12(T3)/13(T3)/14(T3)
XYPLOT ACCE PSDF /19(T3)/20(T3)/21(T3)/22(T3)/23(T3)/24(T3)
XYPRINT ACCE PSDF /1(T3)/2(T3)/3(T3)/4(T3)/5(T3)/6(T3)/7(T3)
XYPRINT ACCE PSDF /8(T3)/9(T3)/10(T3)/11(T3)/12(T3)/13(T3)/14(T3)
XYPRINT ACCE PSDF /19(T3)/20(T3)/21(T3)/22(T3)/23(T3)/24(T3)
$
$   FORCE PSD OUTPUT
$
YTITLE = BENDING MOMENT A2 FORCE PSDF
XYPLOT ELFORCE PSDF /2(3)/3(3)/4(3)/5(3)/7(3)/23(3)/24(3)/27(3)
XYPRINT ELFORCE PSDF /2(3)/3(3)/4(3)/5(3)/7(3)/23(3)/24(3)/27(3)
YTITLE = BENDING MOMENT B2 FORCE PSDF
XYPLOT ELFORCE PSDF /2(5)/3(5)/4(5)/5(5)/7(5)/23(5)/24(5)/27(5)
```

```
XYPRINT ELFORCE PSDF /2(5)/3(5)/4(5)/5(5)/7(5)/23(5)/24(5)/27(5)
YTITLE = SHEAR 2 FORCE PSDF
XYPLOT ELFORCE PSDF /2(7)/3(7)/4(7)/5(7)/7(7)/23(7)/24(7)/27(7)
XYPRINT ELFORCE PSDF /2(7)/3(7)/4(7)/5(7)/7(7)/23(7)/24(7)/27(7)
$
$   STRESS PSD OUTPL
$
YTITLE = BENDING STRESS END A PSDF
XYPLOT STRESS PSDF /2(2)/3(2)/4(2)/5(2)/7(2)/23(2)/24(2)/2
XYPRINT STRESS PSDF /2(2)/3(2)/4(2)/5(2)/7(2)/23(2)/24(2)/27(2)
YTITLE = BENDING STRESS END B PSDF
XYPLOT STRESS PSDF /2(12)/3(12)/4(12)/5(12)/7(12)/23(12)/24(12)/27(12)
XYPRINT STRESS PSDF /2(12)/3(12)/4(12)/5(12)/7(12)/23(12)/24(12)/27(12)
$
BEGIN BULK
$
$.....1..... $.....2..... $.....3..... $.....4..... $.....5..... $.....6..... $.....7..... $.....8..... $.....9..... $.....10.....
$
CBAR     1       1       1       2       19
CBAR     2       2       2       5       19
CBAR     3       3       5       7       19
CBAR     4       3       7       9       19
CBAR     5       13      9       10      19
CBAR     6       13      10      12      19
CBAR     7       13      12      14      19
CBAR     21      10      4       6       19
CBAR     22      11      6       8       19
CBAR     23      11      8       9       19
CBAR     24      12      9       11      19
CBAR     25      12      11      12      19                                      CB25
CB25             56
CBAR     26      12      12      13      19                                      CB26
CB26     56
CBAR     27      12      13      14      19
CELAS2   41      15566   5       3       6       3
CELAS2   42      4330.8  3       3       4       3
CELAS2   43      5814.4  3       4       4       4
CELAS2   44      10.0+5  3       5       4       5
CELAS2   45      4330.8  3       2       4       2
CELAS2   46      10.0+5  3       6       4       6
CELAS2   47      15566   5       2       6       2
$
$.....1..... $.....2..... $.....3..... $.....4..... $.....5..... $.....6..... $.....7..... $.....8..... $.....9..... $.....10.....
$
$CONM2   EID     GRID    CID     MASS    X1      X2      X3                      ONM2
$ONM2    I11     I12     I22     I31     I32     I33
CONM2    1       1       0       0
CONM2    2       2       0       6.6                                             M2
M2       53.742          208                     208
CONM2    3       3       0       1.84                                            M3
M3       14.983
CONM2    4       4       0       0.50302                                         M4
M4       4.076
CONM2    5       5       0       1.06023                                         M5
M5       8.633
```

```
CONM2   6       6       0       6.7201                                  M6
M6      54.72
CONM2   7       7       0       1.74988                                 M7
M7      14.245          20.1                    20.1
CONM2   8       8       0       14.40605                                M8
M8      117.305
CONM2   9       9       0       18.2817                                 M9
M9      148.863         121                     121
CONM2   10      10      0       3.8786                                  M10
M10     51.582          70.3                    70.3
CONM2   11      11      0       12                                      M11
M11     97.713
CONM2   12      12      0       11.84782                                M12
M12     96.489          75.5                    75.5
CONM2   13      13      0       2.74857                                 M13
M13     22.381
CONM2   14      14      0       11.56973                                M14
M14     94.209          70.9                    70.9
$
$       SELECT APPROPRIATE FREQUENCY RANGE
$
EIGR    100     MGIV    20      500                                     EIGR10
EIGR10  MASS
$
$.....1..... $.....2..... $.....3..... $.....4..... $.....5..... $.....6..... $.....7..... $.....8..... $.....9..... $.....10.....
$
GRID    1       0       -3.2    0       0
GRID    2       0       10.12   0       0
GRID    3       0       13.55   0       0
GRID    4       0       13.55   0       0
GRID    5       0       16.2    0       0
GRID    6       0       16.2    0       0
GRID    7       0       24.12   0       0
GRID    8       0       24.12   0       0
GRID    9       0       32.03   0       0
GRID    10      0       42      0       0
GRID    11      0       41.17   0       0
GRID    12      0       50.31   0       0
GRID    13      0       52.98   0       0
GRID    14      0       55.65   0       0
GRID    19      0       68.58   6.4     0                       123456
MAT1    64      16.0+6          0.29    0
MAT1    6061    10.0+6          0.333   0
MAT1    9606    18.0+6          0.26    0
$
$       ELIMINATE NULL COLUMNS IN MASS AND STIFFNESS MATRICES
$
PARAM   ASING   1
PARAM   AUTOSPC YES
$
PARAM   GRDPNT  0
$
$       DEFINE MULTIPLICATION FACTOR TO CONVERT WEIGHT INTO MASS
$
PARAM   WTMASS  0.0025901
```

```
$
$.....1..... $.....2..... $.....3..... $.....4..... $.....5..... $.....6..... $.....7..... $.....8..... $.....9..... $.....10.....
$
PBAR     1        9606     3.14     6.28     6.28     12.56                                 P01A
P01A     2.474874 2.474874 -2.47487 2.474874 -2.47487 -2.47487 2.474874 -2.47487 P01B
P01B     0.5306   0.5306
PBAR     2        9606     5.12     26.96    26.96    53.92                                 P02A
P02A     2.474874 2.474874 -2.47487 2.474874 -2.47487 -2.47487 2.474874 -2.47487 P02B
P02B     0.5306   0.5306
PBAR     3        64       0.9832   5.8452   5.8452   11.6904                               P03A
P03A     2.474874 2.474874 -2.47487 2.474874 -2.47487 -2.47487 2.474874 -2.47487 P03B
P03B     0.5306   0.5306
PBAR     10       6061     1        2        2        4                                     P10A
P10A     2.474874 2.474874 -2.47487 2.474874 -2.47487 -2.47487 2.474874 -2.47487 P10B
P10B     0.5306   0.5306
PBAR     11       6061     0.4      0.66     0.66     1.32                                  P11A
P11A     2.474874 2.474874 -2.47487 2.474874 -2.47487 -2.47487 2.474874 -2.47487 P11B
P11B     0.5306   0.5306
PBAR     12       6061     0.7854   2.454    2.454    4.908                                 P12A
P12A     2.474874 2.474874 -2.47487 2.474874 -2.47487 -2.47487 2.474874 -2.47487 P12B
P12B     0.5306   0.5306
PBAR     13       64       1.0004   5.5629   6.1393   11.702                                P13A
P13A     2.474874 2.474874 -2.47487 2.474874 -2.47487 -2.47487 2.474874 -2.47487 P13B
P13B     0.5306   0.5306
$
$        ATTACH MISSILE SECTION TO SHAKER TABLE AT LOCATIONS 32 AND 55
$
GRID     20       0        32.03    0        5
GRID     21       0        55.65    0        5
GRID     22       0        32.03    0        5
GRID     23       0        55.65    0        5
GRID     24       0        43.84    0        5
$
$        SECTION AND SHAKER TABLE CONNECTIONS
$
RBE2     100      20       135      9
SPC1     10       246      9        20
RBE2     101      21       3        14
RBE2     102      24       3        22       23
SPC1     10       12456    14       21       22       23       24
$
$        SPRING COMPONENT FOR DUAL GRID POINTS
$
CELAS2   51       1.0+5    20       1        22       1
CELAS2   52       1.0+7    20       3        22       3
CELAS2   53       1.0+6    20       5        22       5
CELAS2   54       1.0+7    21       3        23       3
$
$        CONCENTRATED MASS AT GRID POINT 24
$
CONM2    15       24       0        1.0+8
$
$        MODEL CONSTRAINTS
$
SPC1     10       1246     1        THRU     8
```

```
SPC1      10        1246      10        THRU      13
$
$         FREQUENCY RESPONSE ANALYSIS (WHITE NOISE BASE EXCITATION)
$
PARAM     NEWSEQ    3
PARAM     COUPMASS1
$
$         FREQUENCY SELECTION
$
FREQ1     120       20        5         96
$
$         STRUCTURAL DAMPING
$
TABDMP1,13 ,,,,,,,,DAMP          $ 3% DAMPING FOR ALL FREQUENCIES
DAMP,0.0,0.0,1.0,0.03,500.0,0.03,501.0,0.0,+DAMP2
DAMP2,ENDT
$
$         APPLIED LOADING
$
LSEQ      130       10        1
RLOAD1    1         10                            150
DAREA     10        24        3         1.0+8
TABLED1,150,,,,,,,,TABD
TABD,0.0,1.0,500.0,1.0,1000.0,1.0,ENDT
RANDPS,110, 1, 1,1.,,140
TABRND1,140,,,,,,,,TR1A
$
$.....1..... $.....2..... $.....3..... $.....4..... $.....5..... $.....6..... $.....7..... $.....8..... $.....9..... $.....10.....
$
TR1A      20        8.01+5    25        3.14+5    30        1.43+5    35        4.37+4    TR1B
TR1B      40        1.49+4    45        5.71+3    50        2.32+3    55        1.35+3    TR1C
TR1C      60        7.79+2    65        4.36+2    70        2.29+2    75        1.53+2    TR1D
TR1D      80        7.69+1    85        1.81+1    90        7.49+0    95        1.03+2    TR1E
TR1E      100       4.15+2    105       1.17+3    110       2.91+3    115       7.08+3    TR1F
TR1F      120       1.89+4    125       6.89+4    130       6.51+5    135       1.86+5    TR1G
TR1G      140       3.46+4    145       9.75+3    150       2.12+3    155       5.13+2    TR1H
TR1H      160       3.42+3    165       1.29+4    170       4.27+4    175       1.55+5    TR1I
TR1I      180       3.18+5    185       4.81+4    190       1.15+4    195       2.67+3    TR1J
TR1J      200       1.41+3    205       8.93+3    210       6.20+4    215       4.30+4    TR1K
TR1K      220       1.10+4    225       4.24+3    230       1.99+3    235       1.04+3    TR1L
TR1L      240       5.77+2    245       3.35+2    250       1.98+2    255       1.46+2    TR1M
TR1M      260       1.08+2    265       7.85+1    270       5.61+1    275       3.84+1    TR1N
TR1N      280       2.43+1    285       1.34+1    290       7.81+0    295       6.93+1    TR1O
TR1O      300       8.30+2    305       5.79+2    310       3.04+2    315       1.81+2    TR1P
TR1P      320       1.15+2    325       7.50+1    330       4.88+1    335       3.10+1    TR1Q
TR1Q      340       1.89+1    345       1.06+1    350       3.53+0    355       1.90+0    TR1R
TR1R      360       6.34-1    365       5.44-1    370       1.05+0    375       1.81+0    TR1S
TR1S      380       2.62+0    385       3.39+0    390       4.03+0    395       5.25+0    TR1T
TR1T      400       6.55+0    405       7.92+0    410       9.35+0    415       1.08+1    TR1U
TR1U      420       1.23+1    425       1.62+1    430       2.11+1    435       2.70+1    TR1V
TR1V      440       3.43+1    445       4.33+1    450       5.41+1    455       6.71+1    TR1W
TR1W      460       8.29+1    465       8.79+1    470       9.30+1    475       9.79+1    TR1X
TR1X      480       1.03+2    485       1.08+2    490       1.12+2    495       1.17+2    TR1Y
TR1Y      500       1.22+2    ENDT
RANDT1,110,100,0.,,1
$
ENDDATA
```

APPENDIX D

VIBRATION INPUTS, TRANSMISSIBILITIES AND RESPONSES

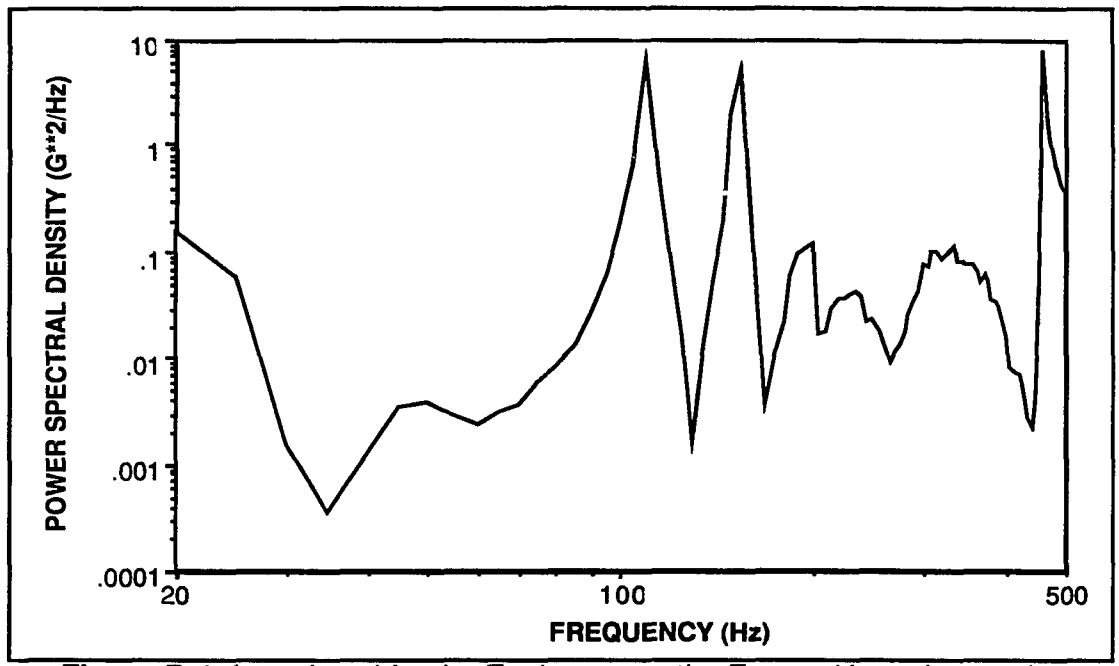

Figure D-1 Input Level for the Equipment at the Forward Location on the Platform

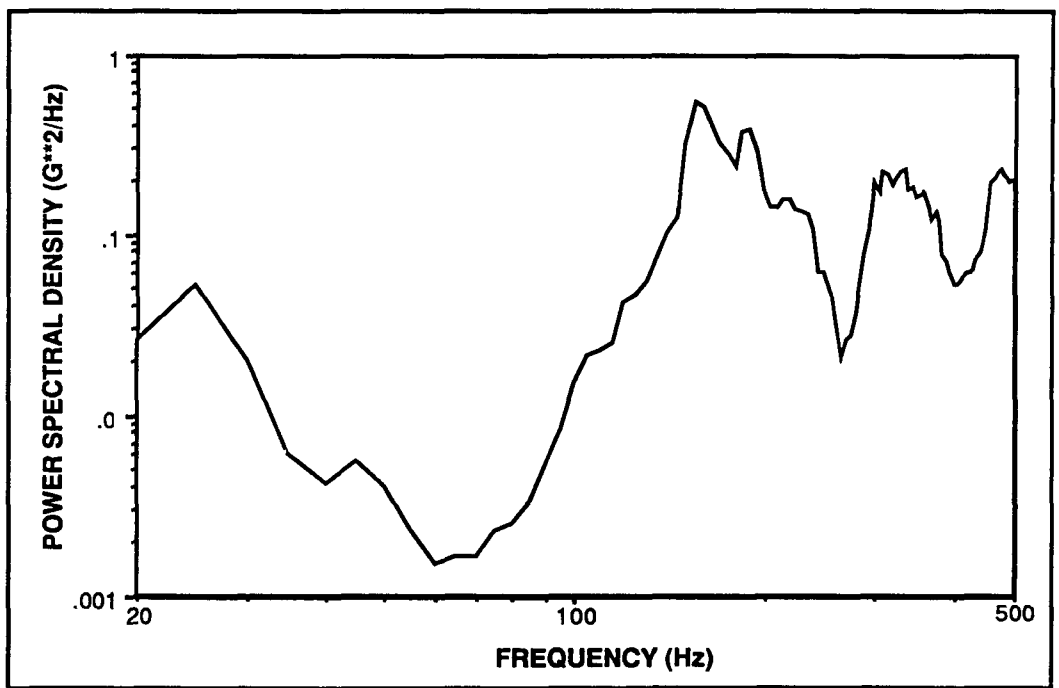

Figure D-2 Response Level for the Equipment at the Forward Location on the Platform

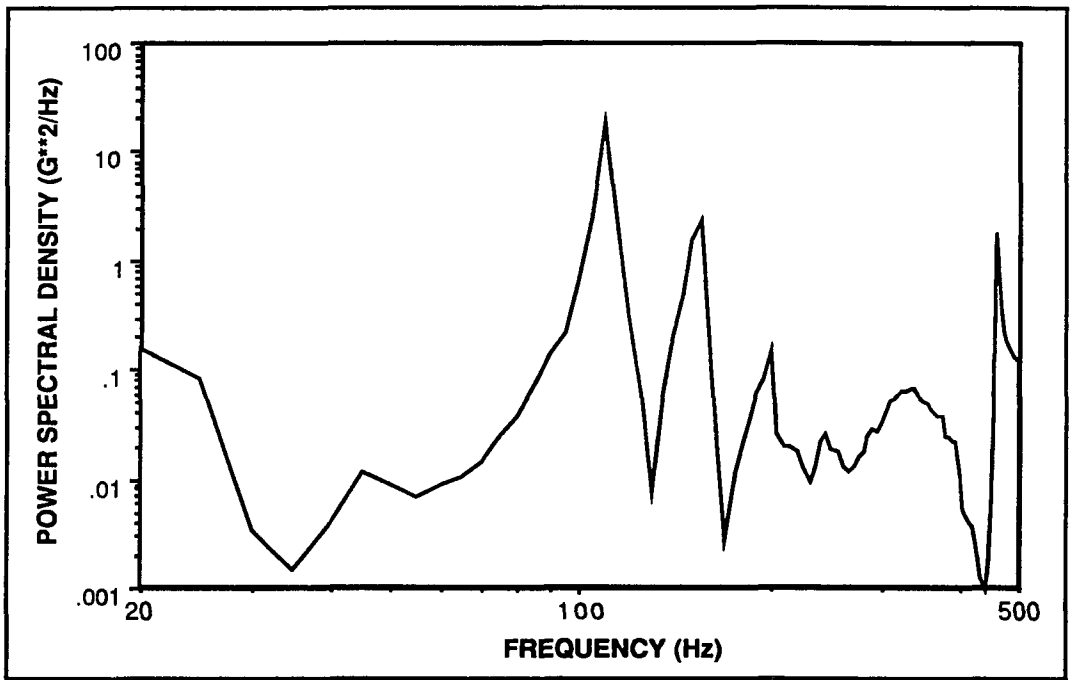

Figure D-3 Input Level for the Equipment at the Rear Location on the Platform

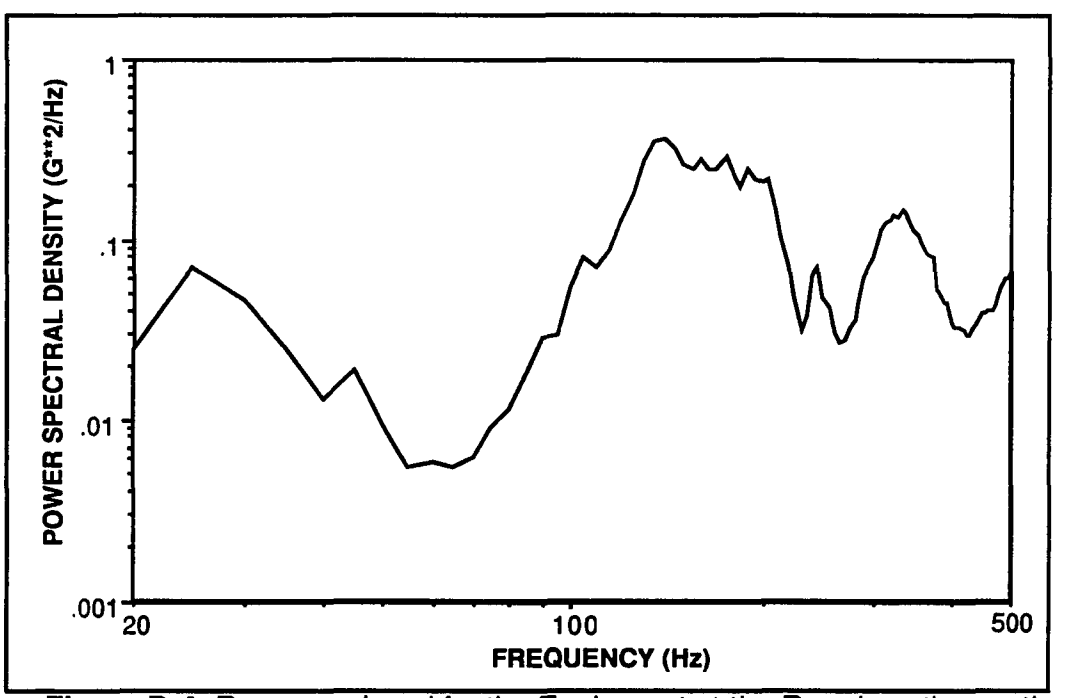

Figure D-4 Response Level for the Equipment at the Rear Location on the Platform

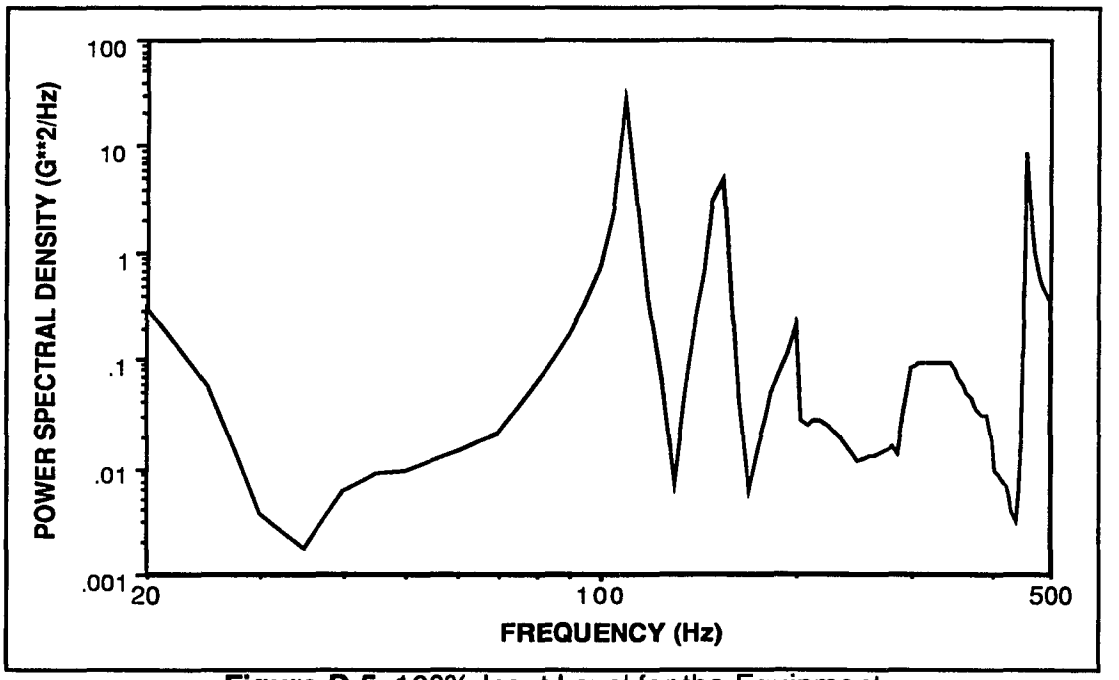

Figure D-5 100% Input Level for the Equipment

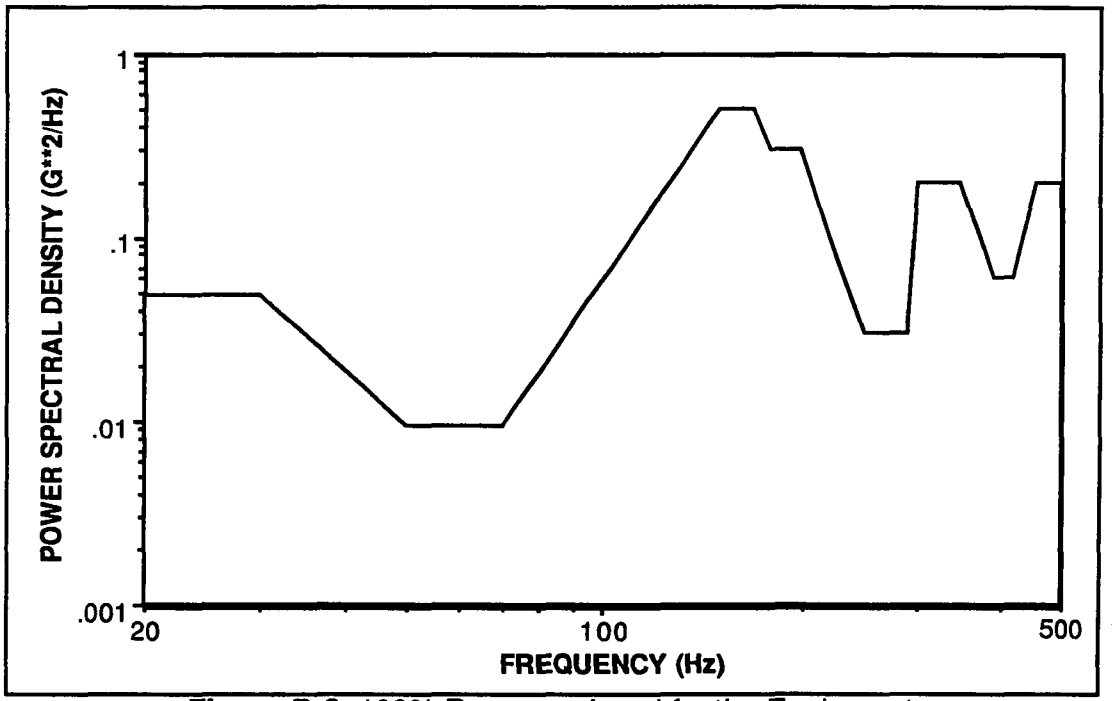

Figure D-6 100% Response Level for the Equipment

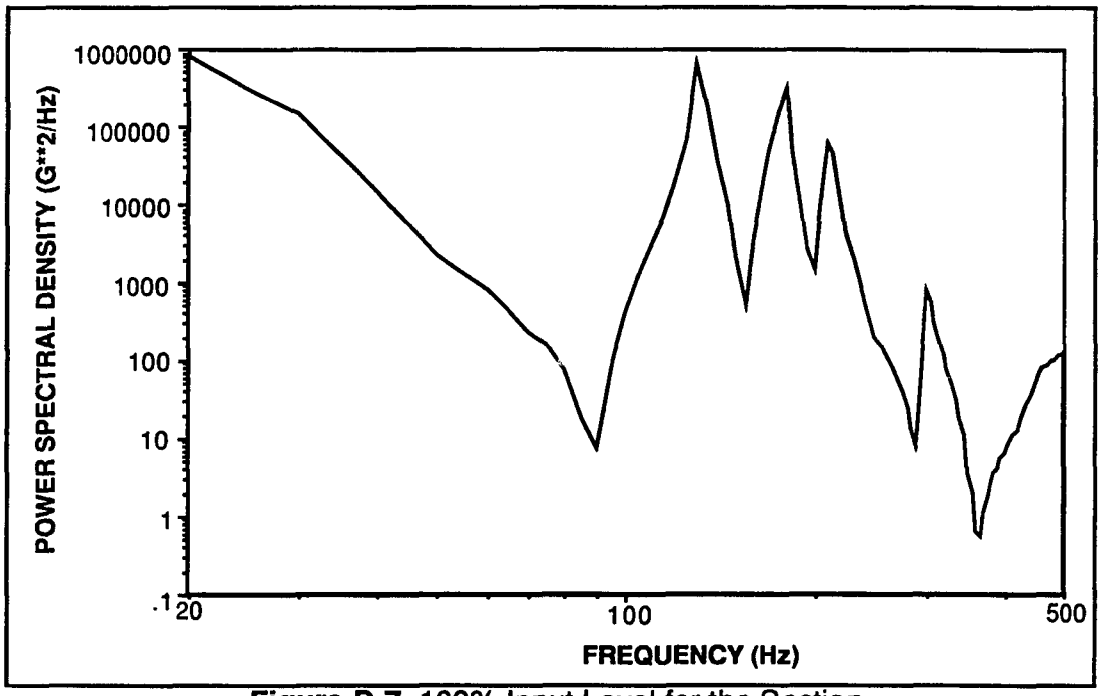

Figure D-7 100% Input Level for the Section

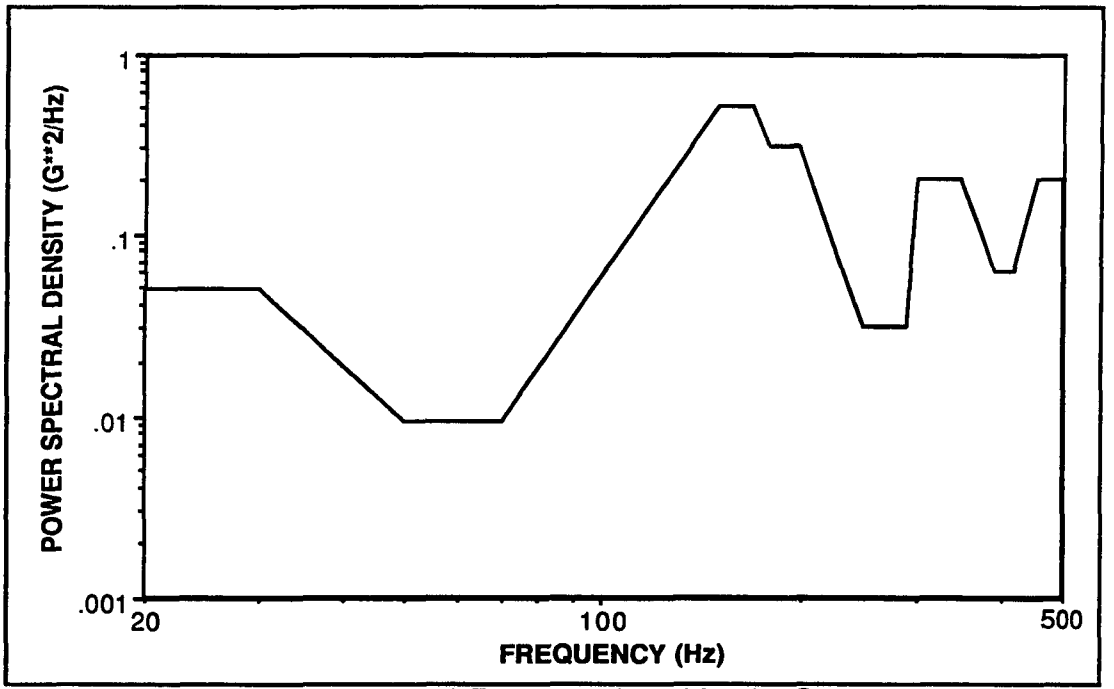

Figure D-8 100% Response Level for the Section

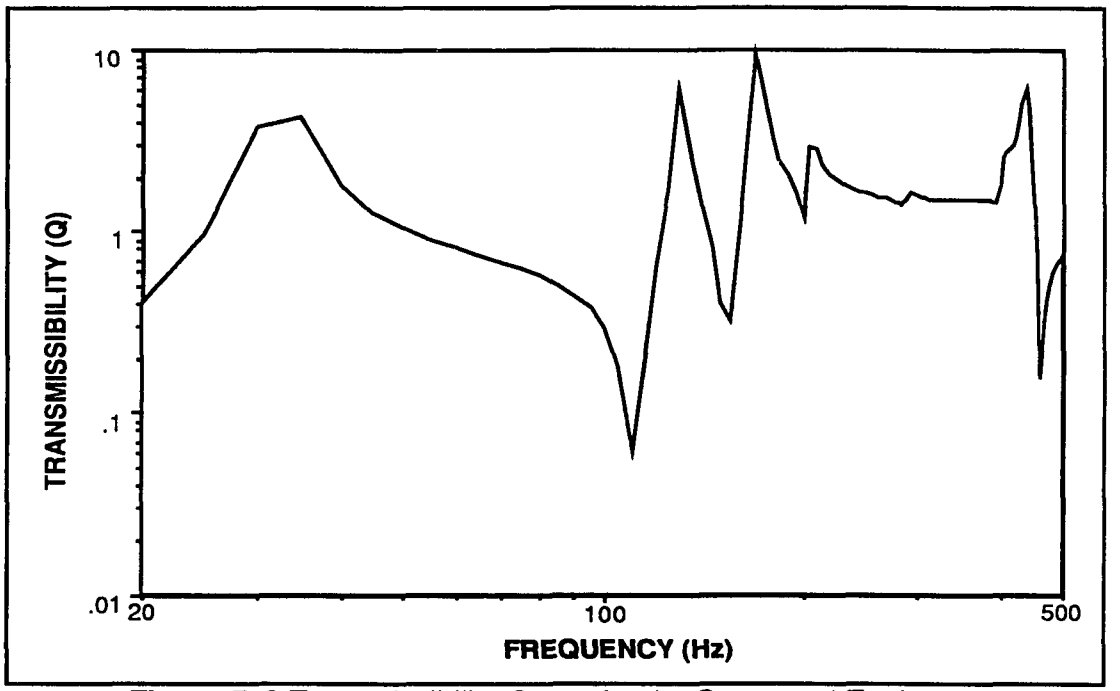

Figure D-9 Transmissibility Curve for the Supported Equipment

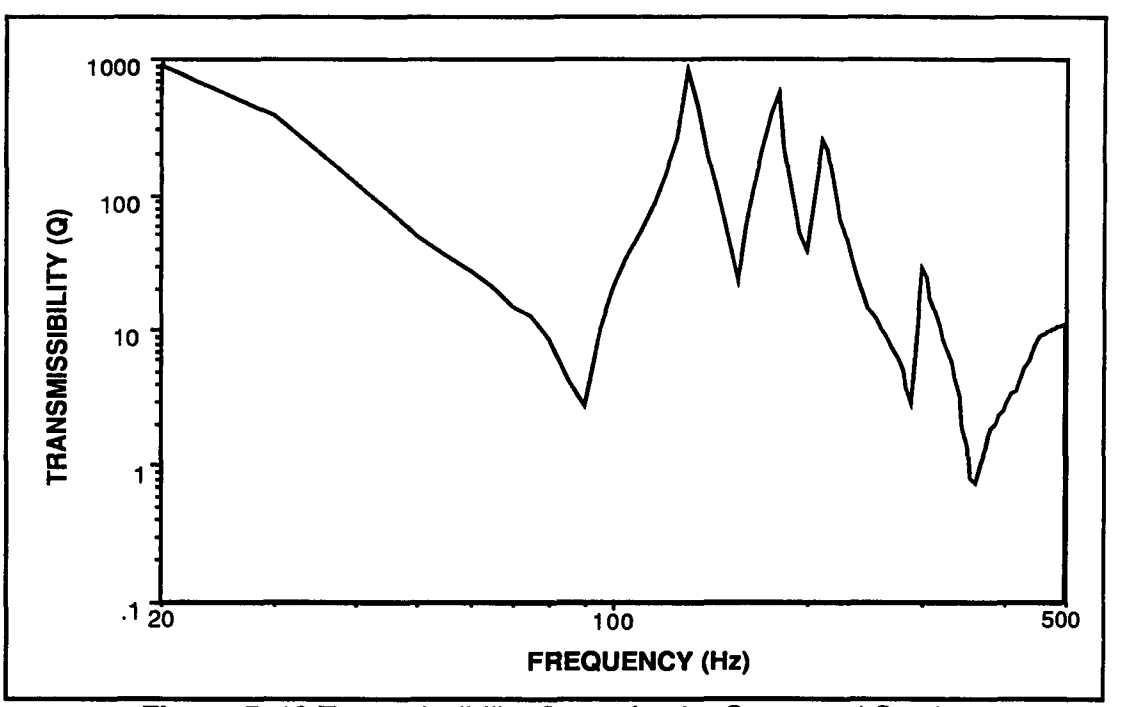

Figure D-10 Transmissibility Curve for the Supported Section

APPENDIX E

STRUCTURAL ANALYSIS RESULTS

RANDOM ANALYSIS OF THE AMRAAM MOUNTED ON A LAU-106
UNIT ACCELERATION IN THE Z PLANE. LADEC (FIG. 4-4) PSD. GRID 133

ACCELERATION (IN/SEC2)**

PLOT TYPE	CURVE TYPE	FRAME NO.	CURVE ID	RMS VALUE	# POS XINGS	XMIN	XMAX	YMIN	X FOR YMIN	YMAX	X FOR YMAX
PSDF	ACCE	1	1(5)	2.64E+04	2.12E+02	20	500	1.04E+01	300	7.43E+07	155
PSDF	ACCE	2	2(5)	1.49E+04	1.94E+02	20	500	4.69E+01	425	2.46E+07	155
PSDF	ACCE	3	3(5)	2.08E+04	1.62E+02	20	500	2.70E+02	435	3.67E+07	155
PSDF	ACCE	4	4(5)	8.69E+03	2.23E+02	20	500	5.89E+02	450	6.33E+06	110
PSDF	ACCE	5	5(5)	9.85E+03	1.81E+02	20	500	7.81E+02	450	1.08E+07	155
PSDF	ACCE	6	6(5)	7.40E+03	2.46E+02	20	500	5.13E+02	245	4.13E+06	110
PSDF	ACCE	7	7(5)	4.48E+03	2.17E+02	20	500	5.40E+02	120	1.64E+06	155
PSDF	ACCE	8	8(5)	5.55E+03	3.68E+02	20	500	1.02E+01	415	2.11E+06	460
PSDF	ACCE	9	9(5)	2.99E+03	3.12E+02	20	500	2.26E+02	60	8.12E+04	155
PSDF	ACCE	10	10(5)	7.38E+03	4.29E+02	20	500	1.22E+01	95	6.67E+06	460
PSDF	ACCE	11	11(5)	9.02E+03	4.27E+02	20	500	3.68E+00	95	8.71E+06	460
PSDF	ACCE	12	12(5)	8.84E+03	4.48E+02	20	500	1.01E-01	85	1.13E+07	460
PSDF	ACCE	13	13(5)	7.22E+03	4.50E+02	20	500	1.25E-01	85	7.66E+06	460
PSDF	ACCE	14	14(5)	5.11E+03	4.50E+02	20	500	3.33E-02	80	3.87E+06	460
PSDF	ACCE	15	15(5)	2.49E+03	4.52E+02	20	500	1.48E-03	80	9.26E+05	460
PSDF	ACCE	16	16(5)	5.37E+02	4.59E+02	20	500	1.69E-05	65	4.43E+04	460
PSDF	ACCE	17	17(5)	2.84E+02	3.80E+02	20	500	2.19E-03	85	6.08E+03	460
PSDF	ACCE	18	19(5)	0.00E+00	0.00E+00	20	500	0.00E+00	20	0.00E+00	20
PSDF	ACCE	19	20(5)	4.03E+02	3.79E+02	20	500	1.68E-03	85	1.32E+04	460
PSDF	ACCE	20	21(5)	2.54E+03	4.56E+02	20	500	7.77E-03	90	9.20E+05	460
PSDF	ACCE	21	22(5)	4.09E+03	4.60E+02	20	500	3.92E-05	55	2.60E+06	460
PSDF	ACCE	22	23(5)	2.42E+04	4.59E+02	20	500	8.11E-02	85	9.01E+07	460
PSDF	ACCE	23	24(5)	3.05E+04	4.54E+02	20	500	7.23E+00	130	1.38E+08	460
PSDF	ACCE	24	25(5)	7.71E+03	2.77E+02	20	500	4.21E+00	130	5.82E+06	200
PSDF	ACCE	25	26(5)	2.19E+04	4.53E+02	20	500	1.49E+01	175	7.49E+07	460
PSDF	ACCE	26	27(5)	1.90E+04	4.52E+02	20	500	2.32E+02	130	5.59E+07	460
PSDF	ACCE	27	28(5)	1.05E+04	3.61E+02	20	500	4.31E+01	425	8.85E+06	460
PSDF	ACCE	28	31(5)	3.78E+04	4.43E+02	20	500	5.14E+02	275	2.02E+08	460
PSDF	ACCE	29	133(5)	1.85E-02	4.46E+02	20	500	3.63E-10	430	4.39E-05	460

RANDOM ANALYSIS OF THE AMRAAM MOUNTED ON A LAU-106
UNIT ACCELERATION IN THE Z PLANE. LADEC (FIG. 4-4) PSD. GRID 133

BENDING MOMENT A2 (IN-LBF)

PLOT TYPE	CURVE TYPE	FRAME NO.	CURVE ID	RMS VALUE	# POS XINGS	XMIN	XMAX	YMIN	X FOR YMIN	YMAX	X FOR YMAX
PSDF	EL FOR	30	2(3)	4.82E+02	2.40E+02	20	500	4.71E-01	60	2.25E+04	155
PSDF	EL FOR	31	3(3)	1.68E+03	1.75E+02	20	500	6.59E+00	265	3.36E+05	155
PSDF	EL FOR	32	4(3)	2.91E+03	1.64E+02	20	500	1.32E+01	305	8.68E+05	155
PSDF	EL FOR	33	5(3)	3.87E+03	1.59E+02	20	500	3.68E+00	500	1.30E+06	155
PSDF	EL FOR	34	6(3)	3.30E+03	1.37E+02	20	500	3.68E-01	265	6.85E+05	155
PSDF	EL FOR	35	7(3)	3.30E+03	1.41E+02	20	500	2.19E-01	370	1.01E+06	20
PSDF	EL FOR	36	8(3)	3.59E+03	5.52E+01	20	500	3.84E+00	440	1.55E+06	20
PSDF	EL FOR	37	9(3)	5.75E+03	1.81E+02	20	500	2.40E+00	415	2.25E+06	20
PSDF	EL FOR	38	10(3)	5.15E+03	2.72E+02	20	500	5.34E+00	80	1.26E+06	460
PSDF	EL FOR	39	12(3)	4.08E+03	2.56E+02	20	500	2.77E+00	80	7.23E+05	155
PSDF	EL FOR	40	13(3)	1.44E+03	1.53E+02	20	500	2.56E-01	85	1.15E+05	155
PSDF	EL FOR	41	14(3)	1.54E+04	3.48E+02	20	500	2.14E+01	360	1.90E+07	460
PSDF	EL FOR	42	18(3)	1.40E+04	4.29E+02	20	500	1.02E+02	130	2.62E+07	460
PSDF	EL FOR	43	19(3)	1.39E+04	4.40E+02	20	500	5.79E+01	130	2.73E+07	460
PSDF	EL FOR	44	20(3)	2.90E+03	4.49E+02	20	500	1.00E+00	130	1.25E+06	460

BENDING MOMENT B2 (IN-LBF)

PSDF	EL FOR	45	2(5)	1.68E+03	1.75E+02	20	500	6.59E+00	265	3.36E+05	155
PSDF	EL FOR	46	3(5)	2.87E+03	1.64E+02	20	500	1.23E+01	305	8.47E+05	155
PSDF	EL FOR	47	4(5)	4.16E+03	1.54E+02	20	500	1.55E+01	310	1.65E+06	155
PSDF	EL FOR	48	5(5)	3.29E+03	1.33E+02	20	500	1.97E-01	430	6.84E+05	155
PSDF	EL FOR	49	6(5)	3.32E+03	1.43E+02	20	500	1.10E-01	365	1.00E+06	20
PSDF	EL FOR	50	7(5)	3.05E+03	5.08E+01	20	500	3.56E+00	385	1.15E+06	20
PSDF	EL FOR	51	8(5)	5.70E+03	1.77E+02	20	500	1.60E+00	415	2.25E+06	20
PSDF	EL FOR	52	9(5)	8.37E+03	2.34E+02	20	500	2.09E+01	80	3.16E+06	155
PSDF	EL FOR	53	10(5)	4.31E+03	2.58E+02	20	500	3.86E+00	80	7.82E+05	155
PSDF	EL FOR	54	12(5)	1.44E+03	1.50E+02	20	500	3.65E-01	85	1.17E+05	155
PSDF	EL FOR	55	13(5)	1.60E+03	2.34E+02	20	500	2.37E-01	80	1.30E+05	155
PSDF	EL FOR	56	14(5)	6.41E+03	2.65E+02	20	500	2.28E+01	130	2.84E+06	20
PSDF	EL FOR	57	18(5)	1.39E+04	4.40E+02	20	500	5.79E+01	130	2.73E+07	460
PSDF	EL FOR	58	19(5)	8.28E+03	4.54E+02	20	500	2.59E+00	130	1.05E+07	460
PSDF	EL FOR	59	20(5)	3.97E+02	4.56E+02	20	500	1.01E-03	70	2.44E+04	460

RANDOM ANALYSIS OF THE AMRAAM MOUNTED ON A LAU-106
UNIT ACCELERATION IN THE Z PLANE. LADEC (FIG. 4-4) PSD. GRID 133

SHEAR FORCE 1 (LBF)

PLOT TYPE	CURVE TYPE	FRAME NO.	CURVE ID	RMS VALUE	# POS XINGS	XMIN	XMAX	YMIN	X FOR YMIN	YMAX	X FOR YMAX
PSDF	EL FOR	60	2(7)	2.02E+02	1.60E+02	20	500	3.75E-02	390	4.99E+03	155
PSDF	EL FOR	61	3(7)	1.65E+02	1.44E+02	20	500	1.28E-02	320	1.86E+03	155
PSDF	EL FOR	62	4(7)	1.65E+02	1.39E+02	20	500	1.55E-03	430	2.00E+03	155
PSDF	EL FOR	63	5(7)	1.91E+02	2.59E+02	20	500	5.31E-03	90	1.90E+03	20
PSDF	EL FOR	64	6(7)	2.06E+02	1.63E+02	20	500	1.21E-02	85	2.19E+03	155
PSDF	EL FOR	65	7(7)	3.49E+02	2.25E+02	20	500	1.69E-02	45	9.59E+03	155
PSDF	EL FOR	66	8(7)	5.85E+02	2.80E+02	20	500	4.53E-03	60	2.12E+04	155
PSDF	EL FOR	67	9(7)	6.64E+02	3.06E+02	20	500	1.83E-02	60	2.66E+04	460
PSDF	EL FOR	68	10(7)	3.05E+02	3.39E+02	20	500	1.44E-02	80	7.27E+03	460
PSDF	EL FOR	69	12(7)	3.17E+02	3.31E+02	20	500	4.74E-03	80	7.54E+03	460
PSDF	EL FOR	70	13(7)	2.49E+02	1.71E+02	20	500	1.91E-02	80	3.55E+03	155
PSDF	EL FOR	71	14(7)	2.37E+03	4.19E+02	20	500	9.86E-02	65	7.02E+05	460
PSDF	EL FOR	72	18(7)	4.21E+02	2.06E+02	20	500	1.46E-03	405	1.30E+04	200
PSDF	EL FOR	73	19(7)	8.32E+02	4.05E+02	20	500	7.37E-01	130	8.05E+04	460
PSDF	EL FOR	74	20(7)	4.33E+02	4.48E+02	20	500	2.69E-02	130	2.78E+04	460

BENDING STRESS A1 (PSI)

PSDF	EL STR	75	2(2)	4.42E+01	2.40E+02	20	500	3.97E-03	60	1.90E+02	155
PSDF	EL STR	76	3(2)	7.13E+02	1.75E+02	20	500	1.18E+00	265	6.02E+04	155
PSDF	EL STR	77	4(2)	1.23E+03	1.64E+02	20	500	2.36E+00	305	1.56E+05	155
PSDF	EL STR	78	5(2)	1.56E+03	1.59E+02	20	500	5.98E-01	500	2.11E+05	155
PSDF	EL STR	79	6(2)	1.33E+03	1.37E+02	20	500	5.98E-02	265	1.11E+05	155
PSDF	EL STR	80	7(2)	1.33E+03	1.41E+02	20	500	3.56E-02	370	1.64E+05	20
PSDF	EL STR	81	8(2)	1.97E+02	5.52E+01	20	500	1.15E-02	440	4.65E+03	20
PSDF	EL STR	82	9(2)	3.15E+02	1.81E+02	20	500	7.21E-03	415	6.77E+03	20
PSDF	EL STR	83	10(2)	5.23E+02	2.72E+02	20	500	5.51E-02	80	1.30E+04	460
PSDF	EL STR	84	12(2)	1.20E+03	2.56E+02	20	500	2.41E-01	80	6.29E+04	155
PSDF	EL STR	85	13(2)	4.24E+02	1.53E+02	20	500	2.23E-02	85	1.00E+04	155
PSDF	EL STR	86	14(2)	4.55E+03	3.48E+02	20	500	1.86E+00	360	1.65E+06	460
PSDF	EL STR	87	18(2)	6.53E+03	4.29E+02	20	500	2.23E+01	130	5.73E+06	460
PSDF	EL STR	88	19(2)	3.81E+03	4.40E+02	20	500	4.38E+00	130	2.07E+06	460
PSDF	EL STR	89	20(2)	7.96E+02	4.49E+02	20	500	7.57E-02	130	9.48E+04	460

RANDOM ANALYSIS OF THE AMRAAM MOUNTED ON A LAU-106
UNIT ACCELERATION IN THE Z PLANE. LADEC (FIG. 4-4) PSD. GRID 133

BENDING STRESS B1 (PSI)

PLOT TYPE	CURVE TYPE	FRAME NO.	CURVE ID	RMS VALUE	# POS XINGS	XMIN	XMAX	YMIN	X FOR YMIN	YMAX	X FOR YMAX
PSDF	EL STR	90	2(12)	1.54E+02	1.75E+02	20	500	5.56E-02	265	2.83E+03	155
PSDF	EL STR	91	3(12)	1.22E+03	1.64E+02	20	500	2.20E+00	305	1.52E+05	155
PSDF	EL STR	92	4(12)	1.76E+03	1.54E+02	20	500	2.78E+00	310	2.96E+05	155
PSDF	EL STR	93	5(12)	1.33E+03	1.33E+02	20	500	3.20E-02	430	1.11E+05	155
PSDF	EL STR	94	6(12)	1.34E+03	1.43E+02	20	500	1.79E-02	365	1.63E+05	20
PSDF	EL STR	95	7(12)	1.23E+03	5.08E+01	20	500	5.79E-01	385	1.87E+05	20
PSDF	EL STR	96	8(12)	3.12E+02	1.77E+02	20	500	4.82E-03	415	6.76E+03	20
PSDF	EL STR	97	9(12)	4.58E+02	2.34E+02	20	500	6.27E-02	80	9.48E+03	155
PSDF	EL STR	98	10(12)	4.37E+02	2.58E+02	20	500	3.99E-02	80	8.07E+03	155
PSDF	EL STR	99	12(12)	4.25E+02	1.50E+02	20	500	3.18E-02	85	1.02E+04	155
PSDF	EL STR	100	13(12)	4.71E+02	2.34E+02	20	500	2.07E-02	80	1.13E+04	155
PSDF	EL STR	101	14(12)	1.89E+03	2.65E+02	20	500	1.99E+00	130	2.47E+05	20
PSDF	EL STR	102	18(12)	6.48E+03	4.40E+02	20	500	1.27E+01	130	5.97E+06	460
PSDF	EL STR	103	19(12)	2.28E+03	4.54E+02	20	500	1.96E-01	130	7.95E+05	460
PSDF	EL STR	104	20(12)	1.09E+02	4.56E+02	20	500	7.66E-05	70	1.84E+03	460

RANDOM ANALYSIS OF THE AMRAAM MOUNTED ON A LAU-106
UNIT ACCELERATION IN THE Z PLANE. LAWUT (FIG. 4-5) PSD. GRID 133

ACCELERATION (IN/SEC2)**

PLOT TYPE	CURVE TYPE	FRAME NO.	CURVE ID	RMS VALUE	# POS XINGS	XMIN	XMAX	YMIN	X FOR YMIN	YMAX	X FOR YMAX
PSDF	ACCE	1	1(5)	2.25E+04	1.63E+02	20	500	4.45E+00	300	3.36E+07	155
PSDF	ACCE	2	2(5)	1.32E+04	1.55E+02	20	500	2.21E+01	425	1.11E+07	155
PSDF	ACCE	3	3(5)	2.43E+04	1.31E+02	20	500	1.20E+02	435	5.43E+07	110
PSDF	ACCE	4	4(5)	1.22E+04	1.45E+02	20	500	2.07E+02	450	1.92E+07	110
PSDF	ACCE	5	5(5)	9.01E+03	1.50E+02	20	500	2.75E+02	450	4.88E+06	155
PSDF	ACCE	6	6(5)	9.89E+03	1.47E+02	20	500	2.13E+02	445	1.25E+07	110
PSDF	ACCE	7	7(5)	4.33E+03	1.77E+02	20	500	6.32E+02	170	9.49E+05	110
PSDF	ACCE	8	8(5)	4.86E+03	2.36E+02	20	500	5.70E+00	415	1.68E+06	110
PSDF	ACCE	9	9(5)	2.57E+03	2.58E+02	20	500	8.03E+02	55	5.37E+04	140
PSDF	ACCE	10	10(5)	4.08E+03	3.75E+02	20	500	4.17E+01	95	1.40E+06	460
PSDF	ACCE	11	11(5)	5.09E+03	3.72E+02	20	500	1.26E+01	95	1.83E+06	460
PSDF	ACCE	12	12(5)	4.42E+03	4.21E+02	20	500	5.56E-01	85	2.37E+06	460
PSDF	ACCE	13	13(5)	3.57E+03	4.25E+02	20	500	6.79E-01	80	1.61E+06	460
PSDF	ACCE	14	14(5)	2.53E+03	4.26E+02	20	500	1.53E-01	80	8.11E+05	460
PSDF	ACCE	15	15(5)	1.22E+03	4.30E+02	20	500	6.77E-03	80	1.94E+05	460
PSDF	ACCE	16	16(5)	2.52E+02	4.52E+02	20	500	5.60E-05	65	9.29E+03	460
PSDF	ACCE	17	17(5)	1.90E+02	3.19E+02	20	500	1.21E-02	85	1.28E+03	460
PSDF	ACCE	18	19(5)	0.00E+00	0.00E+00	20	500	0.00E+00	20	0.00E+00	20
PSDF	ACCE	19	20(5)	2.69E+02	3.16E+02	20	500	9.28E-03	85	2.77E+03	460
PSDF	ACCE	20	21(5)	1.23E+03	4.42E+02	20	500	4.03E-02	90	1.93E+05	460
PSDF	ACCE	21	22(5)	1.91E+03	4.56E+02	20	500	9.07E-05	55	5.45E+05	460
PSDF	ACCE	22	23(5)	1.14E+04	4.51E+02	20	500	4.48E-01	85	1.89E+07	460
PSDF	ACCE	23	24(5)	1.52E+04	4.27E+02	20	500	3.46E+01	130	2.89E+07	460
PSDF	ACCE	24	25(5)	7.53E+03	2.23E+02	20	500	2.01E+01	130	7.31E+06	200
PSDF	ACCE	25	26(5)	1.13E+04	4.13E+02	20	500	1.55E+01	175	1.57E+07	460
PSDF	ACCE	26	27(5)	1.01E+04	3.97E+02	20	500	2.30E+02	170	1.17E+07	460
PSDF	ACCE	27	28(5)	9.39E+03	2.22E+02	20	500	2.04E+01	425	6.90E+06	110
PSDF	ACCE	28	31(5)	2.12E+04	3.75E+02	20	500	5.67E+02	280	4.24E+07	460
PSDF	ACCE	29	133(5)	1.09E-02	3.62E+02	20	500	1.66E-10	430	9.22E-06	460

RANDOM ANALYSIS OF THE AMRAAM MOUNTED ON A LAU-106
UNIT ACCELERATION IN THE Z PLANE. LAWUT (FIG. 4-5) PSD. GRID 133

BENDING MOMENT A2 (IN-LBF)

PLOT TYPE	CURVE TYPE	FRAME NO.	CURVE ID	RMS VALUE	# POS XINGS	XMIN	XMAX	YMIN	X FOR YMIN	YMAX	X FOR YMAX
PSDF	EL FOR	30	2(3)	3.93E+02	1.80E+02	20	500	1.47E+00	55	1.02E+04	155
PSDF	EL FOR	31	3(3)	1.38E+03	1.56E+02	20	500	5.28E+00	390	1.52E+05	155
PSDF	EL FOR	32	4(3)	2.88E+03	1.37E+02	20	500	7.55E+00	305	6.58E+05	110
PSDF	EL FOR	33	5(3)	4.44E+03	1.27E+02	20	500	1.18E+00	495	2.08E+06	110
PSDF	EL FOR	34	6(3)	3.85E+03	1.08E+02	20	500	4.67E-01	265	1.13E+06	110
PSDF	EL FOR	35	7(3)	3.81E+03	8.06E+01	20	500	1.50E-01	370	1.15E+06	25
PSDF	EL FOR	36	8(3)	4.20E+03	4.59E+01	20	500	1.64E+00	440	1.73E+06	25
PSDF	EL FOR	37	9(3)	6.22E+03	1.07E+02	20	500	1.35E+00	415	2.47E+06	25
PSDF	EL FOR	38	10(3)	5.03E+03	1.54E+02	20	500	5.20E+00	390	1.35E+06	110
PSDF	EL FOR	39	12(3)	4.07E+03	1.47E+02	20	500	6.71E+00	430	9.08E+05	110
PSDF	EL FOR	40	13(3)	1.56E+03	1.15E+02	20	500	1.41E+00	85	1.31E+05	110
PSDF	EL FOR	41	14(3)	1.29E+04	2.30E+02	20	500	1.21E+01	360	1.18E+07	200
PSDF	EL FOR	42	18(3)	8.47E+03	3.47E+02	20	500	4.87E+02	130	5.50E+06	460
PSDF	EL FOR	43	19(3)	7.80E+03	3.76E+02	20	500	2.77E+02	130	5.73E+06	460
PSDF	EL FOR	44	20(3)	1.50E+03	4.08E+02	20	500	4.79E+00	130	2.63E+05	460

BENDING MOMENT B2 (IN-LBF)

PSDF	EL FOR	45	2(5)	1.38E+03	1.56E+02	20	500	5.28E+00	390	1.52E+05	155
PSDF	EL FOR	46	3(5)	2.86E+03	1.37E+02	20	500	7.04E+00	305	6.47E+05	110
PSDF	EL FOR	47	4(5)	4.46E+03	1.30E+02	20	500	7.94E+00	310	1.82E+06	110
PSDF	EL FOR	48	5(5)	3.86E+03	1.07E+02	20	500	9.02E-02	430	1.14E+06	110
PSDF	EL FOR	49	6(5)	3.83E+03	8.18E+01	20	500	6.68E-02	365	1.15E+06	25
PSDF	EL FOR	50	7(5)	3.58E+03	4.06E+01	20	500	2.33E+00	385	1.30E+06	25
PSDF	EL FOR	51	8(5)	6.19E+03	1.05E+02	20	500	8.98E-01	415	2.47E+06	25
PSDF	EL FOR	52	9(5)	8.59E+03	1.36E+02	20	500	2.37E+01	430	3.99E+06	110
PSDF	EL FOR	53	10(5)	4.28E+03	1.47E+02	20	500	1.01E+01	275	9.91E+05	110
PSDF	EL FOR	54	12(5)	1.57E+03	1.14E+02	20	500	2.01E+00	85	1.34E+05	110
PSDF	EL FOR	55	13(5)	1.61E+03	1.43E+02	20	500	1.09E+00	80	1.47E+05	110
PSDF	EL FOR	56	14(5)	7.20E+03	1.35E+02	20	500	5.62E+01	170	2.70E+06	20
PSDF	EL FOR	57	18(5)	7.80E+03	3.76E+02	20	500	2.77E+02	130	5.73E+06	460
PSDF	EL FOR	58	19(5)	4.10E+03	4.29E+02	20	500	1.00E+01	65	2.21E+06	460
PSDF	EL FOR	59	20(5)	1.93E+02	4.36E+02	20	500	3.59E-03	65	5.12E+03	460

RANDOM ANALYSIS OF THE AMRAAM MOUNTED ON A LAU-106
UNIT ACCELERATION IN THE Z PLANE. LAWUT (FIG. 4-5) PSD. GRID 133

SHEAR FORCE 1 (LBF)

PLOT TYPE	CURVE TYPE	FRAME NO.	CURVE ID	RMS VALUE	# POS XINGS	XMIN	XMAX	YMIN	X FOR YMIN	YMAX	X FOR YMAX
PSDF	EL FOR	60	2(7)	1.64E+02	1.52E+02	20	500	2.44E-02	390	2.26E+03	155
PSDF	EL FOR	61	3(7)	2.10E+02	1.20E+02	20	500	8.67E-03	315	5.12E+03	110
PSDF	EL FOR	62	4(7)	2.04E+02	1.20E+02	20	500	7.08E-04	430	4.65E+03	110
PSDF	EL FOR	63	5(7)	1.92E+02	1.42E+02	20	500	1.03E-02	375	2.09E+03	25
PSDF	EL FOR	64	6(7)	2.29E+02	1.12E+02	20	500	3.49E-02	500	3.09E+03	110
PSDF	EL FOR	65	7(7)	3.69E+02	1.48E+02	20	500	3.35E-02	270	1.39E+04	110
PSDF	EL FOR	66	8(7)	5.68E+02	1.70E+02	20	500	1.72E-02	60	2.91E+04	110
PSDF	EL FOR	67	9(7)	6.15E+02	1.85E+02	20	500	6.94E-02	60	3.33E+04	110
PSDF	EL FOR	68	10(7)	2.64E+02	1.98E+02	20	500	1.12E-02	325	3.30E+03	110
PSDF	EL FOR	69	12(7)	2.78E+02	1.93E+02	20	500	7.19E-03	350	3.98E+03	110
PSDF	EL FOR	70	13(7)	2.68E+02	1.19E+02	20	500	1.19E-02	500	4.03E+03	110
PSDF	EL FOR	71	14(7)	1.52E+03	3.24E+02	20	500	1.71E-01	310	1.47E+05	460
PSDF	EL FOR	72	18(7)	4.70E+02	1.69E+02	20	500	9.12E-04	405	1.63E+04	200
PSDF	EL FOR	73	19(7)	5.80E+02	2.99E+02	20	500	3.53E+00	130	2.26E+04	200
PSDF	EL FOR	74	20(7)	2.28E+02	4.03E+02	20	500	1.29E-01	130	5.83E+03	460

BENDING STRESS A1 (PSI)

PSDF	EL STR	75	2(2)	3.61E+01	1.80E+02	20	500	1.24E-02	55	8.58E+01	155
PSDF	EL STR	76	3(2)	5.83E+02	1.56E+02	20	500	9.47E-01	390	2.72E+04	155
PSDF	EL STR	77	4(2)	1.22E+03	1.37E+02	20	500	1.35E+00	305	1.18E+05	110
PSDF	EL STR	78	5(2)	1.79E+03	1.27E+02	20	500	1.91E-01	495	3.37E+05	110
PSDF	EL STR	79	6(2)	1.55E+03	1.08E+02	20	500	7.60E-02	265	1.84E+05	110
PSDF	EL STR	80	7(2)	1.54E+03	8.06E+01	20	500	2.43E-02	370	1.87E+05	25
PSDF	EL STR	81	8(2)	2.30E+02	4.59E+01	20	500	4.93E-03	440	5.20E+03	25
PSDF	EL STR	82	9(2)	3.41E+02	1.07E+02	20	500	4.04E-03	415	7.43E+03	25
PSDF	EL STR	83	10(2)	5.11E+02	1.54E+02	20	500	5.36E-02	390	1.39E+04	110
PSDF	EL STR	84	12(2)	1.20E+03	1.47E+02	20	500	5.84E-01	430	7.91E+04	110
PSDF	EL STR	85	13(2)	4.61E+02	1.15E+02	20	500	1.23E-01	85	1.14E+04	110
PSDF	EL STR	86	14(2)	3.81E+03	2.30E+02	20	500	1.06E+00	360	1.02E+06	200
PSDF	EL STR	87	18(2)	3.96E+03	3.47E+02	20	500	1.06E+02	130	1.20E+06	460
PSDF	EL STR	88	19(2)	2.14E+03	3.76E+02	20	500	2.10E+01	130	4.33E+05	460
PSDF	EL STR	89	20(2)	4.14E+02	4.08E+02	20	500	3.62E-01	130	1.99E+04	460

RANDOM ANALYSIS OF THE AMRAAM MOUNTED ON A LAU-106
UNIT ACCELERATION IN THE Z PLANE. LAWUT (FIG. 4-5) PSD. GRID 133

BENDING STRESS B1 (PSI)

PLOT TYPE	CURVE TYPE	FRAME NO.	CURVE ID	RMS VALUE	# POS XINGS	XMIN	XMAX	YMIN	X FOR YMIN	YMAX	X FOR YMAX
PSDF	EL STR	90	2(12)	1.26E+02	1.56E+02	20	500	4.45E-02	390	1.28E+03	155
PSDF	EL STR	91	3(12)	1.21E+03	1.37E+02	20	500	1.26E+00	305	1.16E+05	110
PSDF	EL STR	92	4(12)	1.89E+03	1.30E+02	20	500	1.42E+00	310	3.27E+05	110
PSDF	EL STR	93	5(12)	1.56E+03	1.07E+02	20	500	1.47E-02	430	1.85E+05	110
PSDF	EL STR	94	6(12)	1.54E+03	8.18E+01	20	500	1.09E-02	365	1.87E+05	25
PSDF	EL STR	95	7(12)	1.44E+03	4.06E+01	20	500	3.78E-01	385	2.10E+05	25
PSDF	EL STR	96	8(12)	3.39E+02	1.05E+02	20	500	2.70E-03	415	7.42E+03	25
PSDF	EL STR	97	9(12)	4.71E+02	1.36E+02	20	500	7.13E-02	430	1.20E+04	110
PSDF	EL STR	98	10(12)	4.35E+02	1.47E+02	20	500	1.05E-01	275	1.02E+04	110
PSDF	EL STR	99	12(12)	4.63E+02	1.14E+02	20	500	1.75E-01	85	1.17E+04	110
PSDF	EL STR	100	13(12)	4.76E+02	1.43E+02	20	500	9.46E-02	80	1.28E+04	110
PSDF	EL STR	101	14(12)	2.13E+03	1.35E+02	20	500	4.89E+00	170	2.35E+05	20
PSDF	EL STR	102	18(12)	3.64E+03	3.76E+02	20	500	6.05E+01	130	1.25E+06	460
PSDF	EL STR	103	19(12)	1.13E+03	4.29E+02	20	500	7.57E-01	65	1.67E+05	460
PSDF	EL STR	104	20(12)	5.31E+01	4.36E+02	20	500	2.72E-04	65	3.87E+02	460

RANDOM ANALYSIS OF THE AMRAAM MOUNTED ON A LAU-106
UNIT ACCELERATION IN THE Z PLANE. 32VH (FIG. 4-2) PSD. GRID 133

ACCELERATION (IN/SEC2)**

PLOT TYPE	CURVE TYPE	FRAME NO.	CURVE ID	RMS VALUE	# POS XINGS	XMIN	XMAX	YMIN	X FOR YMIN	YMAX	X FOR YMAX
PSDF	ACCE	1	1(5)	3.04E+04	1.94E+02	20	500	1.10E+01	300	6.85E+07	155
PSDF	ACCE	2	2(5)	1.75E+04	1.77E+02	20	500	5.30E+01	425	2.27E+07	155
PSDF	ACCE	3	3(5)	3.00E+04	1.40E+02	20	500	3.58E+02	435	7.80E+07	110
PSDF	ACCE	4	4(5)	1.45E+04	1.57E+02	20	500	7.98E+02	450	2.75E+07	110
PSDF	ACCE	5	5(5)	1.18E+04	1.64E+02	20	500	1.06E+03	450	9.96E+06	155
PSDF	ACCE	6	6(5)	1.20E+04	1.73E+02	20	500	3.01E+02	250	1.79E+07	110
PSDF	ACCE	7	7(5)	5.50E+03	1.91E+02	20	500	1.31E+03	170	1.51E+06	155
PSDF	ACCE	8	8(5)	6.65E+03	3.12E+02	20	500	1.06E+01	415	2.41E+06	110
PSDF	ACCE	9	9(5)	3.23E+03	2.92E+02	20	500	1.37E+03	70	7.48E+04	170
PSDF	ACCE	10	10(5)	7.56E+03	4.23E+02	20	500	6.52E+01	95	6.92E+06	460
PSDF	ACCE	11	11(5)	9.31E+03	4.20E+02	20	500	1.97E+01	95	9.03E+06	460
PSDF	ACCE	12	12(5)	9.01E+03	4.45E+02	20	500	7.73E-01	85	1.17E+07	460
PSDF	ACCE	13	13(5)	7.35E+03	4.47E+02	20	500	9.61E-01	85	7.94E+06	460
PSDF	ACCE	14	14(5)	5.21E+03	4.48E+02	20	500	2.48E-01	80	4.01E+06	460
PSDF	ACCE	15	15(5)	2.54E+03	4.49E+02	20	500	1.10E-02	80	9.60E+05	460
PSDF	ACCE	16	16(5)	5.44E+02	4.58E+02	20	500	9.50E-05	65	4.59E+04	460
PSDF	ACCE	17	17(5)	2.97E+02	3.72E+02	20	500	1.68E-02	85	6.31E+03	460
PSDF	ACCE	18	19(5)	0.00E+00	0.00E+00	20	500	0.00E+00	20	0.00E+00	20
PSDF	ACCE	19	20(5)	4.22E+02	3.71E+02	20	500	1.29E-02	85	1.37E+04	460
PSDF	ACCE	20	21(5)	2.57E+03	4.55E+02	20	500	4.93E-02	90	9.54E+05	460
PSDF	ACCE	21	22(5)	4.15E+03	4.60E+02	20	500	1.55E-04	55	2.69E+06	460
PSDF	ACCE	22	23(5)	2.45E+04	4.58E+02	20	500	6.22E-01	85	9.34E+07	460
PSDF	ACCE	23	24(5)	3.12E+04	4.50E+02	20	500	3.12E+01	130	1.43E+08	460
PSDF	ACCE	24	25(5)	9.36E+03	2.54E+02	20	500	1.82E+01	130	1.07E+07	200
PSDF	ACCE	25	26(5)	2.27E+04	4.45E+02	20	500	2.13E+01	175	7.76E+07	460
PSDF	ACCE	26	27(5)	1.99E+04	4.38E+02	20	500	4.78E+02	170	5.79E+07	460
PSDF	ACCE	27	28(5)	1.31E+04	3.01E+02	20	500	2.84E+01	240	9.91E+06	110
PSDF	ACCE	28	31(5)	3.98E+04	4.27E+02	20	500	3.57E+02	290	2.09E+08	460
PSDF	ACCE	29	133(5)	1.97E-02	4.23E+02	20	500	4.59E-10	430	4.55E-05	460

RANDOM ANALYSIS OF THE AMRAAM MOUNTED ON A LAU-106
UNIT ACCELERATION IN THE Z PLANE. 32VH (FIG.4-2) PSD. GRID 133

BENDING MOMENT A2 (IN-LBF)

PLOT TYPE	CURVE TYPE	FRAME NO.	CURVE ID	RMS VALUE	# POS XINGS	XMIN	XMAX	YMIN	X FOR YMIN	YMAX	X FOR YMAX
PSDF	EL FOR	30	2(3)	5.44E+02	2.22E+02	20	500	1.42E+00	290	2.08E+04	155
PSDF	EL FOR	31	3(3)	1.86E+03	1.68E+02	20	500	6.92E+00	290	3.10E+05	155
PSDF	EL FOR	32	4(3)	3.69E+03	1.47E+02	20	500	1.49E+01	390	9.44E+05	110
PSDF	EL FOR	33	5(3)	5.51E+03	1.37E+02	20	500	3.71E+00	500	2.98E+06	110
PSDF	EL FOR	34	6(3)	4.57E+03	1.22E+02	20	500	5.23E-01	265	1.62E+06	110
PSDF	EL FOR	35	7(3)	4.22E+03	1.21E+02	20	500	1.97E-01	370	1.93E+06	20
PSDF	EL FOR	36	8(3)	4.44E+03	5.27E+01	20	500	5.27E+00	440	2.97E+06	20
PSDF	EL FOR	37	9(3)	7.22E+03	1.54E+02	20	500	2.49E+00	415	4.33E+06	20
PSDF	EL FOR	38	10(3)	6.36E+03	2.30E+02	20	500	6.93E+00	390	1.94E+06	110
PSDF	EL FOR	39	12(3)	5.09E+03	2.15E+02	20	500	9.07E+00	275	1.30E+06	110
PSDF	EL FOR	40	13(3)	1.85E+03	1.35E+02	20	500	1.96E+00	85	1.87E+05	110
PSDF	EL FOR	41	14(3)	1.78E+04	3.14E+02	20	500	1.83E+01	360	1.97E+07	460
PSDF	EL FOR	42	18(3)	1.49E+04	4.12E+02	20	500	4.40E+02	130	2.72E+07	460
PSDF	EL FOR	43	19(3)	1.45E+04	4.28E+02	20	500	2.50E+02	130	2.83E+07	460
PSDF	EL FOR	44	20(3)	2.99E+03	4.42E+02	20	500	4.32E+00	130	1.30E+06	460

BENDING MOMENT B2 (IN-LBF)

PSDF	EL FOR	45	2(5)	1.86E+03	1.68E+02	20	500	6.92E+00	290	3.10E+05	155
PSDF	EL FOR	46	3(5)	3.65E+03	1.47E+02	20	500	1.43E+01	305	9.28E+05	110
PSDF	EL FOR	47	4(5)	5.59E+03	1.37E+02	20	500	1.40E+01	310	2.62E+06	110
PSDF	EL FOR	48	5(5)	4.57E+03	1.20E+02	20	500	2.49E-01	430	1.64E+06	110
PSDF	EL FOR	49	6(5)	4.25E+03	1.22E+02	20	500	9.73E-02	365	1.93E+06	20
PSDF	EL FOR	50	7(5)	3.76E+03	4.81E+01	20	500	3.18E+00	385	2.21E+06	20
PSDF	EL FOR	51	8(5)	7.17E+03	1.51E+02	20	500	1.66E+00	415	4.32E+06	20
PSDF	EL FOR	52	9(5)	1.05E+04	1.96E+02	20	500	3.86E+01	275	5.73E+06	110
PSDF	EL FOR	53	10(5)	5.36E+03	2.17E+02	20	500	9.33E+00	275	1.42E+06	110
PSDF	EL FOR	54	12(5)	1.86E+03	1.33E+02	20	500	2.54E+00	275	1.92E+05	110
PSDF	EL FOR	55	13(5)	2.00E+03	1.99E+02	20	500	1.76E+00	80	2.11E+05	110
PSDF	EL FOR	56	14(5)	8.61E+03	2.08E+02	20	500	9.85E+01	130	5.45E+06	20
PSDF	EL FOR	57	18(5)	1.45E+04	4.28E+02	20	500	2.50E+02	130	2.83E+07	460
PSDF	EL FOR	58	19(5)	8.47E+03	4.50E+02	20	500	1.12E+01	130	1.09E+07	460
PSDF	EL FOR	59	20(5)	4.05E+02	4.53E+02	20	500	5.61E-03	70	2.53E+04	460

RANDOM ANALYSIS OF THE AMRAAM MOUNTED ON A LAU-106
UNIT ACCELERATION IN THE Z PLANE. 32VH (FIG.4-2) PSD. GRID 133

SHEAR FORCE 1 (LBF)

PLOT TYPE	CURVE TYPE	FRAME NO.	CURVE ID	RMS VALUE	# POS XINGS	XMIN	XMAX	YMIN	X FOR YMIN	YMAX	X FOR YMAX
PSDF	EL FOR	60	2(7)	2.21E+02	1.56E+02	20	500	3.26E-02	390	4.60E+03	155
PSDF	EL FOR	61	3(7)	2.55E+02	1.26E+02	20	500	1.36E-02	320	7.35E+03	110
PSDF	EL FOR	62	4(7)	2.48E+02	1.23E+02	20	500	1.62E-03	390	6.67E+03	110
PSDF	EL FOR	63	5(7)	2.34E+02	2.20E+02	20	500	1.19E-02	375	3.65E+03	20
PSDF	EL FOR	64	6(7)	2.71E+02	1.40E+02	20	500	5.79E-02	385	4.43E+03	110
PSDF	EL FOR	65	7(7)	4.73E+02	1.84E+02	20	500	3.60E-02	270	1.99E+04	110
PSDF	EL FOR	66	8(7)	7.51E+02	2.30E+02	20	500	2.75E-02	60	4.18E+04	110
PSDF	EL FOR	67	9(7)	8.34E+02	2.55E+02	20	500	8.05E-02	265	4.78E+04	110
PSDF	EL FOR	68	10(7)	3.59E+02	2.96E+02	20	500	1.63E-02	325	7.54E+03	460
PSDF	EL FOR	69	12(7)	3.76E+02	2.87E+02	20	500	1.28E-02	350	7.81E+03	460
PSDF	EL FOR	70	13(7)	3.20E+02	1.48E+02	20	500	3.69E-02	500	5.78E+03	110
PSDF	EL FOR	71	14(7)	2.56E+03	3.97E+02	20	500	3.01E-01	310	7.27E+05	460
PSDF	EL FOR	72	18(7)	5.71E+02	1.83E+02	20	500	1.66E-03	405	2.38E+04	200
PSDF	EL FOR	73	19(7)	9.20E+02	3.77E+02	20	500	3.18E+00	130	8.34E+04	460
PSDF	EL FOR	74	20(7)	4.47E+02	4.40E+02	20	500	1.16E-01	130	2.88E+04	460

BENDING STRESS A1 (PSI)

PSDF	EL STR	75	2(2)	4.99E+01	2.22E+02	20	500	1.19E-02	290	1.75E+02	155
PSDF	EL STR	76	3(2)	7.89E+02	1.68E+02	20	500	1.24E+00	290	5.55E+04	155
PSDF	EL STR	77	4(2)	1.56E+03	1.47E+02	20	500	2.67E+00	390	1.69E+05	110
PSDF	EL STR	78	5(2)	2.22E+03	1.37E+02	20	500	6.02E-01	500	4.84E+05	110
PSDF	EL STR	79	6(2)	1.84E+03	1.22E+02	20	500	8.50E-02	265	2.64E+05	110
PSDF	EL STR	80	7(2)	1.70E+03	1.21E+02	20	500	3.20E-02	370	3.14E+05	20
PSDF	EL STR	81	8(2)	2.43E+02	5.27E+01	20	500	1.58E-02	440	8.92E+03	20
PSDF	EL STR	82	9(2)	3.96E+02	1.54E+02	20	500	7.48E-03	415	1.30E+04	20
PSDF	EL STR	83	10(2)	6.46E+02	2.30E+02	20	500	7.16E-02	390	2.00E+04	110
PSDF	EL STR	84	12(2)	1.50E+03	2.15E+02	20	500	7.90E-01	275	1.13E+05	110
PSDF	EL STR	85	13(2)	5.45E+02	1.35E+02	20	500	1.71E-01	85	1.63E+04	110
PSDF	EL STR	86	14(2)	5.24E+03	3.14E+02	20	500	1.59E+00	360	1.71E+06	460
PSDF	EL STR	87	18(2)	6.96E+03	4.12E+02	20	500	9.60E+01	130	5.94E+06	460
PSDF	EL STR	88	19(2)	3.99E+03	4.28E+02	20	500	1.89E+01	130	2.14E+06	460
PSDF	EL STR	89	20(2)	8.21E+02	4.42E+02	20	500	3.27E-01	130	9.83E+04	460

RANDOM ANALYSIS OF THE AMRAAM MOUNTED ON A LAU-106
UNIT ACCELERATION IN THE Z PLANE. 32VH (FIG. 4-2) PSD. GRID 133

BENDING STRESS B1 (PSI)

PLOT TYPE	CURVE TYPE	FRAME NO.	CURVE ID	RMS VALUE	# POS XINGS	XMIN	XMAX	YMIN	X FOR YMIN	YMAX	X FOR YMAX
PSDF	EL STR	90	2(12)	1.71E+02	1.68E+02	20	500	5.83E-02	290	2.61E+03	155
PSDF	EL STR	91	3(12)	1.55E+03	1.47E+02	20	500	2.56E+00	305	1.66E+05	110
PSDF	EL STR	92	4(12)	2.37E+03	1.37E+02	20	500	2.51E+00	310	4.69E+05	110
PSDF	EL STR	93	5(12)	1.84E+03	1.20E+02	20	500	4.05E-02	430	2.66E+05	110
PSDF	EL STR	94	6(12)	1.71E+03	1.22E+02	20	500	1.58E-02	365	3.13E+05	20
PSDF	EL STR	95	7(12)	1.52E+03	4.81E+01	20	500	5.17E-01	385	3.60E+05	20
PSDF	EL STR	96	8(12)	3.93E+02	1.51E+02	20	500	5.00E-03	415	1.30E+04	20
PSDF	EL STR	97	9(12)	5.78E+02	1.96E+02	20	500	1.16E-01	275	1.72E+04	110
PSDF	EL STR	98	10(12)	5.44E+02	2.17E+02	20	500	9.63E-02	275	1.47E+04	110
PSDF	EL STR	99	12(12)	5.48E+02	1.33E+02	20	500	2.21E-01	275	1.68E+04	110
PSDF	EL STR	100	13(12)	5.91E+02	1.99E+02	20	500	1.53E-01	80	1.83E+04	110
PSDF	EL STR	101	14(12)	2.54E+03	2.08E+02	20	500	8.58E+00	130	4.74E+05	20
PSDF	EL STR	102	18(12)	6.78E+03	4.28E+02	20	500	5.46E+01	130	6.18E+06	460
PSDF	EL STR	103	19(12)	2.33E+03	4.50E+02	20	500	8.45E-01	130	8.24E+05	460
PSDF	EL STR	104	20(12)	1.11E+02	4.53E+02	20	500	4.24E-04	70	1.91E+03	460

RANDOM ANALYSIS ON THE AMRAAM SECTION W/ SHAKER TABLE
UNIT ACCELERATION IN THE Z PLANE. 32VH (FIG.4-2) PSD. GRID 24

ACCELERATION (IN/SEC2)**

PLOT TYPE	CURVE TYPE	FRAME NO.	CURVE ID	RMS VALUE	# POS XINGS	XMIN	XMAX	YMIN	X FOR YMIN	YMAX	X FOR YMAX
PSDF	ACCE	1	1(5)	4.50E+06	1.77E+02	20	500	1.28E+05	275	1.75E+12	180
PSDF	ACCE	2	2(5)	2.60E+06	1.76E+02	20	500	9.10E+04	280	5.86E+11	180
PSDF	ACCE	3	3(5)	5.21E+06	1.36E+02	20	500	1.01E+05	360	3.12E+12	130
PSDF	ACCE	4	4(5)	2.46E+06	1.63E+02	20	500	1.76E+04	385	4.90E+11	130
PSDF	ACCE	5	5(5)	1.73E+06	1.75E+02	20	500	4.04E+04	350	2.58E+11	180
PSDF	ACCE	6	6(5)	1.98E+06	1.68E+02	20	500	3.68E+04	370	2.83E+11	130
PSDF	ACCE	7	7(5)	6.89E+05	1.74E+02	20	500	1.51E+03	395	4.05E+10	180
PSDF	ACCE	8	8(5)	8.85E+05	2.00E+02	20	500	2.74E+05	355	5.27E+10	210
PSDF	ACCE	9	9(5)	3.22E+03	2.92E+02	20	500	1.37E+03	50	7.49E+04	160
PSDF	ACCE	10	10(5)	1.82E+05	1.80E+02	20	500	9.62E+04	285	2.68E+09	180
PSDF	ACCE	11	11(5)	5.51E+05	2.10E+02	20	500	3.41E+02	35	1.94E+10	180
PSDF	ACCE	12	12(5)	1.07E+05	1.90E+02	20	500	2.32E+04	50	8.66E+08	180
PSDF	ACCE	13	13(5)	5.06E+04	1.91E+02	20	500	4.86E+03	50	1.94E+08	180
PSDF	ACCE	14	14(5)	6.84E+03	1.92E+02	20	500	8.08E+01	50	3.52E+06	180
PSDF	ACCE	15	19(5)	0.00E+00	0.00E+00	20	500	0.00E+00	20	0.00E+00	20
PSDF	ACCE	16	20(5)	3.22E+03	2.92E+02	20	500	1.37E+03	50	7.49E+04	160
PSDF	ACCE	17	21(5)	6.84E+03	1.92E+02	20	500	8.08E+01	50	3.52E+06	180
PSDF	ACCE	18	22(5)	3.34E-01	1.56E+02	20	500	1.05E-08	270	9.86E-03	130
PSDF	ACCE	19	23(5)	3.34E-01	1.56E+02	20	500	1.05E-08	270	9.86E-03	130
PSDF	ACCE	20	24(5)	3.34E-01	1.56E+02	20	500	1.05E-08	270	9.86E-03	130

RANDOM ANALYSIS ON THE AMRAAM SECTION W/ SHAKER TABLE
UNIT ACCELERATION IN THE Z PLANE. 32VH (FIG.4-2) PSD. GRID 24

BENDING MOMENT A2 (IN-LBF)

PLOT TYPE	CURVE TYPE	FRAME NO.	CURVE ID	RMS VALUE	# POS XINGS	XMIN	XMAX	YMIN	X FOR YMIN	YMAX	X FOR YMAX
PSDF	EL FOR	21	2(3)	6.56E+04	1.70E+02	20	500	1.16E+03	420	2.64E+08	180
PSDF	EL FOR	22	3(3)	2.90E+05	1.68E+02	20	500	9.72E+03	420	5.53E+09	180
PSDF	EL FOR	23	4(3)	6.25E+05	1.28E+02	20	500	1.14E+04	290	2.94E+10	20
PSDF	EL FOR	24	5(3)	7.69E+05	1.07E+02	20	500	4.57E+02	500	5.39E+10	20
PSDF	EL FOR	25	7(3)	3.42E+04	1.50E+02	20	500	1.52E+02	85	5.47E+07	130
PSDF	EL FOR	26	23(3)	1.56E+05	1.48E+02	20	500	5.15E+02	350	2.27E+09	130
PSDF	EL FOR	27	24(3)	2.61E+05	5.85E+01	20	500	9.48E+04	290	1.04E+10	20
PSDF	EL FOR	28	27(3)	4.84E+04	1.45E+02	20	500	1.64E+03	285	1.05E+08	180

BENDING MOMENT B2 (IN-LBF)

PSDF	EL FOR	29	2(5)	2.90E+05	1.68E+02	20	500	9.72E+03	420	5.53E+09	180
PSDF	EL FOR	30	3(5)	6.21E+05	1.28E+02	20	500	1.12E+04	290	2.91E+10	20
PSDF	EL FOR	31	4(5)	1.01E+06	1.16E+02	20	500	6.25E+03	285	8.90E+10	20
PSDF	EL FOR	32	5(5)	3.60E+05	1.16E+02	20	500	8.10E+03	285	1.01E+10	20
PSDF	EL FOR	33	7(5)	2.40E+05	1.41E+02	20	500	3.07E+04	285	2.46E+09	180
PSDF	EL FOR	34	23(5)	2.97E+05	9.84E+02	20	500	1.55E+03	340	1.05E+10	200
PSDF	EL FOR	35	24(5)	2.41E+05	1.63E+02	20	500	1.59E+04	40	3.39E+09	130
PSDF	EL FOR	36	27(5)	9.83E+04	1.46E+02	20	500	7.32E+03	285	4.43E+08	180

SHEAR FORCE 1 (LBF)

PSDF	EL FOR	37	2(7)	3.69E+04	1.68E+02	20	500	1.13E+02	420	9.13E+07	180
PSDF	EL FOR	38	3(7)	4.91E+04	9.50E+01	20	500	1.22E+02	270	2.47E+08	20
PSDF	EL FOR	39	4(7)	5.09E+04	9.85E+01	20	500	1.11E+02	420	2.58E+08	20
PSDF	EL FOR	40	5(7)	4.13E+04	9.81E+01	20	500	2.74E+00	340	1.75E+08	20
PSDF	EL FOR	41	7(7)	4.85E+04	1.49E+02	20	500	2.05E+03	285	1.11E+08	180
PSDF	EL FOR	42	23(7)	4.30E+04	1.27E+02	20	500	6.49E+01	350	1.62E+08	20
PSDF	EL FOR	43	24(7)	4.21E+04	1.25E+02	20	500	9.08E+02	100	1.42E+08	20
PSDF	EL FOR	44	27(7)	1.87E+04	1.48E+02	20	500	2.84E+02	285	1.63E+07	180

RANDOM ANALYSIS ON THE AMRAAM SECTION W/ SHAKER TABLE
UNIT ACCELERATION IN THE Z PLANE. 32VH (FIG.4-2) PSD. GRID 24

BENDING STRESS A1 (PSI)

PLOT TYPE	CURVE TYPE	FRAME NO.	CURVE ID	RMS VALUE	# POS XINGS	XMIN	XMAX	YMIN	X FOR YMIN	YMAX	X FOR YMAX
PSDF	EL STR	45	2(2)	6.02E+03	1.70E+02	20	500	9.78E+00	420	2.22E+06	180
PSDF	EL STR	46	3(2)	1.23E+05	1.68E+02	20	500	1.74E+03	420	9.91E+08	180
PSDF	EL STR	47	4(2)	2.64E+05	1.28E+02	20	500	2.04E+03	290	5.26E+09	20
PSDF	EL STR	48	5(2)	3.10E+05	1.07E+02	20	500	7.43E+01	500	8.75E+09	20
PSDF	EL STR	49	7(2)	1.38E+04	1.50E+02	20	500	2.47E+01	85	8.88E+06	130
PSDF	EL STR	50	23(2)	5.85E+05	1.48E+02	20	500	7.24E+03	350	3.19E+10	130
PSDF	EL STR	51	24(2)	2.63E+05	5.85E+01	20	500	9.64E+04	290	1.06E+10	20
PSDF	EL STR	52	27(2)	4.88E+04	1.45E+02	20	500	1.67E+03	285	1.07E+08	180

BENDING STRESS B1 (PSI)

PSDF	EL STR	53	2(12)	2.66E+04	1.68E+02	20	500	8.19E+01	420	4.66E+07	180
PSDF	EL STR	54	3(12)	2.63E+05	1.28E+02	20	500	2.01E+03	290	5.22E+09	20
PSDF	EL STR	55	4(12)	4.29E+05	1.16E+02	20	500	1.12E+03	285	1.60E+10	20
PSDF	EL STR	56	5(12)	1.45E+05	1.16E+02	20	500	1.32E+03	285	1.64E+09	20
PSDF	EL STR	57	7(12)	9.66E+04	1.41E+02	20	500	4.98E+03	285	4.00E+08	180
PSDF	EL STR	58	23(12)	1.11E+06	9.84E+01	20	500	2.18E+04	340	1.48E+11	20
PSDF	EL STR	59	24(12)	2.43E+05	1.63E+02	20	500	1.61E+04	40	3.45E+09	130
PSDF	EL STR	60	27(12)	9.91E+04	1.46E+02	20	500	7.44E+03	285	4.50E+08	180

GLOSSARY

The definitions of the terminology used in this study are reprinted from the Shock and Vibration Handbook (Harris 1988, pp. 1-18 to 1-20). The Shock and Vibration Handbook is perhaps one the most complete and comprehensive works published on the subject of vibration. Since, it is such an authoritative work, only those technical terms that were used in this study are reprinted below in order to "standardize" the usage of the terminology.

Acceleration. Vector quality that specifies the time rate of change of velocity.
Broad-band Random Vibration. Random vibration having its frequency components distributed over a broad frequency band.
Cycle. Complex sequence of values of a periodic quantity that occur during a period.
Degrees-of-freedom. The number of degrees-of-freedom of a mechanical system is equal; to the minimum number of independent coordinates required to define completely the positions of all parts of the system at any instant of time. In general, it is equal to the number of independent displacements that are possible.
Displacement. Vector quantity that specifies the change of position of a body or particle and is usually measured from the mean position or position of rest. In general, it can be represented as a rotational vector or a translational vector, or both.
Ensemble. A collection of signals.
Frequency. The frequency of a function periodic in time is the reciprocal of the period. The unit is the cycle per unit time and must be specified: the unit cycle per second is called Hertz (Hz).
Induced Environment. Those conditions generated as a result of the operation of a structure or equipment.
Fundamental Frequency. The fundamental frequency of an oscillating system is the lowest frequency, and is associated with the fundamental mode.

Linear System. A system is linear if for every element in the system the response is proportional to the excitation. This definition implies that the dynamic properties of each element in the system can be represented as a set of linear differential equations with constant coefficients, and that for the system as a whole superposition holds.

Mode of Vibration. In a system under going vibration, a mode of vibration is a characteristic pattern assumed by the system in which the motion of every particle is simple harmonic with the same frequency. Two or more modes may exist concurrently in a multiple degree-of-freedom system.

Multiple Degree-of-freedom system. A multiple degree-of-freedom system is one for which two or more coordinates are required to define completely the position of the system at any instant.

Narrow-band Random Vibration. Random vibration having frequency components only within a narrow band. It has the appearance of a sine wave whose amplitude varies in an unpredictable manner.

Natural Environments. Those conditions generated by the forces of nature and whose effects are experienced when the equipment or structure is at rest as well as when it is in operation.

Natural Frequency. The frequency of free vibration of a system. For a multiple degree-of-freedom system, the natural frequencies are the frequencies of the normal modes of vibration.

Nonstationary Process. A process that is not stationary. The statistical averages computed over an ensemble of time history records are not invariant with respect to translations in time, but are a function of the times being analyzed (Bendat and Piersol 1986, p. 542).

Peak-to-peak Value. The algebraic difference between the extremes of a quantity.

Period. The smallest increment of the independent variable for which the function repeats itself.

Power Spectral Density (PSD). The limiting mean-square value (e.g., of acceleration, velocity, displacement, stress or other random variable) per unit bandwidth, i.e., the limit of the mean-square value in a given rectangular

bandwidth divided by the bandwidth, as the bandwidth approaches zero.

Random Vibration. Vibration whose instantaneous magnitude is not specified for any given instant of time. The instantaneous magnitudes of a random vibration are specified only by probability distribution functions giving the probable fraction of the total time that the magnitude (or some sequence of magnitudes) lies within a specified range. Random vibration contains no periodic or quasi-periodic constituents. If random vibration has instantaneous magnitude that occur according to the Gaussian distribution, it is called "Gaussian random vibration."

Resonance. Resonance of a system in forced vibration exists when any change, however small, in the frequency of excitation causes a decrease in the response of the system.

Response. The response of a device or system is the motion (or other output) resulting from an excitation (stimulus) under specified conditions.

Root Mean Square (RMS). The positive square root of the mean square value. The RMS value is equal to the standard deviation if the mean value is zero (Bendat and Piersol 1986, p. 543).

Single Degree-of-freedom system. A system for which only one coordinate is required to define completely the configuration of the system at given instant.

Stationary Process. A stationary process is an ensemble of signals such that an average of values over the ensemble at any given time is independent of time.

Steady-state Vibration. Exists in a system if the velocity of each particle is a continuing periodic quantity.

Stiffness. The ratio of change of force (or torque) to the corresponding change in translational (or rotational) deflection of an elastic element.

Transmissibility. The nondimensional ratio of the response amplitude of a system in steady-state forced vibration to the excitation amplitude. The ratio may be one of forces, displacements, velocities, or acceleration.

Vibration. An oscillation wherein the quantity is a parameter that defines the motion of a mechanical system.

White Noise. A noise whose power spectral density is substantially independent of frequency over a specified range.

REFERENCES

1. Brown Dave. Senior Scientist. "AMRAAM IMV Vibration Data Base." Tucson: Hughes Aircraft Company,1989.

2. Curtis, Allen J., Nickolas G. Tinling, and Henry T. Abstein, Jr. Selection and Performance of Vibration Tests. Shock and Vibration Center, Monograph SVM-8. Washington: GPO, 1971.

3. Curtis, Allen J. "Review of Missile Shock and Vibration Problems," Colloquium on Experimental Techniques in Shock and Vibration at the Winter Annual Meeting of the ASME. (New York: ASME, 1962), 107-120.

4. Curtis, Allen J. "Concepts in Vibration Data Analysis." Shock and Vibration Handbook. 3rd ed. Ed, Cyril M. Harris. New York: McGraw-Hill, 1988.

5. Department of Defense. Military Standard, Environmental Test Methods and Engineering Guidelines. MIL-STD-810E. Washington: GPO, 1989.

6. Department of Defense. Military Standard, Environmental Criteria and Guidelines for Air-Launched Weapons. MIL-STD-1670A. Washington: GPO, 1976.

7. Fackler, Warren C. Equivalence Techniques for Vibration Testings. Shock and Vibration Monograph, SVM-9. Washington: GPO, 1972.

8. Fischer, Edward G., and Harold M. Forkois. "Practice of Equipment Design." Shock and Vibration Handbook. 3rd ed. Ed, Cyril M. Harris. New York: McGraw-Hill, 1988.

9. Gallagher, V. M., Wadsworth T. M., York R. L. Sidewinder Fatigue Spectra Development. Technical Report NWC TP6833. China Lake: NWC, 1987.

10. Hughes Aircraft Company. CDRL A03H. "Missile and Launcher Vibration, Shock and Acoustic Analysis Report." 32050-2584, Revision A1. Tucson: Hughes Aircraft Company, Oct 1989.

REFERENCES -- Continued

11. Johnson, Lt Col T. L., Stuart , Senior Engineer R. M., and Topham, Capt K. C. "F-15 Mission Profile for the AMRAAM Qualification Program." Unpublished. Eglin AFB FL. Jul 1989.

12. Miles, John W., and William T. Thomson. "Statistical Concepts in Vibration." Shock and Vibration Handbook. 3rd ed. Ed, Cyril M. Harris. New York: McGraw-Hill, 1988.

13. Morrow, Charles T. "Introduction to Data Reduction, Testings, and Specifications." Shock and Vibration Handbook. 3rd ed. Ed, Cyril M. Harris. New York: McGraw-Hill, 1988.

14. Piersol, Allen G. Vibration and Acoustic Test Criteria for Captive Flight of Externally Carried Stores. AFFDL-TR-71-158, Wright-Patterson AFB: WRDC, 1971.

15. Scheidter, Roy A. "F-15 Signal Data Recorder Computer Tapes." St. Louis: McDonnell Douglas Corporation, 22 May 1989.

16. Smith C. R. Fatigue Strength of Riveted Joints. Reprinted in CDRL A02W. "Fatigue Stress Analysis Report -Airframe Final." 32050-2584, Revision A1. Tucson: Hughes Aircraft Company, Oct 1989.

17. Steinberg, David S. Vibration Analysis For Electronic Equipment. 2nd ed. New York: John Wiley and Sons, 1988.

18. Stuart, Robert M. Presentation to a General Officer. "Captive Flight Vibration Requirement for AMRAAM on the F-15." Tucson: Hughes Aircraft Company, 8 August 1989.